5-1-1983

A Theoretical Model for Captive Columns in Bending

Michael J. Gilberg

A THEORETICAL MODEL FOR CAPTIVE COLUMNS IN BENDING

by

Michael J. Gilberg
Bachelor of Science, University of North Dakota, 1980

A Thesis

Submitted to the Graduate Faculty

of the

University of North Dakota

in partial fulfillment of the requirements

for the degree of

Master of Science

Grand Forks, North Dakota

May 1983

This Thesis submitted by Michael J. Gilberg in partial fulfillment of the requirements for the Degree of Master of Science from the University of North Dakota is hereby approved by the Faculty Advisory Committee under whom the work has been done.

J. Peter Saddler
(Chairman)

Ed Adams

Albert E. Amuta J.

This thesis meets the standards for appearance and conforms to the style and format requirements of the Graduate School of the University of North Dakota, and is hereby approved.

O. William Johnson
Dean of the Graduate School

Permission

Title A THEORETICAL MODEL FOR CAPTIVE COLUMNS IN BENDING

Department Mechanical Engineering

Degree Master of Science

In presenting this thesis in partial fulfillment of the requirements for a graduate degree from the University of North Dakota, I agree that the Library of the University shall make it freely available for inspection. I further agree that permission for extensive copying for scholarly purposes may be granted by the professor who supervised my thesis work or, in his absence, by the Chairman of the Department or the Dean of the Graduate School. It is understood that any copying or publication or other use of this thesis or part thereof for financial gain shall not be allowed without that due recognition shall be given to me and to the University of North Dakota in any scholarly use which may be made of any material in my thesis.

Signature Michael J. Gilberg

Date 3/18/83

TABLE OF CONTENTS

	PAGE
LIST OF FIGURES	vii
LIST OF TABLES	x
ACKNOWLEDGEMENTS	xi
ABSTRACT	xii
NOMENCLATURE	1
CHAPTER 1 - INTRODUCTION	5
CHAPTER 2 - THEORETICAL EQUATIONS	11
Initial Application of Classical Beam Theory	11
Conservation of Energy	14
Elastic Strain Energy Due to Normal Bending Stress	16
Effect of the Wrap Upon the Flexural Rigidity	19
Elastic Strain Energy Due to Shear Stress	22
Beam Stiffness	35
CHAPTER 3 - COMPUTER MODEL	38
General Computer Model	38
Simple-Supported Beam	44
CHAPTER 4 - TEST SPECIMENS AND PHYSICAL TESTING	49
Captive Column Test Specimens	49
Test Apparatus	54
CHAPTER 5 - RESULTS	58
Experimental Results	58
Analytical Results	67
Computer Model Results	67

TABLE OF CONTENTS (Continued)

	PAGE
Conclusions	69
CHAPTER 6 - ANALYTICAL RESULTS	70
Approximate Beam Stiffness	70
Predicted Captive Column Behavior	73
Cap Elastic Modulus	74
Cap Diameter	76
Span Length	76
Cap Centerline Distance	79
Core Panels and Wrap	81
Cross-Section Geometry	88
Other Design Parameters	92
Experimental Verification	94
Sources of Error in the Analytical Approach	115
CHAPTER 7 - COMPUTER MODEL RESULTS	120
Computer Model Versus Experimentally Determined Beam Stiffness	120
Computer Model Versus Analytical Beam Stiffness	121
Cross-Sectional Deformation	124
Wrap Pretension	124
CHAPTER 8 - OTHER FLEXURAL LOADING CONDITIONS	132
Castigliano's Thereom	132
Cantilevered Beam, Uniform Load	135
Simple-Supported Beam, Concentrated Midspan Load	138
CHAPTER 9 - CONCLUSION	141

TABLE OF CONTENTS (Continued)

	PAGE
Physical Testing	141
Analytical Development	143
Computer Model	144
Dynamic Analysis	144
APPENDICES	146
APPENDIX A - MOMENT OF INERTIA EQUATIONS	147
APPENDIX B - WRAP SHEAR STIFFNESS AND EQUIVALENT WRAP WIDTH	151
APPENDIX C - SOLUTION OF INTEGRALS NEEDED FOR THE ELASTIC STRAIN ENERGY DUE TO SHEAR STRESS	161
APPENDIX D - BEAM STIFFNESS FOR OTHER CAPTIVE COLUMN CROSS-SECTIONS	165
APPENDIX E - COMPUTER PROGRAMS	183
REFERENCES	193

LIST OF FIGURES

FIGURE NO.		PAGE
1	CAPTIVE COLUMN COMPONENTS	6
2	CAPTIVE COLUMN GEOMETRIES	8
3	DEFLECTION OF A BEAM DUE TO A BENDING MOMENT AND A SHEAR FORCE	13
4	SHEAR AND MOMENT DIAGRAMS FOR A SIMPLE-SUPPORTED BEAM WITH A CONCENTRATED MIDSPAN LOAD	18
5	WRAP STRESSES DUE TO A PURE BENDING MOMENT	20
6	BEAM CROSS-SECTION FOR SHEAR STRESS DISTRIBUTION . .	23
7	SHEAR STIFFNESS OF A WRAP PANEL	28
8	SIMPLIFIED SQUARE CROSS-SECTION	30
9	FINITE ELEMENT CAPTIVE COLUMN CORE	40
10	FINITE ELEMENT CAPTIVE COLUMN CAP	41
11	FINITE ELEMENT CAPTIVE COLUMN WRAP	43
12	SIMPLE-SUPPORTED BEAM WITH A CONCENTRATED MIDSPAN LOAD	45
13	NODE NUMBERING FOR A SQUARE CROSS-SECTION CAPTIVE COLUMN	47
14	TEST CONFIGURATION FOR SMALL CAPTIVE COLUMNS	55
15	TEST CONFIGURATION FOR LARGE CAPTIVE COLUMNS	55
16	LOAD DISTRIBUTIONS AND END SUPPORTS	57
17	BEAM STIFFNESS VS. CAP ELASTIC MODULUS	75
18	BEAM STIFFNESS VS. CAP DIAMETER	77
19	BEAM STIFFNESS VS. SPAN LENGTH	78
20	BEAM STIFFNESS VS. CAP CENTERLINE DISTANCE	80
21	WRAP PARAMETERS FOR CONSTANT WRAP DENSITY	84

LIST OF FIGURES (Continued)

FIGURE NO.		PAGE
22	WRAP PARAMETERS FOR CONSTANT AMOUNT OF WRAP MATERIAL	86
23	BEAM STIFFNESS AS A FUNCTION OF CORE PANEL AND WRAP SHEAR STIFFNESSES	87
24	CAPTIVE COLUMN CROSS-SECTIONAL SHAPES	89
25	BEAM STIFFNESS VS. SPAN LENGTH, CAPTIVE COLUMN NUMBER 16	96
26	BEAM STIFFNESS VS. SPAN LENGTH, CAPTIVE COLUMN NUMBERS 17 AND 20	97
27	BEAM STIFFNESS VS. SPAN LENGTH, CAPTIVE COLUMN NUMBERS 18 AND 21	98
28	BEAM STIFFNESS VS. SPAN LENGTH, CAPTIVE COLUMN NUMBER 19	99
29	BALSA WOOD MATERIAL PROPERTIES	105
30	BEAM STIFFNESS VS. WRAP DENSITY	107
31	BEAM STIFFNESS VS. WRAP ANGLE	109
32	BEAM STIFFNESS VS. SPAN LENGTH, WRAP DENSITY = 2.5 STRANDS/INCH	111
33	BEAM STIFFNESS VS. SPAN LENGTH, WRAP DENSITY = 7.5 STRANDS/INCH	112
34	BEAM STIFFNESS VS. SPAN LENGTH, WRAP DENSITY = 15.0 STRANDS/INCH	113
35	CROSS-SECTIONAL DEFORMATION DUE TO LATERAL EXPANSION AND CONTRACTION	118
36	BEAM STIFFNESS VS. LOAD FOR 1.0 POUND OF WRAPPING TENSION	129
37	BEAM STIFFNESS VS. WRAPPING TENSION	130
38	CANTILEVERED BEAM, UNIFORM LOAD	136
39	SIMPLE-SUPPORTED BEAM, CONCENTRATED MIDSPAN LOAD	136
40	CAPTIVE COLUMN CROSS-SECTIONS	150

LIST OF FIGURES (Continued)

FIGURE NO.		PAGE
41	PANEL OF WRAP STRANDS, ONE DIRECTION OF WRAP	153
42	PANEL OF WRAP STRANDS, TWO DIRECTIONS OF WRAP . . .	159
43	SQUARE CROSS-SECTION CAPTIVE COLUMN, ROTATED 45° . .	167
44	TRIANGULAR CROSS-SECTION CAPTIVE COLUMN	173

LIST OF TABLES

TABLE NO.		PAGE
1	DIMENSIONAL PROPERTIES	50
2	MATERIAL PROPERTIES	53
3	BEAM STIFFNESS VALUES	60
4	COMPUTED CAPTIVE COLUMN PROPERTIES	68
5	BEAM STIFFNESS FOR CORE THICKNESS TESTS	104
6	ANALYTICAL METHOD VS. COMPUTER MODEL	122

ACKNOWLEDGEMENTS

The author expresses his appreciation to Dr. J. Peter Sadler, Albert E. Anuta, and Dr. Edmon L. Adams for serving as consultants on the faculty advisory committee for this thesis. Gratitude is also extended to Dr. Ronald Apanian and Bill Heglund for suggestions and criticisms in the preparation of this thesis; to Curtis Larsen, Steve Apanian, and Dave O'Shea for their work in captive column fabrication and testing; and to Lawrence Bosch, captive column inventor and patent holder.

The assistance of the clerical and drafting staff of the Engineering Experiment Station in the preparation of the rough and final drafts of this thesis is deeply appreciated.

The funding support of the North Dakota State Highway Department and the Federal Highway Administration is recognized and appreciated.

ABSTRACT

A theoretical model for the determination of the beam stiffness of a captive column loaded as a simple-supported beam with a concentrated midspan load is described. A captive column is a high strength, light-weight composite structural member. Due to the composite nature of a captive column, the deflection due to shear forces, which is neglected in typical beam applications, must be included in the determination of the lateral deflection. The total deflection is obtained by setting the elastic strain energy stored in the captive column equal to the work that is applied to the column. The effects of changes in individual design parameters are investigated using the theoretical model. Experimental data was obtained to verify the theoretical model and the effects of changes in individual design parameters. Comparisons are also made between beam stiffness values obtained from the theoretical model and a finite element computer model.

Comparisons between beam stiffness values obtained from the theoretical model, experimental testing, and the finite element model indicate that the theoretical model can be used to determine captive column beam stiffness or to predict the effect of a change in an individual design parameter. Sources of error in the experimental results and possible areas of improvement in the theoretical model are identified and discussed.

NOMENCLATURE

a	y-intercept for "best fit" straight line
A	Cross-sectional area
A_{1mno}	Area used in computing the first moment of area
A_s	Cross-sectional area of a wrap strand
b	Width of the cross-section at the height h
b_{caps}	Width of the caps
b_{center}	Width of the centerpiece
b_{eq}	Equivalent cross-section width
b_{panels}	Width of the core panels
b_{wrap}	Width of the wrap
$B_1 - B_4$	Constants used in approximate beam stiffness equations
$c_1 - c_{18}$	Constants used in the elastic strain energy due to shear stress equations
d	Cap diameter
d_{wrap}	Wrap strand diameter
D	Cap centerline distance
E	Elastic modulus
E_{cap}	Cap material elastic modulus
E_{center}	Core centerpiece elastic modulus
E_{panel}	Core panel material elastic modulus
E_{wrap}	Wrap material elastic modulus
$(EI)_{caps}$	Flexural rigidity of the caps
$(EI)_{center}$	Flexural rigidity of the core centerpiece
$(EI)_{eq}$	Equivalent flexural rigidity

NOMENCLATURE (Continued)

$(EI)_{panels}$	Flexural rigidity of the core panels
F	Arbitrary force used in Castigliano's theorem
F_s	Wrap strand force
G	Shear modulus
G_{cap}	Cap material elastic modulus
G_{center}	Core centerpiece material elastic modulus
G_{panel}	Core panel material elastic modulus
G_{wrap}	Wrap material elastic modulus
h	Distance from the neutral axis
h_{panel}	Core panel weight
$h_1 - h_6$	Distances from the neutral axis
$H_1 - H_4$	Constants used in approximate beam stiffness equations
I	Moment of inertia
I_{caps}	Moment of inertia of the caps
I_{center}	Moment of inertia of the core centerpiece
I_{panels}	Moment of inertia of the core panels
$J_1 - J_6$	Integrals used in the elastic strain energy due to shear stress equations
k	Beam stiffness
K	Constant value used in the elastic strain energy due to shear stiffness equations
l	Amount of wrap material per lineal inch
ℓ	Length of a wrap strand
L	Span length
m	Slope of the "best fit" straight line
M	Bending moment

NOMENCLATURE (Continued)

N	Number of wrap strands
NA	Neutral axis
P	Concentrated midspan load
P_{eq}	Equivalent shear force
Q	First moment of area outside of the height h
Q_{caps}	First moment of area of the caps
Q_{center}	First moment of area of the core centerpiece
Q_{eq}	Equivalent first moment of area
Q_{panels}	First moment of area of the core panels
Q_{wrap}	First moment of area of the wrap
t_{panel}	Core panel thickness
$(tG)_{panel}$	Core panel shear stiffness
U_{normal}	Elastic strain energy due to normal bending stress
U_{shear}	Elastic strain energy due to shear stresses
U_{total}	Total elastic strain energy
V	Shear force
w_{cap}	Cap width
w_{center}	Core centerpiece width
w'_{center}	Equivalent core centerpiece width
w_{wrap}	Wrap panel width
$(wG)_{wrap}$	Wrap panel shear stiffness
W	Uniform load
W_{ext}	External work
x_o	Distance from an end support
y	Distance from the neutral axis
$\overline{y}$	Distance from the neutral axis to the centroid of the area above h

NOMENCLATURE (Continued)

γ	Shear strain
δ	Lateral deflection of a beam
Δ	Axial deflection of a wrap strand
$\Delta_{deflection}$	Change in the lateral deflection
Δ_{load}	Change in the applied load
π	Pi = 3.1415927...
ρ	Wrap density
σ	Normal stress
τ	Shear stress
ϕ	Wrap angle

CHAPTER 1

INTRODUCTION

A captive column is a high-strength, light-weight composite structural member. The high strength, while maintaining light weight, is attained by taking full advantage of the mechanical properties of the three major components which make up a captive column: the caps, the core, and the wrap (see Figure 1).

The primary emphasis in the design of a captive column is to place material with high strength and a high elastic modulus (the caps) at as great a distance as possible from the neutral axis. By doing this, the moment of inertia of the member is increased, which increases the flexural load carrying capacity of a captive column beam or girder and the critical buckling load of an axially loaded captive column.

In order to maintain the caps at a specified distance from the neutral axis, there must be a way to prevent the caps from movement relative to each other and to prevent buckling of an individual cap. A light-weight core section is used to prevent inward buckling of the caps. The core section consists of core panels, one for each cap, joined to a common centerpiece. The core panel material must possess a relatively high compressive strength in the direction perpendicular to the caps. The wrap, which is a fibrous material or fine wire helically wound around the core and caps, is used to prevent outward or lateral buckling of the caps. The material used for the wrap should have a high tensile strength and elastic modulus. Together, the core and the wrap maintain the

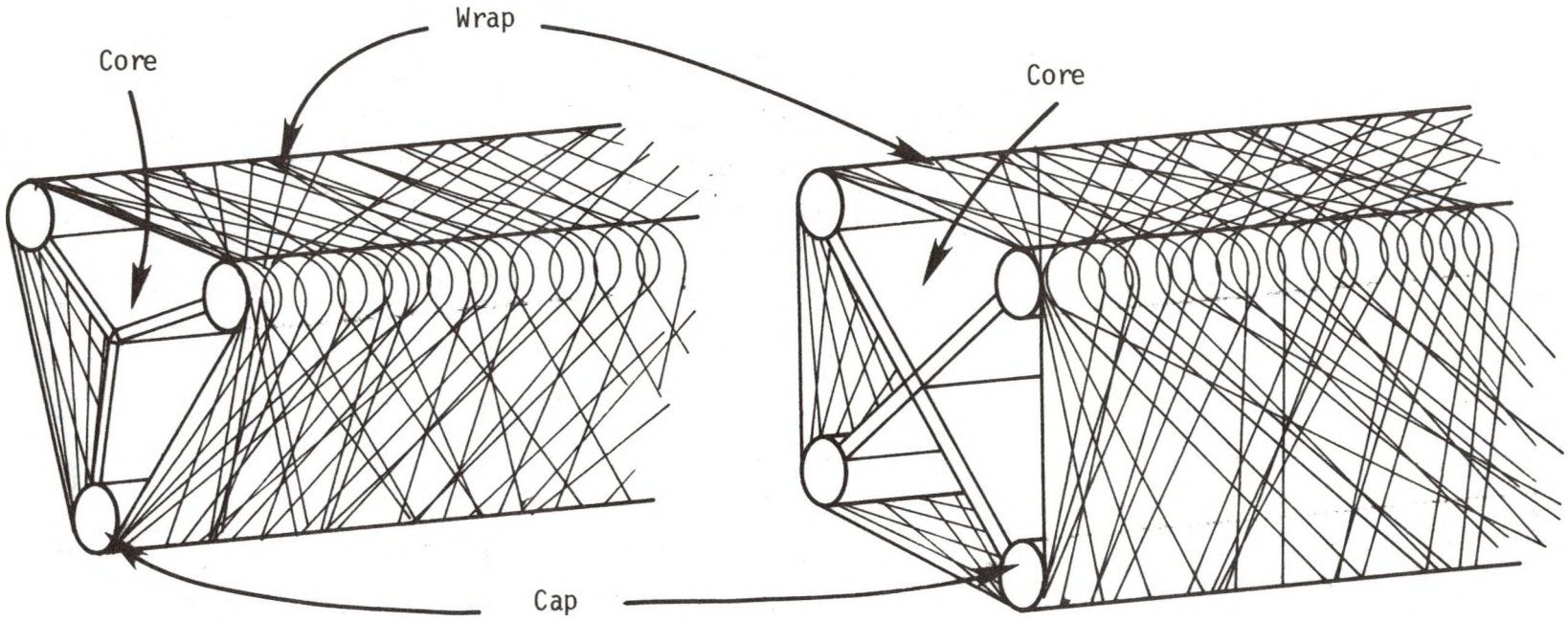

FIGURE 1 - CAPTIVE COLUMN COMPONENTS

cross-sectional geometry. The caps are essentially held captive, which leads to the name "captive column".

A multitude of cross-sectional geometries for cap placement are possible, with the number of possibilities limited by the designer's imagination and economic construction techniques. Shown in Figure 1 are two of the simplest, and thus the most common cross-sectional geometries in use. In Figure 2, three other geometries are shown, along with a comparison between straight and tapered members. The cross-sectional geometry which is used in a design will be dependent upon the application.

The Engineering Experiment Station at the University of North Dakota is currently conducting research which is aimed at determining how the captive column reacts to various load conditions. This research is being done under a grant from the North Dakota State Highway Department and the Federal Highway Administration. The main emphasis of the research is the application of captive columns to highway-related structures.

Triangular and square cross-section captive columns have been built and tested. The range of size for these captive columns varied from a length of 2.5 feet with a 1.25 inch square cross-section, to a length of 20 feet with an 11 inch triangular cross-section. Steel and fiberglass reinforced polyester rods have been used as caps. The core material has been balsa wood or acrylic sheet. Kevlar 49, which is an aramid fiber manufactured by DuPont Company, has been used as the wrap material. These materials represent a small part of the wide spectrum of possible materials that can be used in the construction of captive columns. Larsen [1] conducted an extensive study of possible materials in a previous report.

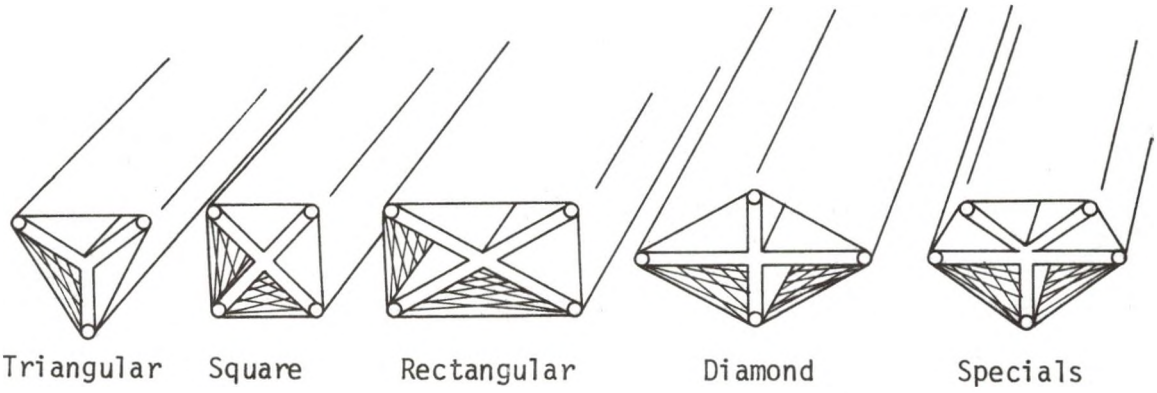

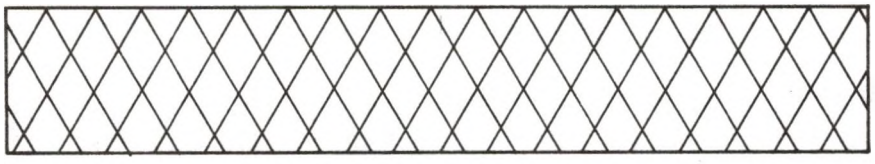

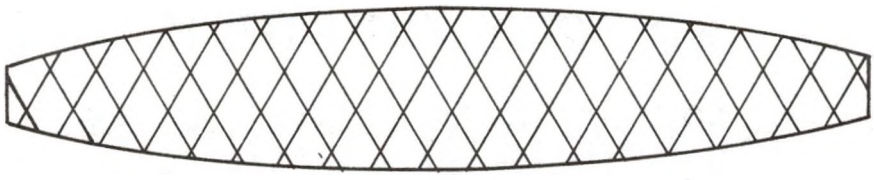

FIGURE 2 - CAPTIVE COLUMN GEOMETRIES

At the present time, information concerning the structural behavior of captive columns is very limited [1-3]. This information is necessary before an engineer can properly design a structure which will incorporate captive columns. Design information similar to that for common structural members (steel beams, reinforced concrete, wood trusses, etc.) must be obtained. Unfortunately, design information for captive columns is difficult to obtain due to the complexities involved in the interrelationship between the caps, core, and wrap and the many parameters involved in captive column design. The wrap is a good example of the many design parameters in a captive column. Proper design of the wrap involves the selection of a wrap material, the cross-sectional shape and size, the wrap density, the wrap angle, the wrapping tension, and the correct adhesive to bond the wrap to the cap. These parameters depend upon the stresses which the wrap will be subjected to in the given application.

Kipp [2] has developed a finite element computer model for the structural analysis of captive columns. This model can be used to determine the deflection of any point of the captive column and to determine the stress condition within individual components for a wide variety of load conditions. The previously mentioned physical testing was used to verify that the computer model yields information which is acceptable for engineering design and analysis [2,3]. A computer with large storage capabilities and access to a general purpose finite element computer program are required for the use of this computer model.

Initial research has established a method of applying classical beam theory to predict the beam stiffness of a captive column loaded as a

simple-supported beam with a concentrated midspan load. The beam stiffness is determined by dividing the applied load by the computed deflection due to the bending moment only. In some cases, this method provides an accurate prediction of the actual beam stiffness, but in other cases, a large difference exists between the predicted and experimentally determined values. Examination of the data indicates that the deflection due to shear force, which is neglected in typical beam applications, may be the primary cause of the discrepancies in the results.

There were three objectives of the research presented in this thesis: 1) the application of classical beam theory to the determination of beam stiffness, 2) the identification of the major captive column design parameters, and 3) the investigation of the interrelationships of the captive column components in beam applications. The application of classical beam theory will include the deflection due to the bending moment and the deflection due to the shear force. Comparisons will be made between experimentally determined beam stiffness values and values predicted by the classical beam theory approach and by the computer model. These comparisons will indicate the effectiveness of the two methods in accounting for the interrelationships of the various captive column components.

The emphasis of this research is on captive columns loaded as simple-supported beams with a concentrated midspan load. However, a chapter is also included that deals with the applicability of the two methods for predicting beam stiffness for other load conditions.

CHAPTER 2

THEORETICAL EQUATIONS

The equations needed to calculate the theoretically determined beam stiffness will be developed in this chapter. These equations are developed by applying the principle of conservation of energy to classical beam theory.

Initial Application of Classical Beam Theory

The initial application of classical beam theory used the well known equation for the midspan deflection of a simple-supported beam with a concentrated midspan load [2,3]. This equation is shown below:

$$\delta = \frac{PL^3}{48\ EI} \tag{1}$$

where δ = deflection

P = applied load

L = span length

E = elastic modulus

I = moment of inertia.

Equation (1) is based upon a beam composed of a homogeneous, linearly elastic, isotropic material. A captive column is constructed of more than one material, with a possibility of one or more of the materials being anisotropic. Because of the nonhomogeneity of the captive column, an equivalent flexural rigidity, $(EI)_{eq}$, was developed.

This flexural rigidity is the summation of the flexural rigidities for the individual components that make up the captive column [2,3]:

$$(EI)_{eq} = (EI)_{caps} + (EI)_{panels} + (EI)_{center} \qquad (2)$$

where $(EI)_{eq}$ = equivalent flexural rigidity

$(EI)_{caps}$ = flexural rigidity of the caps

$(EI)_{panels}$ = flexural rigidity of the core panels

$(EI)_{center}$ = flexural rigidity of the core centerpiece.

The moment of inertia for the various components can be derived from standard equations. The necessary formulas for square and triangular cross-section captive columns can be found in Appendix A.

As noted by an examination of equation (2), the effect of the wrap is neglected in the computation of the equivalent flexural rigidity. The wrap flexural rigidity was neglected because the wrap moment of inertia is small in comparison with the cap and core panel moments of inertia [2]. The effect of the wrap on the equivalent flexural rigidity will be examined in greater detail later in this chapter.

The deflection computed by using equation (1) is the deflection due to the bending moment. Derivation of the equation is based upon the fundamental hypothesis of flexure theory [4]. This hypothesis states that plane sections normal to the neutral axis remain plane and normal to the neutral axis after the beam is subjected to a bending moment. A segment of a homogeneous, rectangular beam is shown in Figures 3A through 3D. Two plane sections, which are parallel to each other in Figure 3A, remain plane after being subjected to a bending moment, Figure 3B, but are no longer parallel to each other. If shear forces exist on the beam, the plane sections become curved, Figure 3C, due to the mutual sliding of

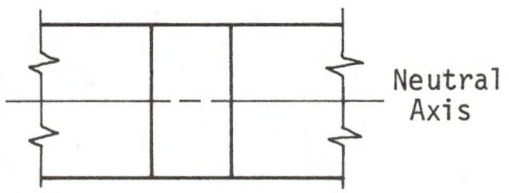

A) No Deflection

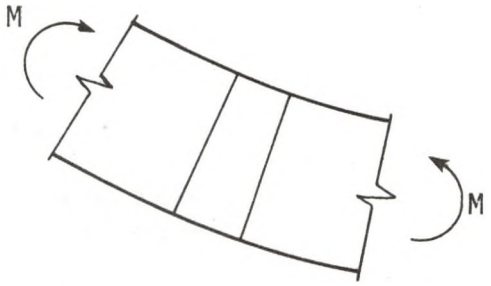

B) Deflection Due to a Bending Moment

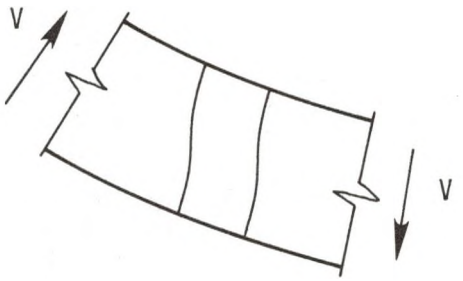

C) Deflection Due to a Shear Force

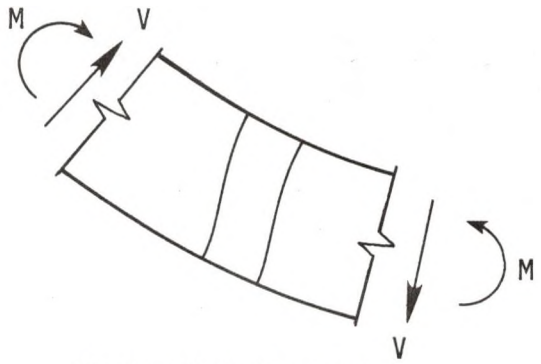

D) Total Deflection

FIGURE 3 - DEFLECTION OF A BEAM DUE TO A BENDING MOMENT AND A SHEAR FORCE

adjacent axial planes along each other [5]. This cross-section curvature results in additional deflection of the beam, which will be referred to as the deflection due to shear force. The total deflection of the beam is the sum of the deflections due to the bending moment and the shear force, Figure 3D.

For typical beams, the deflection due to shear force is very small and is neglected in the majority of cases. For a captive column, the deflection due to shear force may be significant and in some cases it is greater than the deflection due to the bending moment. The equations needed to calculate the total deflection will be derived in the following section.

Conservation of Energy

Work done on a body is measured by the product of the force applied to the body and the displacement of the body. The forces applied to a body produce stresses within the body. In a solid deformable body, a stress multiplied by its respective area is a force. The product of this force and the deformation, which is a displacement, is the work done on the body due to externally applied forces. This work is stored in the body as elastic strain energy. The elastic strain energy stored in the body can be equated to the work applied to the body by using the principle of conservation of energy. The deflection of axially loaded members, torsional members, and beams may be determined by using this principle.

When a concentrated external force is gradually applied to a simple-supported beam, the external work is equal to one-half of the total force multiplied by the deflection in the direction of its action. This external force produces stresses within the beam in the form of normal bending stresses and shear stresses. The work associated with

these stresses is stored in the form of elastic strain energy. Using the principle of conservation of energy, the following equation is obtained:

$$W_{ext} = U_{total}$$
$$\frac{P\delta}{2} = U_{normal} + U_{shear} \tag{3}$$

where W_{ext} = external work

P = applied load

δ = deflection at the load in the direction of the load

U_{total} = total elastic strain energy

U_{normal} = elastic strain energy due to normal bending stresses

U_{shear} = elastic strain energy due to shear stresses.

For a linearly elastic material, stress is proportional to strain. When a perfectly elastic body is subjected to a stress, no energy is dissipated and the work done on the body is stored as recoverable elastic strain energy. Equations have been developed for the elastic strain energy stored in a perfectly elastic body per unit volume of a linearly elastic material [4]. By integrating over the volume of the body the following equations are obtained:

$$U_{normal} = \int_{Volume} \frac{\sigma^2 dV}{2E} \tag{4}$$

$$U_{shear} = \int_{Volume} \frac{\tau^2 dV}{2G} \tag{5}$$

where σ = normal bending stress

E = elastic modulus

τ = shear stress

G = shear modulus.

Elastic Strain Energy Due to Normal Bending Stress

The beams under consideration in this research are captive columns with a constant cross-section, and therefore, the moment of inertia will be constant along the length of the beam. By using a transformed section of the captive column cross-section, the normal stress will vary linearly from the neutral axis according to the following formula:

$$\sigma = \frac{My}{I} \tag{6}$$

where M = bending moment

y = distance from neutral axis

I = moment of inertia.

The transformed section is developed in such a way that the resisting forces of the section are equivalent to the resisting forces of the actual cross-section. Substituting equation (6) into equation (4) and using dxdA as the incremental volume yields the following equation:

$$U_{normal} = \int_{Volume} \frac{M^2 y^2}{2EI^2} \, dxdA \tag{7}$$

The bending moment at any section of a beam is constant and the order of integration in equation (7) is arbitrary. Furthermore, the moment of inertia is defined by the following equation:

$$I = \int_{area} y^2 dA \tag{8}$$

By rearranging the terms in equation (7), and using the above statements and equation (8), the following result is obtained:

$$U_{normal} = \int_{length} \frac{M^2}{2EI^2}\, dx \int_{area} y^2 dA$$

$$U_{normal} = \int_0^L \frac{M^2}{2EI}\, dx \qquad (9)$$

where L = span length

EI = flexural rigidity.

The shear and bending moment diagrams for a simple-supported beam with a concentrated midspan load are shown in Figure 4. The bending moment varies linearly from zero at either end of the beam to a maximum value at the midspan of the beam. The bending moment for the left half of the beam may be represented by the following equation:

$$M = \frac{Px}{2} \quad \text{for} \quad 0 < x < \frac{L}{2} \qquad (10)$$

Substituting equation (10) into equation (9), and using symmetry to reduce the integral, the following equation is obtained:

$$U_{normal} = \frac{P^2 L^3}{96(EI)_{eq}} \qquad (11)$$

This equation yields the strain energy stored in the beam that is attributable to the normal bending stress.

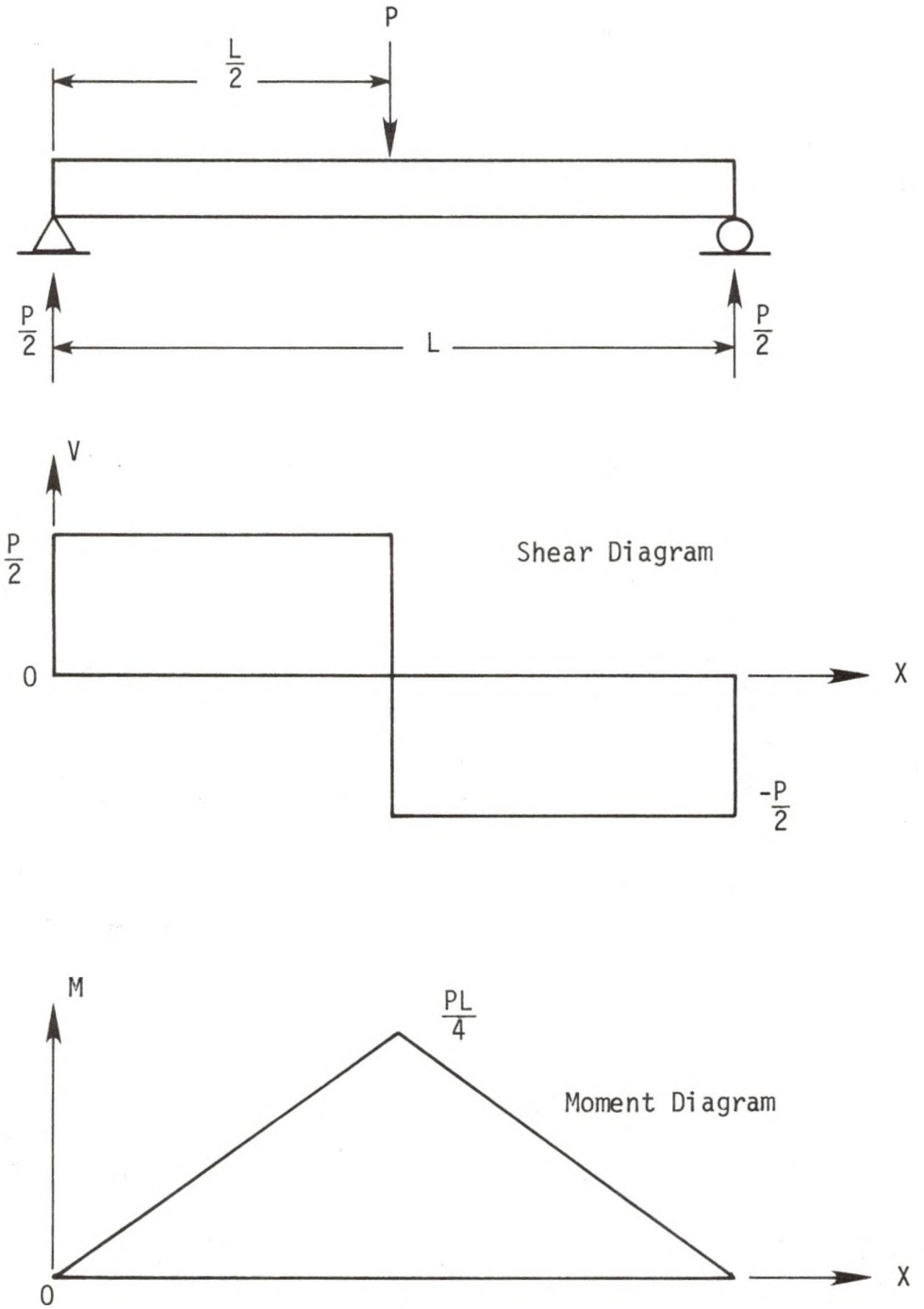

FIGURE 4 - SHEAR AND MOMENT DIAGRAMS FOR A SIMPLE-SUPPORTED BEAM WITH A CONCENTRATED MIDSPAN LOAD

Notice that the equivalent flexural rigidity, computed by using equation (2), is used in equation (11). This value is easier to compute than transforming the section and will yield the same result for the elastic strain energy.

Effect of the Wrap Upon the Flexural Rigidity

The effect of the wrap on the equivalent flexural rigidity was initially neglected because the moment of inertia for the wrap is small in comparison with the core panel and cap moments of inertia. This is a true statement, but it does not represent a fair comparison. The comparison should be made between the wrap flexural rigidity and the core panel and cap flexural rigidities. When this comparison is made, the effect of the wrap on the flexural rigidity may become large enough so that it should not be neglected.

Because the captive column is a complex structural member, questions exist regarding the role of the wrap in resisting external forces and moments applied to the structure. For the following discussion, consider a square cross-section captive column subjected to a pure bending moment. In Figure 5A, assume that the wrap strands are rigid truss members pin-connected to the caps. Under the application of the bending moment, the wrap strands on the concave and convex sides of the captive column will be subjected to compressive and tensile stresses, respectively, thus decreasing the curvature of the member, see Figure 5B. Because the wrap strands are oriented at an angle to the longitudinal axis, the stress can be divided into two components; one parallel and one perpendicular to the longitudinal axis. The component of the stress that is perpendicular to the neutral axis will tend to push the caps on the concave side apart and pull the caps on the convex side together (Figure 5C). This distortion

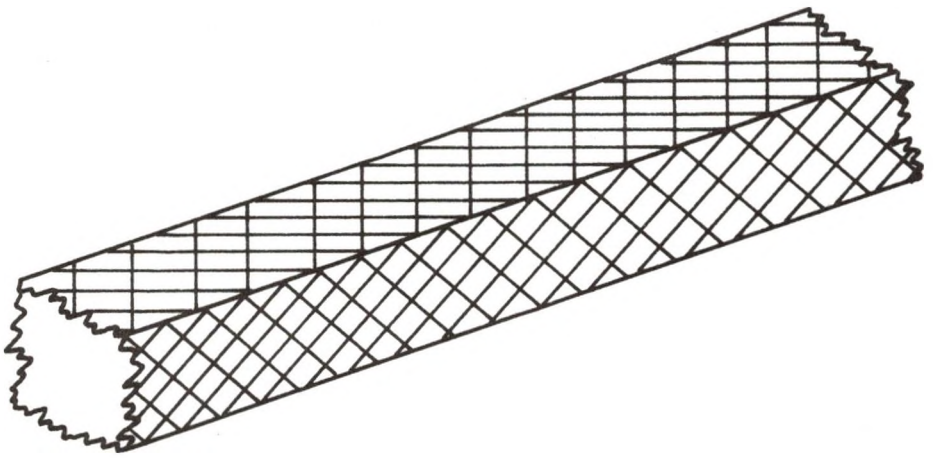

A) Portion of a Captive Column

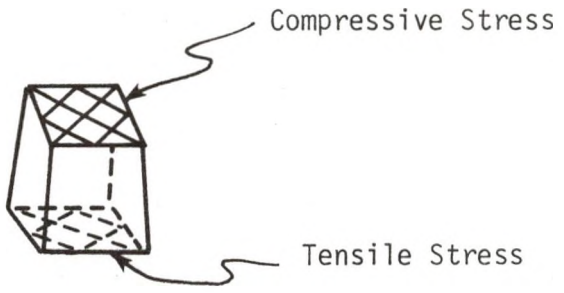

B) Wrap on Concave and Convex Sides

C) Distortion of Cross-Section

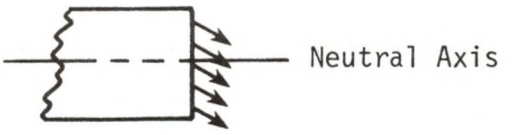

D) Free Body Diagram Showing Side Wrap Forces

FIGURE 5 - WRAP STRESSES DUE TO A PURE BENDING MOMENT

of the cross-section will increase the curvature of the captive column. It is believed that the difference between the decrease in curvature due to the parallel component of the wrap stress and the increase in curvature due to the cross-sectional deformation is negligible in most cases. It is also believed that any stress in the wrap strands on the sides of the captive column will be fairly uniform, at any given section, from cap to cap. Therefore, any horizontal component of stress above the neutral axis will be balanced by an equal stress below the neutral axis (Figure 5D). For these reasons, the contribution of the wrap is neglected in the computation of the equivalent flexural rigidity for a captive column.

The above discussion for a square cross-section captive column can be expanded to a cross-section of any shape. By examining the resulting stress components in the wrap strands it is expected that the contribution of the wrap to the flexural rigidity will be negligible.

This discussion is not intended to dispel the importance of the wrap in the captive column structure. The wrap, as stated in Chapter 1, provides resistance to outward or lateral buckling of the caps. An additional role of the wrap is to prevent cross-sectional deformation due to load conditions other than a pure bending moment. In virtually all applications, including the one under consideration in this research effort, a captive column will be subjected to shear forces. The role of the wrap in resisting shear forces may be very significant.

The inventor of the captive column claims that substantially all types of loading of a captive column results in tensile or compressive forces in the structure [6]. He further claims that by properly designing the wrap, virtually all of the shear forces applied to a captive

column can be transferred into axial forces in the wrap. If this statement is true, the wrap will be a significant factor in the computation of the elastic strain energy due to shear stresses. A method to determine the contribution of the wrap in resisting shear force will be developed in the following section. The truth of the inventors claim will become apparent in Chapter 6.

Elastic Strain Energy Due to Shear Stress

The elastic strain energy due to shear stresses is computed by using equation (5). In order to perform the integration needed for this equation, the shear stress at any point within the captive column must be determined. The shear stress at any distance, h, from the neutral axis of an isotropic, linearly elastic, homogeneous beam is computed by using the following formula:

$$\tau = \frac{VQ}{Ib} \tag{12}$$

where V = shear force

Q = first moment of area outside of height h

I = moment of inertia

b = width of the cross-section at the height h.

A cross-section of a beam is shown in Figure 6A with the dimensions labeled. The first moment of area may be computed by using either of the following formulas:

$$Q = \int_{A_{lmno}} y dA \tag{13}$$

$$Q = A_{lmno}\bar{y} \tag{14}$$

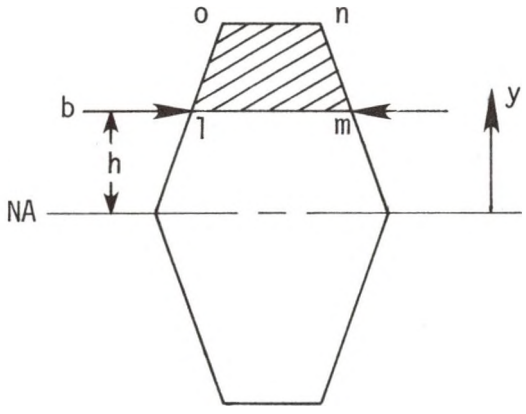

A) Isotropic, Homogeneous Beam

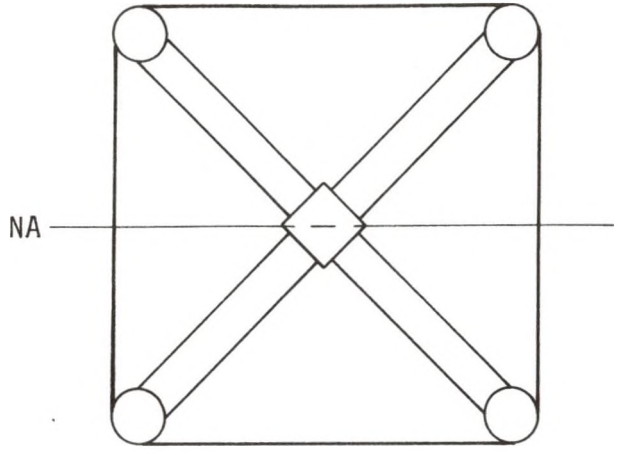

B) Captive Column Cross-Section

FIGURE 6 - BEAM CROSS-SECTION FOR SHEAR STRESS DETERMINATION

where y = distance from the neutral axis

A_{lmno} = area above h

$\bar{y}$ = distance from the neutral axis to the centroid of the area above h.

Since the shear stress is squared in the integral of equation (5), the sign of the shear force is insignificant. By examining the shear diagram of Figure 4, it is apparent that the magnitude of the shear force is equal to a constant value of one half of the applied load, P. For a captive column, the equivalent moment of inertia, computed by dividing the equivalent flexural rigidity of equation (2) by the cap elastic modulus, is used in equation (12). The cap elastic modulus is used in computing the equivalent moment of inertia because the flexural rigidity of the caps is by far the largest component of the equivalent flexural rigidity. As previously stated, this value is constant along the length of the captive columns under consideration. Substituting the above values for the shear force and moment of inertia into equation (12) yields the following:

$$\tau = \frac{VQ}{Ib}$$

$$\tau = \left[\frac{P\ E_{caps}}{2(EI)_{eq}}\right]\left[\frac{Q}{b}\right] \qquad (15)$$

The first bracketed term in equation (15) is a constant value. The second term is a function of the vertical distance from the neutral axis. Since the shear stress is a function of vertical distance only and is not a function of axial position, the incremental volume, dV, may be replaced by the following:

$$dV = LdA \qquad (16)$$

where L = span length

dA = incremental area of the cross-section.

Substituting equations (15) and (16) into equation (5) and simplifying yields the following:

$$U_{shear} = \int_{volume} \frac{\tau^2}{2G} \, dV$$

$$U_{shear} = \frac{P^2 L}{8G} \left[\frac{E_{cap}}{(EI)_{eq}} \right]^2 \int_{area} \left(\frac{Q}{b} \right)^2 dA \qquad (17)$$

The above expression is valid provided that the equivalent flexural rigidity and the magnitude of the shear force are constant along the length of the span. The terms that are not within the integral yield a constant value for any given cross-sectional geometry. The integral is dependent upon the particular orientation of the cross section under consideration. The solution of this integral for a square cross-section captive column, oriented as in Figure 6B, will be developed in the remainder of this section.

The solution of the integral found in equation (17) is complicated due to three main reasons: 1) the possibility of a different material for each component of the cross-section, 2) the nature of the wrap strands in resisting shear force, and 3) the effect of a thin member positioned such that the vertical shear force acts at an angle to the member. Each of these complications will be addressed in the development of the solution to the integral. In the development, it will be assumed that the components of the cross-section are joined together in a fashion

such that no slippage occurs between adjacent components. This implies that the strain on one side of an adhesive joint is equivalent to the strain on the other side of the joint.

An equivalent moment of inertia has been developed for the captive column cross-section. Due to the composite nature of the captive column, a similar development is needed in the computation of the first moment of area, Q, and the width of the cross-section, b. The equivalent quantities are determined in a similar fashion to the development of the equivalent moment of inertia:

$$Q_{eq} = \frac{(QG)_{caps} + (QG)_{panels} + (QG)_{center} + (QG)_{wrap}}{G_{cap}} \tag{18}$$

$$b_{eq} = \frac{(bG)_{caps} + (bG)_{panels} + (bG)_{center} + (bG)_{wrap}}{G_{cap}} \tag{19}$$

where Q_{eq} = equivalent first moment of area

QG = first moment of area of a component multiplied by its shear modulus

b_{eq} = equivalent cross-section width

bG = width of a component multiplied by its shear modulus

G_{cap} = cap shear modulus.

The use of equations (18) and (19) results in a transformed section with the same resistance to shear force as the actual section. The cap shear modulus is used as the divisor in the two equations because the cap elastic modulus was used in the computation of the equivalent moment of inertia.

The first moment of area for each of the components in equation (18) is dependent upon the geometry of that component. The wrap is composed of individual strands, assumed to be uniformly distributed along the

length of the captive column. The wrap strands on the top and bottom of the cross-section shown in Figure 6B are assumed to offer negligible resistance to vertical shear force. In order to determine the first moment of area for the individual strands of wrap on the sides of the cross-section, an equivalent width must be developed for a panel of wrap strands. This width is determined by considering the stress needed to distort a panel of wrap strands by an angle γ. Two parameters of the wrap are used in this analysis. As shown in Figure 7A, the wrap angle, ϕ, is defined to be the angle between the wrap strands and the longitudinal axis of the captive column. Wrap density, ρ, is defined to be the number of wrap strands, in a given helical direction, per lineal inch of captive column.

Four rigid links are shown in Figure 7B. If the links are connected by frictionless pins, the assemblage will have no resistance to an applied shear stress. By adding wrap strands, which are represented by pin-connected links, the assemblage will have resistance to an applied shear stress (Figure 7C). This resistance is defined to be the shear stiffness of the wrap and is represented by the following equation:

$$(wG)_{wrap} = \rho\, A_s\, E \sin\phi \cos^2\phi \qquad (20)$$

where $(wG)_{wrap}$ = shear stiffness of the panel of wrap strands

ρ = wrap density

A_s = cross-sectional area of one wrap strand

E = wrap material elastic modulus

ϕ = wrap angle.

The wrap is uniformly distributed along the length of the captive column; therefore, an equivalent width of the wrap panel is obtained by dividing shear stiffness by the shear modulus of the wrap material.

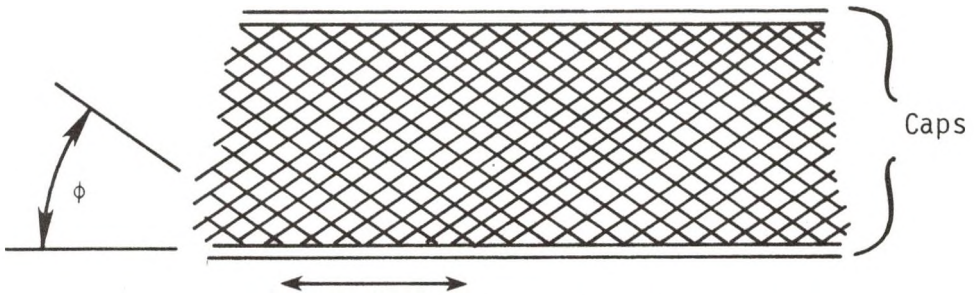

ρ Strands/Inch in Each Helical Direction

A) Captive Column Wrap

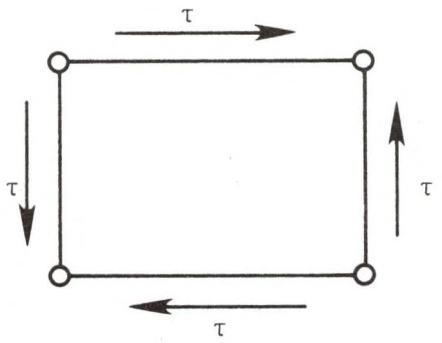

B) Four Pin-Connected Links

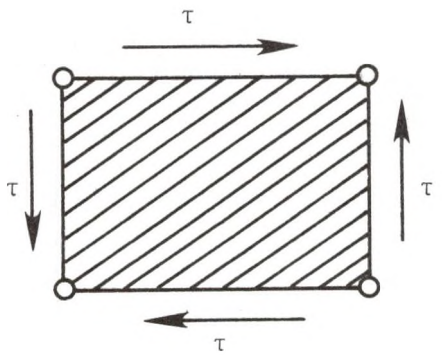

C) Four Pin-Connected Links With Wrap Strands

FIGURE 7 - SHEAR STIFFNESS OF A WRAP PANEL

$$w_{wrap} = \frac{(wG)_{wrap}}{G_{wrap}}$$

$$w_{wrap} = \frac{\rho\ A_s\ E\ \sin\phi\ \cos^2\phi}{G_{wrap}} \qquad (21)$$

Equation (21) represents the equivalent width of one side of wrap strands if there is no wrap pretension. With no pretension, the wrap strands will merely relax under an axial compressive force. For this reason, Figure 7C shows the wrap strands in one direction only. If the pretension is greater than the maximum compressive force that the strands will be subjected to, all of the wrap strands will resist the shear force. This pretension is defined to be the ideal pretension. In this case, the equivalent width will be the width calculated by using equation (21) multiplied by two. Derivation of equations (20) and (21) is found in Appendix B.

The centerpiece and caps are transformed into square regions with areas equivalent to the areas of the actual regions. These transformations are made in order to simplify the determination of the first moment of area. The error introduced by this simplification is negligibly small. The captive column cross-section, before and after the transformations are made, is shown in Figure 8, with the necessary quantities defined below:

D = cap centerline distance

d = cap diameter

t_{panel} = thickness of a core panel

w_{center} = width of the core centerpiece

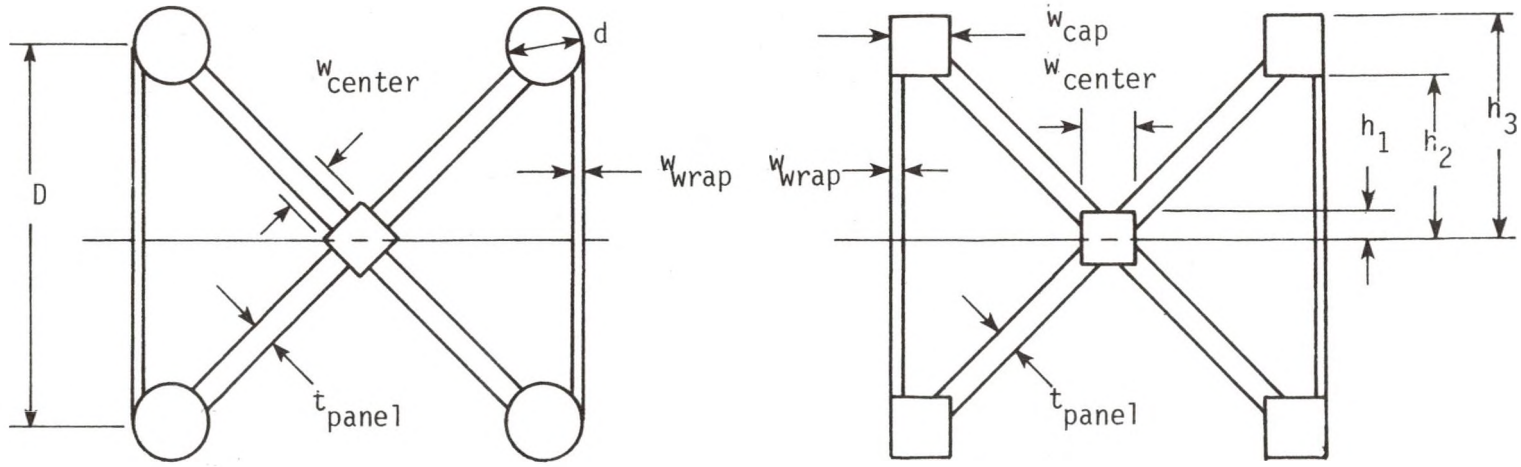

FIGURE 8 - SIMPLIFIED SQUARE CROSS-SECTION

$$w_{cap} = \frac{\sqrt{\pi}\, d}{2} \tag{22}$$

$$h_1 = w_{center}/2 \tag{23}$$

$$h_2 = (D - w_{cap})/2 \tag{24}$$

$$h_3 = (D + w_{cap})/2 \tag{25}$$

The first moment of area for each of the components is shown below. These values were computed using equation (13).

Caps

$$Q(0, h_2) = w_{cap} (h_3^2 - h_2^2) \tag{26}$$

$$Q(h_2, h_3) = w_{cap} (h_3^2 - y^2) \tag{27}$$

Core Panels

$$Q(0, h_1) = \sqrt{2}\, t_{panel}(h_2^2 - h_1^2) \tag{28}$$

$$Q(h_1, h_2) = \sqrt{2}\, t_{panel}(h_2^2 - y^2) \tag{29}$$

$$Q(h_2, h_3) = 0 \tag{30}$$

Core Centerpiece

$$Q(0, h_1) = \frac{w_{center}}{2} (h_1^2 - y^2) \tag{31}$$

$$Q(h_1, h_3) = 0 \tag{32}$$

Wrap

$$Q(0, h_2) = w_{wrap}(h_2^2 - y^2) \tag{33}$$

$$Q(h_2, h_3) = 0 \tag{34}$$

The width of each component, b, is needed for the solution of equation (19). The widths of the caps, core centerpiece, and wrap are given by the following equations.

$$b_{caps} = 2\, w_{cap} \tag{35}$$

$$b_{center} = w_{center} \tag{36}$$

$$b_{wrap} = 2\, w_{wrap} \tag{37}$$

The core panels of the cross-section shown in Figure 8 are oriented at a 45° angle to the neutral plane. The horizontal width of a section is normally used to compute the shear stress. For thin sections, however, the thickness of the section is used to compute the shear stress [4]. For this reason, the following equation is used for the core panels:

$$b_{panels} = 2\, t_{panels} \tag{38}$$

By substituting equations (26) through (38) into equations (18) and (19), three equations for the equivalent first moment of area divided by the equivalent cross-section width are derived. One equation will be derived for each of the following ranges of vertical distance: 1) $0 < y < h_1$, 2) $h_1 < y < h_2$, and 3) $h_2 < y < h_3$.

Since the width of each component is independent of the height for the above three ranges of vertical distance, the incremental area, dA, in equation (17) can be reduced to the following values:

$$dA = \frac{[2(wG)_{wrap} + (wG)_{center}]}{G_{cap}} dy, \text{ for } 0 < y < h_1 \tag{39}$$

$$dA = \frac{[2(wG)_{wrap} + 2\sqrt{2}(tG)_{panels}]}{G_{cap}} dy, \text{ for } h_1 < y < h_2 \qquad (40)$$

$$dA = 2\, w_{cap}\, dy, \text{ for } h_2 < y < h_3 \qquad (41)$$

The shear moduli ratios are again used to obtain an equivalent cross-section composed of the cap material.

Substituting equations (39) through (41) into equation (17), and using the horizontal plane of symmetry, the elastic strain energy due to shear force is computed as follows:

$$U_{shear} = \frac{P^2 L}{8G} \left[\frac{E_{caps}}{(EI)_{eq}}\right]^2 \int_{area} \left(\frac{Q}{b}\right)^2 dA$$

$$U_{shear} = K[J_1 + J_2 + J_3] \qquad (42)$$

where $$K = \frac{P^2 L}{4G_{cap}} \left[\frac{E_{cap}}{(EI)_{eq}}\right]^2$$

$$J_1 = \int_0^{h_1} \left(\frac{Q_{eq}}{b_{eq}}\right)^2 dA$$

$$J_2 = \int_{h_1}^{h_2} \left(\frac{Q_{eq}}{b_{eq}}\right)^2 dA$$

$$J_3 = \int_{h_2}^{h_3} \left(\frac{Q_{eq}}{b_{eq}}\right)^2 dA$$

By substituting the appropriate values into the three integrals and performing the integrations, the following results are obtained:

$$J_1 = c_1[c_2^2 h_1 - \frac{2}{3} c_2 c_3 h_1^3 + \frac{c_3^2}{5} h_1^5] \tag{43}$$

$$J_2 = c_4[c_5^2(h_2 - h_1) - \frac{2}{3} c_5 c_6(h_2^3 - h_1^3) + \frac{c_6^2}{5}(h_2^5 - h_1^5)] \tag{44}$$

$$J_3 = c_7[c_8^2(h_3 - h_2) - \frac{2}{3} c_8 c_9(h_3^3 - h_2^3) + \frac{c_9^2}{5}(h_3^5 - h_2^5)] \tag{45}$$

where $c_1 = \dfrac{1}{G_{cap}[2(wG)_{wrap} + (wG)_{center}]}$

$$c_2 = (h_3^2 - h_2^2)(wG)_{cap} + \sqrt{2}(h_2^2 - h_1^2)(tG)_{panel} + \frac{h_1^2}{2}(wG)_{center} + h_2^2 (wG)_{wrap}$$

$$c_3 = \frac{1}{2}(wG)_{center} + (wG)_{wrap}$$

$$c_4 = \frac{(wG)_{wrap} + \sqrt{2}(tG)_{panel}}{2G_{cap}[(wG)_{wrap} + (tG)_{panel}]^2}$$

$$c_5 = (h_3^2 - h_2^2)(wG)_{cap} + h_2^2[\sqrt{2}(tG)_{panel} + (wG)_{wrap}]$$

$$c_6 = \sqrt{2}(tG)_{panel} + (wG)_{wrap}$$

$$c_7 = \frac{1}{2w_{cap}}$$

$$c_8 = h_3^2 w_{cap}$$

$$c_9 = w_{cap}$$

For the interested reader, the solution of the above integrals can be found in Appendix C.

Beam Stiffness

All of the quantities needed to determine the elastic strain energy stored in the captive column have now been computed. By substituting equations (11) and (42) into equation (3) and simplifying, the following relationship for deflection is obtained:

$$\frac{P\delta}{2} = U_{normal} + U_{shear}$$

$$\frac{P\delta}{2} = \frac{P^2L^3}{96(EI)_{eq}} + \frac{P^2L}{4G_{cap}}\left[\frac{E_{cap}}{(EI)_{eq}}\right]^2 [J_1 + J_2 + J_3]$$

$$\delta = \frac{PL^3}{48\ (EI)_{eq}}\left[1 + \frac{24\ (E_{cap})^2}{L^2 G_{cap}(EI)_{eq}}\ (J_1 + J_2 + J_3)\right] \qquad (46)$$

The first term in the brackets of equation (46) accounts for the deflection due to the bending moment only. If the second term is neglected, equation (1) and equation (46) are equivalent. This is to be expected because the deflection due to shear forces is neglected in the derivation of equation (1).

Beam stiffness is defined to be the amount of force needed to produce a unit of deflection. By dividing the deflection computed by using equation (46) into the applied load, the beam stiffness is found to be:

$$k = \frac{48(EI)_{eq}}{L^3\left[1 + \dfrac{24(E_{cap})^2}{L^2\ G_{cap}\ (EI)_{eq}}\ (J_1 + J_2 + J_3)\right]} \qquad (47)$$

where k = beam stiffness.

The above stiffness was determined by using the equivalent wrap panel width for the case when there is no pretension. If the pretension is sufficiently great to keep all of the wrap strands in tension under the applied load, the stiffness will be increased. To determine this stiffness, replace w_{wrap} in the constant values c_1 through c_6 with $2w_{wrap}$.

As previously noted, equation (47) applies for a square cross-section captive column positioned as shown in Figure 6B. If the captive column is rotated to a different orientation, or if a different cross-section is used, a different value for the elastic strain energy due to shear forces will result. The development of the equations needed to find the elastic strain energy due to shear forces for a square cross-section captive column rotated 45° and for a triangular cross-section captive column can be found in Appendix D. The development begins with equation (17) and follows the same steps used in the development of equation (42). The beam stiffness equations for the above cases can also be found in Appendix D.

Due to the large number of captive columns that were analyzed in this research effort, computer programs for the determination of beam stiffness were written for square and triangular cross-section captive columns. These programs may be found in Appendix E.

There are limitations in the use of equation (46) that should be discussed at this time. The major limitation is that this direct method can only be used to determine the deflection at the location of the applied load. To determine the deflection at other locations,

Castigliano's theorem must be used. This method will be discussed in Chapter 8.

The contribution of the wrap in maintaining the cross-sectional geometry is neglected in the development of equation (46). The wrap decreases the cross-sectional deformation caused by loads that are not applied with a line of action through the centroid of the cross-section. This deformation will lead to an increase in the deflection in the vicinity of the applied load. The computed deflection is the deflection of the cross-section at the neutral axis of the captive column. The deflection of the cross-section at locations other than the neutral axis may not be the same due to the cross-sectional deformation. A further limitation is the fact that a range of stiffness values exists for various wrap pretensions, from the case of no pretension to an ideal pretension.

The above limitations should be considered when using equation (46). The verification of the method of applying classical beam theory which has been presented here will be discussed in Chapter 6.

CHAPTER 3

COMPUTER MODEL

A brief description of a finite element computer model will be given in this chapter. This model, which was developed by Kipp [2], can be used to conduct a complete structural analysis of a captive column under various load conditions. The input data needed to compute beam stiffness will be discussed here in greater detail.

General Computer Model

The computer model uses the Structural Analysis Program (SAP IV), which is a general purpose finite element program [7]. The model uses standard element types and can easily be adapted for use with other commerically available finite element programs.

A number of possible element combinations were considered for the computer model of a captive column. The final model was selected because it is adaptable to a wide variety of captive column geometries, material types, and load conditions while still yielding predictions of captive column behavior that are acceptable for engineering purposes.

Axial-force truss elements, beam elements, and plane stress elements are used in the computer model. The input data required by the SAP IV program for each of the element types is summarized below:

1. Truss element - coordinates of two nodal points (one at each end of the element), elastic modulus, and cross-sectional area,

2. Beam element - coordinates of three nodal points (one at each end of the element and one to define the local coordinate system), elastic modulus, Poisson's ratio, cross-sectional area, and the moments of inertia in the local coordinate system,

3. Plane stress element - coordinates of four nodal points (one at each corner of the element), elastic moduli and Poisson's ratios for the three local coordinate directions of the element, shear modulus, and the element thickness.

By using the correct material and geometrical properties, a wide variety of materials, both isotropic and anisotropic, and cross-sectional shapes can be considered for each of the components of the captive column.

The following paragraphs will give a brief description of the finite element computer model. References [2] and [3] are recommended if a more specific description of the model is desired.

The core of a captive column is modeled by using a series of beam and plane stress elements. Figure 9 shows a portion of a core section for a triangular cross-section captive column. The plane stress element and the two radial beam elements represent a segment of a core panel. The plane stress element is used to represent the in-plane stiffness of the core panel, with the radial beam element used to represent the out-of-plane stiffness. Although the two elements physically occupy the same space in the core panel, the geometrical properties of the beam elements are specified in such a way that there is no addition to the in-plane stiffness of the core panel. These core panel segments are connected to a series of beam elements, which represent the centerpiece of the core.

The caps, shown in Figure 10, are represented by beam elements. The two nodal points used to define the ends of each beam element are also two of the nodal points used for the adjoining core panel segment. By using common nodal points, the cap beam elements are modeled as being rigidly attached to the core panel at these two points.

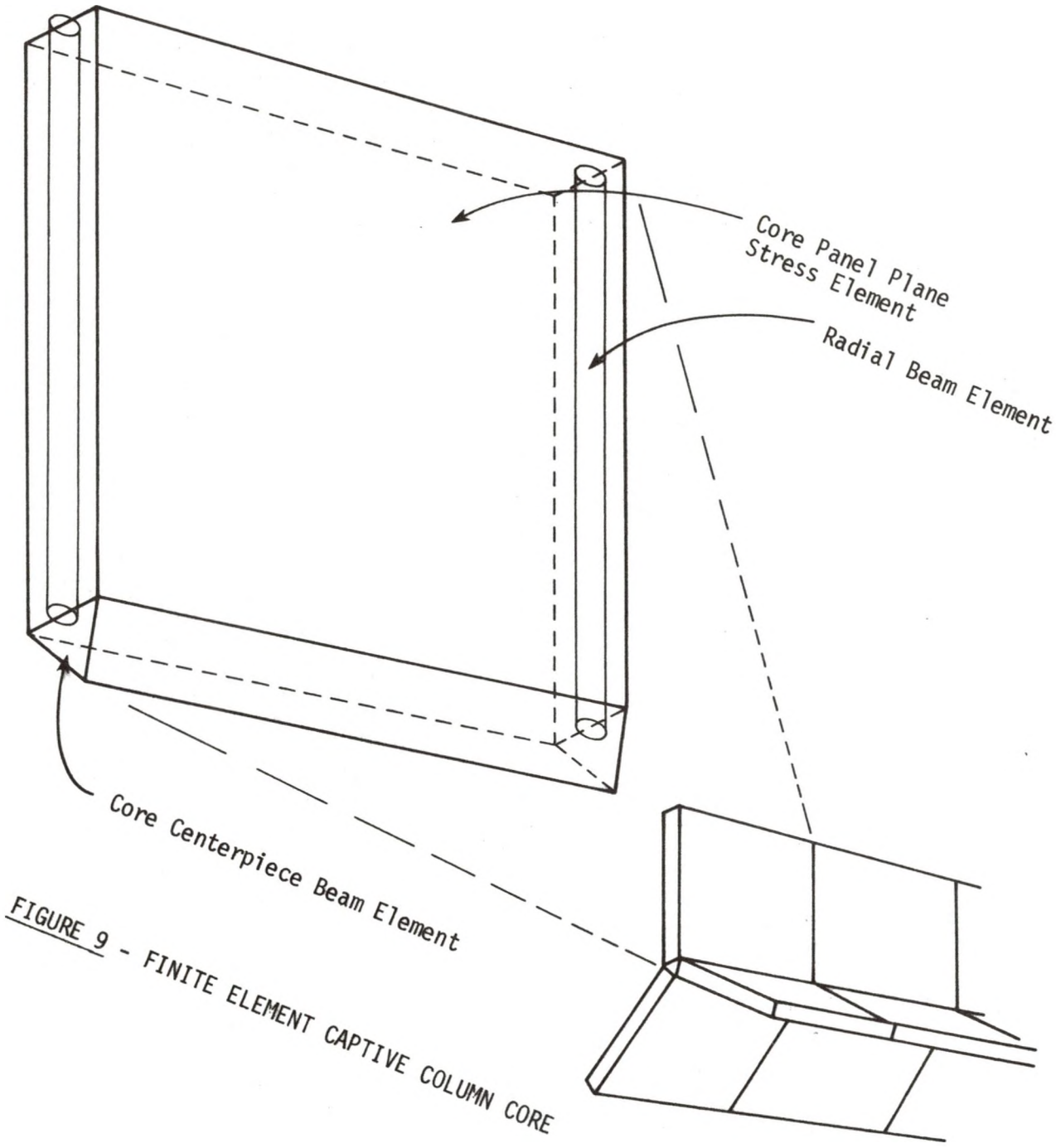

FIGURE 9 - FINITE ELEMENT CAPTIVE COLUMN CORE

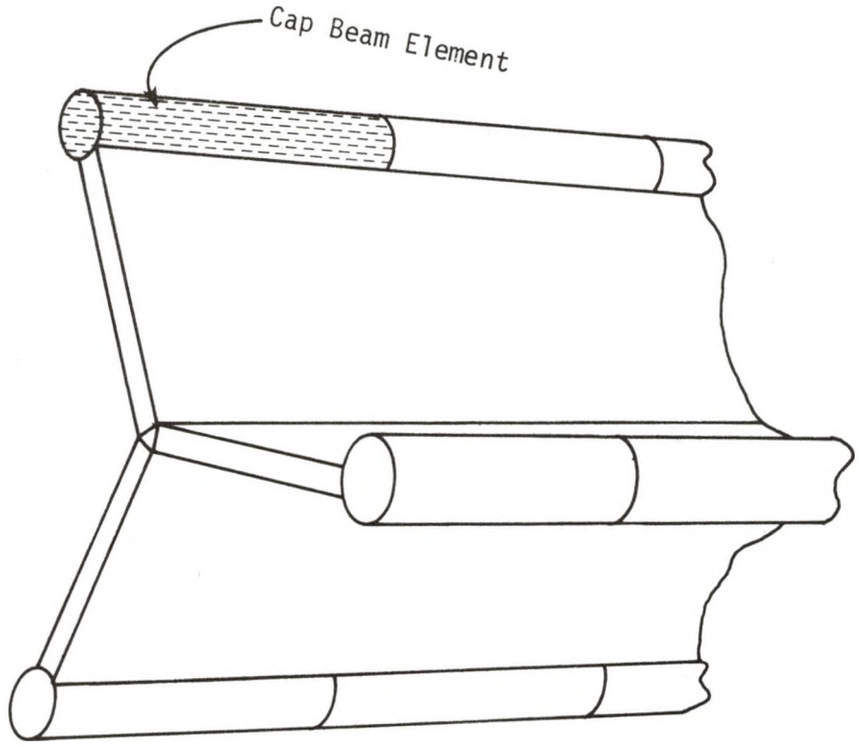

FIGURE 10 - FINITE ELEMENT CAPTIVE COLUMN CAP

Truss elements are used to model the wrap. As shown in Figure 11, a single element is used to model a group of individual strands. This approximation is required in order to reduce the size of the system of equations, thus reducing the computer solution time. This representation of the wrap is not believed to have any significant effect on the structural behavior. The nodal points used to define the truss elements are the same points that are used in defining the cap and core panel elements, thus implying rigid attachment of the wrap to the caps. Any wrap angle can be modeled by varying the location of these nodal points along the length of the captive column model.

The wrap strands in a captive column cannot carry compressive loads. The truss elements used to represent a group of wrap strands can carry both tensile and compressive loads, and therefore, a method was devised to identify the truss elements that are subjected to compressive loads. The truss elements so identified are then assigned a very small elastic modulus, which in effect, removes them from the model. This method requires a multi-step process which consists of identifying elements that are carrying a compressive load and then assigning the low modulus to these elements. This process is repeated until all of the wrap elements in the model are either carrying a tensile load or have been assigned the low modulus.

To reduce the amount of relaxation of the wrap strands upon the application of a load, pretension can be applied to the wrap strands during construction. This wrap pretension can be modeled in the wrap truss elements of the computer model by using the thermal stress capabilities of SAP IV. Any degree of pretension can be modeled by properly assigning the nodal point temperatures, the truss element zero

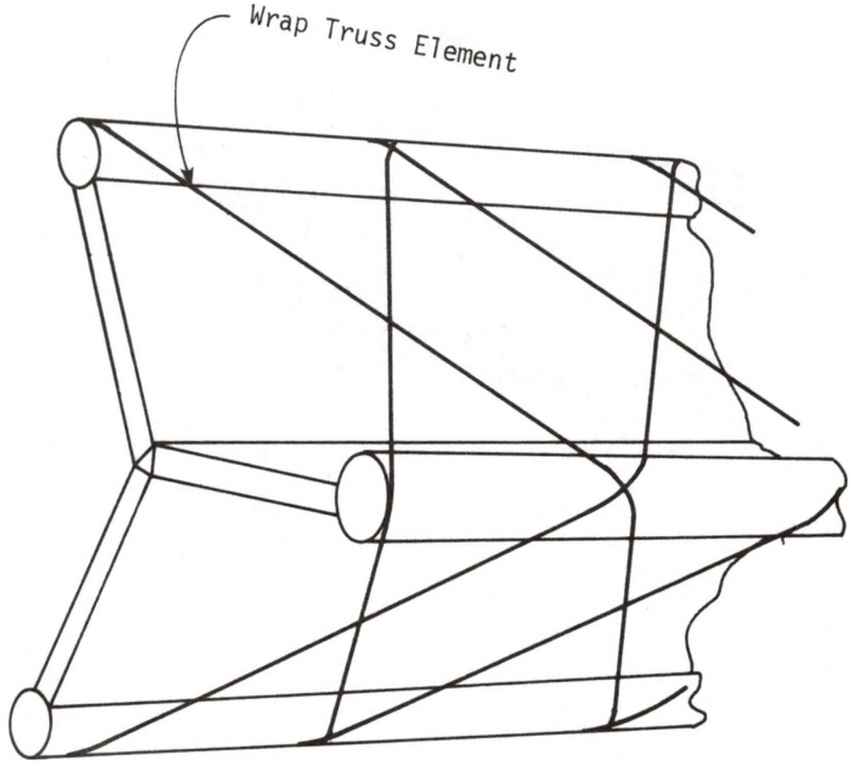

FIGURE 11 - FINITE ELEMENT CAPTIVE COLUMN WRAP

stress temperature, and the truss element coefficient of thermal expansion. The use of thermal stress to model wrap pretension will be examined in greater detail in Chapter 7.

After the nodal point coordinates and the required information for each of the element groups have been specified, a wide variety of load conditions can be investigated by properly assigning boundary conditions and the magnitude and location of external forces and moments. When symmetry in the captive column geometry and the load condition exists, the correct assignment of boundary conditions will enable the user to obtain the desired information by modeling a portion of the captive column. The output from the SAP IV program consists of displacements, both translational and rotational, for all of the nodal points and stress information for all of the elements.

Simple-Supported Beam

A vertical transverse plane of symmetry exists through the midspan of a simple-supported beam with a concentrated midspan load. The captive columns under consideration have a constant cross-section along the longitudinal axis. By using the symmetry of the load condition and the captive column geometry, the analysis using the full captive column can be reduced to an analysis using one half of the captive column (see Figure 12). The boundary conditions at the midspan are specified in such a way that the nodal points in the vertical transverse plane can not translate in the axial direction or rotate about the axis normal to the plane of the paper. This reduced model will result in a reduction in the size of the system of equations, thus decreasing the computer solution time.

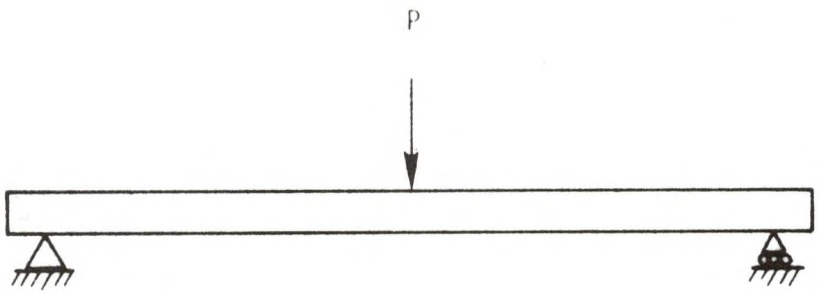

A) Full Beam Analysis

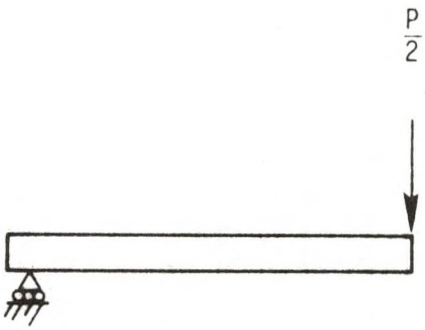

B) Half Beam Analysis

FIGURE 12 - SIMPLE-SUPPORTED BEAM WITH CONCENTRATED MIDSPAN LOAD

An example of the nodal point numbering scheme for a square cross-section captive column is shown in Figure 13, with the boundary conditions and applied forces necessary to model the load condition of Figure 12A listed in the lower, right-hand corner. The boundary conditions specify that there is no vertical translation of the bottom two cap beam element nodal points, nodes 6 and 9, at the support end of the captive column. The applied load, P, is reduced by a factor of two to account for the symmetry of loading. This reduced load is equally divided between the top two cap beam element nodal points, nodes 62 and 63, at the midspan of the captive column. These boundary conditions at the support and the division of the load between two nodal points represent the support and load configuration of the physical testing of square captive columns that was done in this research effort. The following chapter will give specific information concerning the end supports and the loading apparatus for square and triangular cross-section captive columns.

The numbering scheme shown in Figure 13 is an example of a possible configuration. The total number of nodal points and elements will depend upon the length of the span and the wrap angle.

As defined in Chapter 2, the beam stiffness is determined by dividing the applied load by the deflection at the location and in the direction of the applied load. The total load, P, that is being modeled, not the reduced load, P/4, should be used in the determination of the beam stiffness.

The computer model, unlike the previously developed theoretical approach, will yield information concerning the distortion of the cross-section due to the applied load. For the square cross-section captive

Note: Nodal points on the neutral axis, which are numbered in multiples of 5, from 5 through 65, are not shown.

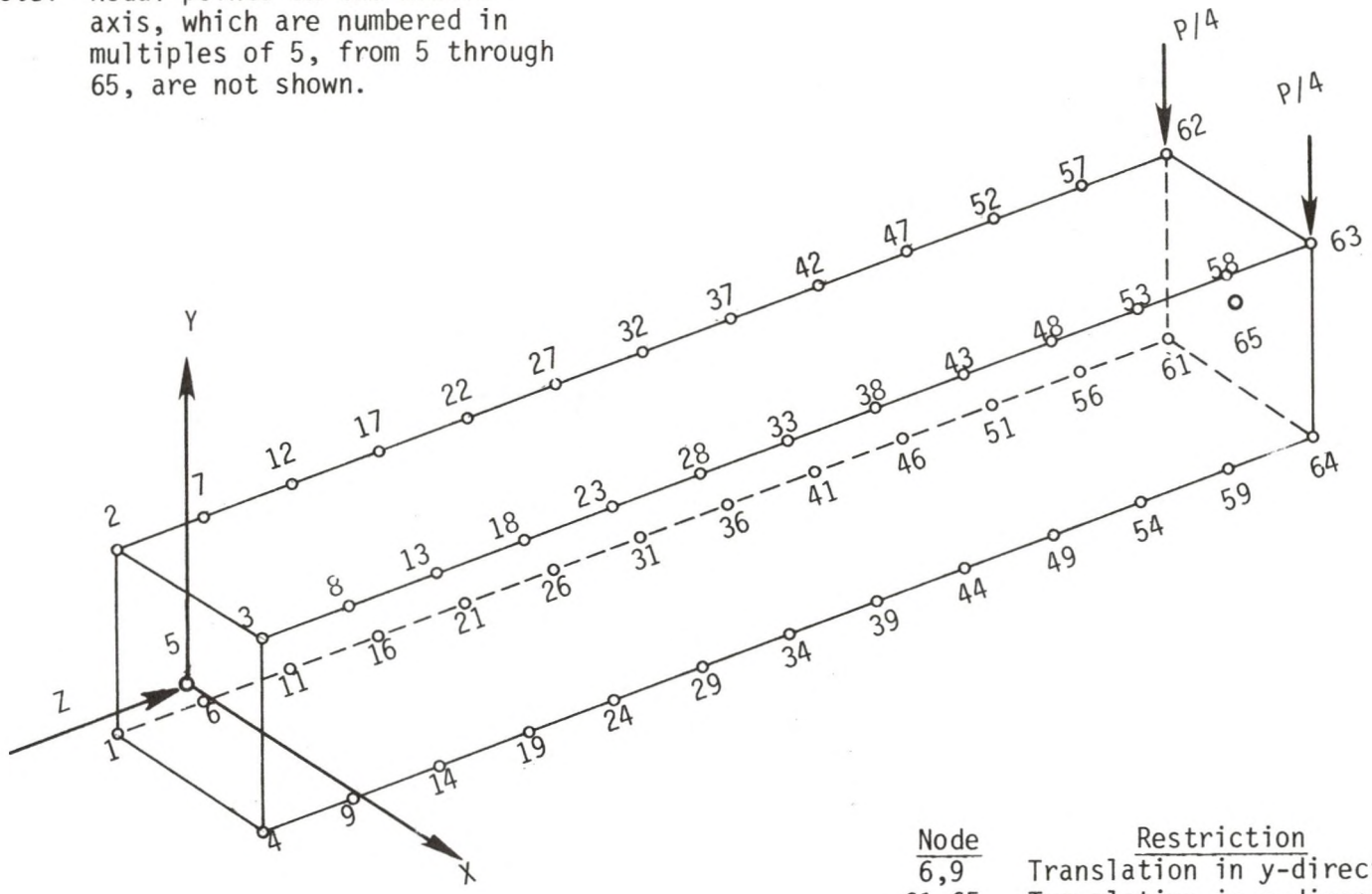

Node	Restriction
6,9	Translation in y-direction
61-65	Translation in z-direction
	rotation about x-axis

FIGURE 13 - NODE NUMBERING FOR A SQUARE CROSS-SECTION CAPTIVE COLUMN

column shown in Figure 13, four stiffness values may be computed depending upon which of the following four deflections is used: 1) the deflection of the top cap nodal points (nodes 62 and 63), 2) the deflection of the centerpiece nodal point (node 65), 3) the deflection of the bottom cap nodal points (nodes 61 and 64), or 4) an average value. Any difference between the four stiffness values will depend upon the amount of cross-sectional deformation. The computer model also yields the deflection of any nodal point within the model.

CHAPTER 4

TEST SPECIMENS AND PHYSICAL TESTING

Forty-eight captive columns were constructed and tested during the various phases of this research effort. A description of each captive column will be given in this chapter, along with a brief description of the physical testing that was used to obtain beam stiffness values for the captive columns.

Captive Column Test Specimens

All of the captive columns that were built and tested in this research effort had either a square or triangular cross-section that was constant along the length of the member. These captive columns were tested in order to determine whether the analytical approach and/or the computer model yield adequate predictions of beam stiffness. Identification of the effects of the various design parameters on stiffness was accomplished by holding all of the parameters constant except the parameter under consideration.

All of the test specimens were built and tested in the Structures Laboratory, which is located in Upson Hall at the University of North Dakota. Construction of the core assembly and attachment of the caps was done strictly by hand. A semi-automated wrapping machine was used to apply the helically wound wrap. Structural adhesives were used to bond the various components together.

The physical dimensions and materials used for all of the test specimens are listed in Table 1. The physical properties for all of the materials are listed in Table 2. When balsa wood was used as the core

TABLE 1

DIMENSIONAL PROPERTIES

Captive Column Number	Core Panel Thickness (in), Material	Core Centerpiece Width (in), Material	Cap Diameter (in), Material	Wrap Density (strands/in), Diameter (in), Wrapping Tension (lbs), Angle (degrees)	Distance Between Cap Centers (in)
1	3/16,BW	3/16,DF	1/8,FRP	32.0,0.0054,low,45	1.250
2	3/16,BW	3/16,DF	1/4,FRP	34.6,0.0054,low,45	1.156
3	3/16,BW	3/16,DF	1/8,ST	32.1,0.0054,low,45	1.246
4	3/16,BW	3/16,DF	1/4,ST	34.2,0.0054,low,45	1.168
5	3/16,BW	3/16,DF	1/8,FRP	21.4,0.0054,low,45	1.865
6	3/16,BW	3/16,DF	1/4,FRP	22.5,0.0054,low,45	1.781
7	3/16,BW	3/16,DF	1/8,ST	21.2,0.0054,low,45	1.885
8	3/16,BW	3/16,DF	1/4,ST	22.6,0.0054,low,45	1.767
9	3/16,ACR	3/16,ACR	1/8,FRP	29.8,0.0054,low,45	1.344
10	3/16,ACR	3/16,ACR	1/8,ST	30.1,0.0054,low,45	1.328
11	3/16,ACR	3/16,ACR	1/4,ST	22.2,0.0054,low,45	1.805
12	1/4,BW	1/4,DF	3/8,FRP	16.1,0.0054,med,45	3.719
13	1/4,BW	3/4,DF	3/8,FRP	16.4,0.0054,med,45	3.660
14	1/4,BW	1/4,DF	1/2,FRP	16.6,0.0054,med,45	3.613
15	1/4,BW	3/4,DF	1,2/FRP	16.5,0.0054,med,45	3.633
16	3/8,BW	1,DF	3/8,FRP	14.3,0.0076,med,45	7.000
17	5/16,BW	1,DF	1/2,FRP	13.8,0.0132,med,45	7.223
18	3/8,BW	1,DF	1/2,ST	14.2,0.0132,high,45	7.078
19	3/16,ACR	5/8,ACR	1/2,ST	11.8,0.0132,high,45	6.790
20	3/8,BW	1,DF	1/2,FRP	13.3,0.0132,high,45	10.062

TABLE 1 (Continued)

Captive Column Number	Core Panel Thickness (in), Material	Core Centerpiece Width (in), Material	Cap Diameter (in), Material	Wrap Density (strands/in), Diameter (in), Wrapping Tension (lbs), Angle (degrees)	Distance Between Cap Centers (in)
21	3/8,BW	1,DF	1/2,ST	13.2,0.0132,high,45	10.092
22	1/2,BW	1-1/8,DF	1/2,ST	11.3,0.0132,high,45	8.880
23	1/2,BW	1-1/8,DF	1/2,ST	11.0,0.0132,high,45	9.094
24	1/2,BW	1-1/8,DF	5/8,ST	13.3,0.0132,high,45	10.062
25	3/16,BW	5/8,DF	3/8,ST	No Wrap	3.188
26	3/16,BW	5/8,DF	3/8,ST	6.3,0.0076,1.5,45	3.180
27	3/16,BW	5/8,DF	3/8,ST	18.9,0.0076,0.75,45	3.180
28	3/16,BW	5/8,DF	3/8,ST	18.9,0.0076,1.5,45	3.180
29	3/16,BW	5/8,DF	3/8,ST	18.9,0.0076,4.0,45	3.172
30	3/16,BW	5/8,DF	3/8,ST	37.8,0.0076,1.5,45	3.172
31	3/16,BW	5/8,DF	3/8,ST	63.2,0.0076,1.5,45	3.164
32	3/8,BW	1,DF	1/2,ST	17.7,0.0076,4.0,60	3.711
33	3/8,BW	1,DF	1/2,ST	18.3,0.0076,4.0,45	3.711
34	3/8,BW	1,DF	1/2,ST	15.6,0.0076,4.0,30	3.711
35	3/8,BW	1,DF	1/2,ST	17.6,0.0076,4.0,60	3.750
36	3/8,BW	1,DF	1/2,ST	18.1,0.0076,4.0,45	3.750
37	3/8,BW	1,DF	1/2,ST	15.4,0.0076,4.0,30	3.750
38	1/4,BW	3/4,DF	3/8,ST	2.5,0.0132,1.5,45	4.000
39	1/4,BW	3/4,DF	3/8,ST	2.5,0.0132,4.5,45	4.000
40	1/4,BW	3/4,DF	3/8,ST	2.5,0.0132,6.0,45	4.000

TABLE 1 (Continued)

Captive Column Number	Core Panel Thickness (in), Material	Core Centerpiece Width (in), Material	Cap Diameter (in), Material	Wrap Density (strands/in), Diameter (in), Wrapping Tension (lbs), Angle (degrees)	Distance Between Cap Centers (in)
41	1/4,BW	3/4,DF	3/8,ST	7.5,0.0132,1.5,45	4.000
42	1/4,BW	3/4,DF	3/8,ST	7.5,0.0132,4.5,45	4.000
43	1/4,BW	3/4,DF	3/8,ST	7.5,0.0132,6.0,45	4.000
44	1/4,BW	3/4,DF	3/8,ST	15.0,0.0132,1.5,45	4.000
45	1/4,BW	3/4,DF	3/8,ST	15.0,0.0132,4.5,45	4.000
46	1/4,BW	3/4,DF	3/8,ST	15.0,0.0132,6.0,45	4.000
47	3/8,BW	1,DF	3/8,ST	7.5,0.0132,4.5,45	4.000
48	1/2,BW	1-1/8,DF	3/8,ST	7.5,0.0132,4.5,45	4.000

Captive columns numbered 1-4, 9-19, 22, 23, 25-48 have square cross-sections
Captive columns numbered 5-8, 20, 21, 24 have triangular cross-sections

Legend
BW - balsa wood
ACR - acrylic
DF - Douglas fir
FRP - fiberglass reinforced polyester
ST - steel

TABLE 2

MATERIAL PROPERTIES

Material	Cap		Core Panel		Centerpiece	Wrap
	Steel	FRP	Balsa Wood	Acrylic Sheet	Douglas Fir	Kevlar 49, Type 965
Modulus of Elasticity (psi)	30×10^6	6×10^6	E_n 13,400 E_s 400,000 E_t 13,400	450,000	E_n 71,000 E_s 1.2×10^6 E_t 71,000	18×10^6
Shear Modulus (psi)	11.5×10^6	1×10^6	18,000	173,076	85,000	---
Poisson's Ratio	0.3	---	μ_{ns} 0.3 μ_{nt} 0.3 μ_{st} 0.04	0.3	μ_{ns} 0.35 μ_{nt} 0.35 μ_{st} 0.02	---
Weight (lb/in^3)	0.282	0.072	0.0041	0.043	0.018	0.056

panel material, the grain of the wood was directed radially outward from the centerpiece. The wood was oriented in this way so that the core panels could resist the compressive force applied to the core assembly during the wrapping operation.

The beam stiffness of a captive column is dependent, to a certain degree, upon the amount of wrap pretension. This pretension is applied to the wrap while it is being wound onto the captive column. The tension value listed in Table 1 is the tension in the wrap strands during the winding operation. In Chapter 6, it will be shown that the pretension of the wrap on the captive column is less than this wrapping tension. It was difficult initially to monitor and control the amount of tension in the wrap strands during the wrapping operation. The lack of control over the wrapping tension necessitated the use of a subjective value (low, medium, or high) for approximately half of the test specimens. Improvements in the wrapping machine allowed for better control of the tension applied to each wrap strand. A numerical value is listed in Table 1 for specimens built after these improvements were made.

Test Apparatus

All of the captive columns were loaded as simple-supported beams with a concentrated midspan load. The wide variation in specimen length required the use of two test set-ups. The test set-up used for specimens under thirty inches in length is shown in Figure 14. A hydraulic testing machine, Versa Tester Model 30M, was used to apply the load. The load measurement device was a Lebow 1K load cell with a Vishay Ellis digital strain indicator. A Soil-Test dial indicator was used to measure the deflection of the loading platen.

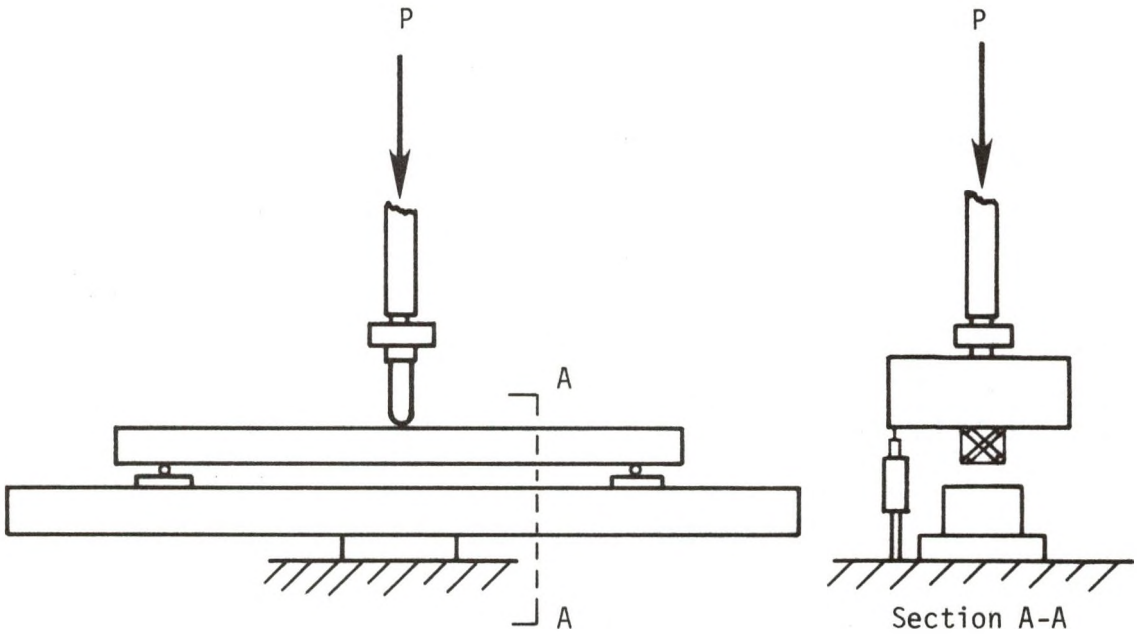

FIGURE 14 - TEST CONFIGURATION FOR SMALL CAPTIVE COLUMNS

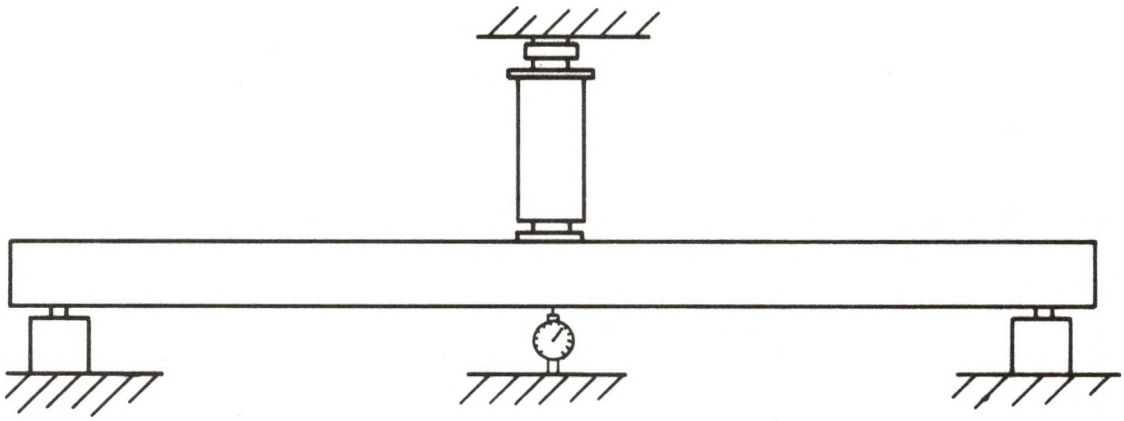

FIGURE 15 - TEST CONFIGURATION FOR LARGE CAPTIVE COLUMNS

An Enerpac hydraulic ram and hand pump were used to apply the load to specimens over thirty inches in length, see Figure 15. The load cell and strain indicator described above were used to measure the applied load. Soil-Test dial indicators were used to measure the deflection of the top and/or bottom caps at midspan.

When square cross-section captive columns were tested, a narrow steel bar was placed between the loading device and the specimen, see Figure 16A. By doing this, the applied load was equally divided between the two upper caps. The captive columns were supported at the two ends by narrow steel bars in contact with the two lower caps.

Two methods of load distribution were used for triangular cross-section captive columns. When the specimen was tested with an apex down, Figure 16B, the method described above was used. Rigid frames were used to support the three caps at each end of the specimen, see Figure 16C. When the specimen was tested with an apex up, Figure 16D, a rigid frame was used to distribute the load between the three caps. Narrow steel bars were used as end supports for the two lower caps.

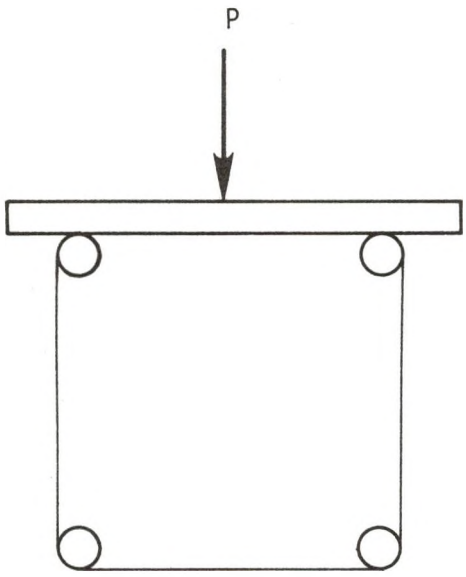

A) Load Distribution, Square Cross-Section

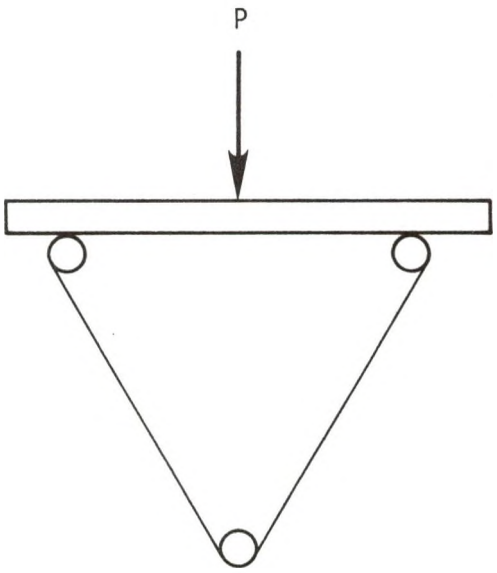

B) Load Distribution, Triangular Cross-Section (Apex Down)

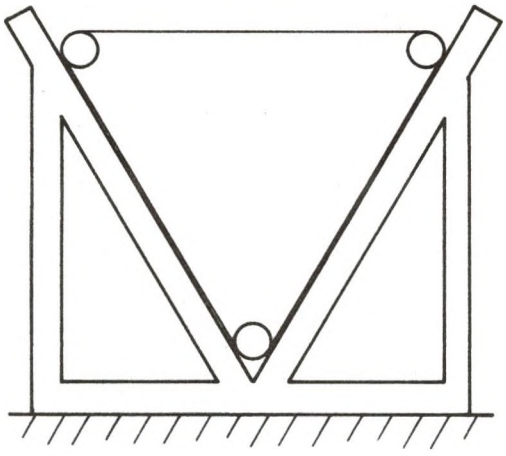

C) End Support, Triangular Cross-Section

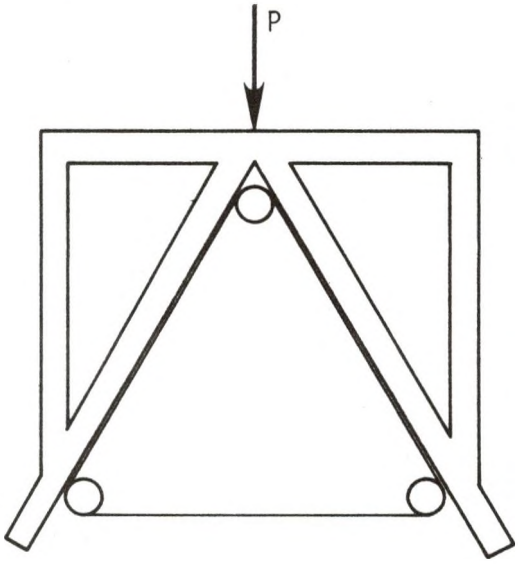

D) Load Distribution, Triangular Cross-Section (Apex Up)

FIGURE 16 - LOAD DISTRIBUTIONS AND END SUPPORTS

CHAPTER 5

RESULTS

The beam stiffness values determined experimentally will be presented in this chapter, along with the test procedure used to obtain these results. The analytical approach developed in Chapter 2 and the computer model described in Chapter 3 were used to predict beam stiffness values for the physical test specimens. These values are also presented in this chapter.

Experimental Results

Each of the captive columns listed in Table 1 was tested using one of the test set-ups described in the previous chapter. Approximately one half of the captive columns were tested more than once, using either a different test span or, in the case of triangular cross-section specimens, a different angular orientation of the specimen (apex up versus apex down).

The data collected for each test consisted of a change in deflection for a change in load, rather than absolute deflection for an absolute load. A small initial load, varying from twenty pounds for small specimens to one hundred pounds for large specimens, was applied and measurements were made relative to this point. This initial load was applied to ensure that the steel bars or rigid frames used to distribute the load or as end supports were in full contact with the caps.

The experimental data proved to be quite linear in nature. The general linear model (GLM) method was used to compute the equation of the best fit straight line for each of the tests:

$$\Delta_{deflection} = m(\Delta_{load}) + a \tag{48}$$

where $\Delta_{deflection}$ = change in deflection

Δ_{load} = change in load

m = slope of the best fit line

a = zero intercept of the best fit line.

The value of the zero-intercept, for virtually all of the tests, was statistically insignificant. The beam stiffness is determined by taking the reciprocal of the slope:

$$k = \frac{1}{m} = \frac{\Delta_{load}}{\Delta_{deflection}} \tag{49}$$

To ensure repeatability of the tests, data was obtained for at least two load cycles for each specimen. In some cases, the test specimen was rotated about its axis (90 degrees for square cross-sections and 120 degrees for triangular cross-sections) and the tests were repeated. This was done to yield information concerning the symmetry of the cross-section. The results of these multiple tests indicated that the structural response was repeatable and that the captive columns tested were very close to being symmetric. The results presented here are based on all of the data that was collected for each set of tests.

The experimentally determined beam stiffness values can be found in Table 3, along with the values predicted by the analytical approach and the computer model. For tests done on triangular cross-section captive columns, a triangle is drawn next to the captive column number. This triangle indicates the orientation, apex up or apex down, of the captive column for that test. Due to distortion of the cross-section during loading, the deflection was not the same for all of the caps at the

TABLE 3

BEAM STIFFNESS VALVES

Test Number	Captive Column Number	Span (in)	Gage Point	Beam Stiffness (lbs/in)				
				Experimental	Analytical		Computer Model	
					No Pretension	Ideal Pretension	No Pretension	Ideal Pretension
1	1	26.5	TC	381	270	279	257	281
2	1	21.7	TC	515	469	492	436	496
3	1	16.9	TC	909	911	979	805	981
4	2	26.5	TC	817	807	880	676	837
5	2	21.7	TC	1290	1330	1500	1060	1400
6	2	16.9	TC	2140	2370	2810	1740	2540
7	3	26.5	TC	760	1030	1170	822	1090
8	3	21.7	TC	1160	1630	1930	1220	1760
9	3	16.9	TC	1770	2740	3450	1890	3010
10	4	26.5	TC	1690	2260	2930	1550	2510
11	4	21.7	TC	2330	3210	4400	2170	3690
12	4	16.9	TC	3640	4760	6890	3810	5690
13	5-Δ	28.0	AVG	293	238	247	244	264
14	6-Δ	28.0	AVG	681	701	787	678	821
15	7-Δ	28.0	AVG	757	858	1000	823	1050
16	8-Δ	28.0	AVG	1460	1620	2180	1540	2350
17	9	28.0	TC	439	358	359	372	379
18	10	28.0	TC	1250	1350	1370	1240	1300
19	11	28.0	TC	5660	6630	6900	4270	5120
20	12	50.8	BC	2090	1720	2000	1520	2000
21	13	50.8	BC	1980	1840	2100	1510	1970
22	14	50.8	BC	3950	2250	2730	1900	2650
23	15	50.8	BC	3000	2530	3020	1940	2690

TABLE 3 (Continued)

Test Number	Captive Column Number	Span (in)	Gage Point	Beam Stiffness (lbs/in)				
				Experimental	Analytical		Computer Model	
					No Pretension	Ideal Pretension	No Pretension	Ideal Pretension
24	16	216.0	BC	173	147	149	145	150
25	16	187.2	BC	266	221	226	217	228
26	16	158.4	BC	429	352	363	344	367
27	16	129.6	BC	750	609	636	589	646
28	16	100.8	BC	1450	1170	1250	1110	1280
29	17	216.0	BC	303	276	283	266	284
30	17	187.2	BC	465	416	428	398	432
31	17	158.4	BC	734	664	692	626	701
32	17	129.6	BC	1310	1150	1220	1060	1240
33	17	100.8	BC	2330	2210	2420	1970	2510
34	18	216.0	BC	1150	1120	1220	966	1190
35	18	187.2	BC	1680	1610	1800	1350	1750
36	18	158.4	BC	2550	2410	2780	1940	2680
37	18	129.6	BC	3980	3780	4580	2900	4380
38	18	100.8	BC	6760	6300	8150	4540	7710
39	19	216.0	BC	1140	1160	1190	1110	1170
39	19	216.0	TC	1100	1160	1190	1070	1150
40	19	187.2	BC	1650	1720	1780	1620	1740
40	19	187.2	TC	1580	1720	1780	1530	1690
41	19	158.4	BC	2550	2670	2800	2470	2720
41	19	158.4	TC	2390	2670	2800	2280	2590
42	19	129.6	BC	4140	4430	4720	3980	4560
42	19	129.6	TC	3740	4430	4720	3510	4210
43	19	100.8	BC	7530	7980	8730	6860	8330
43	19	100.8	TC	6460	7980	8730	5580	7230

TABLE 3 (Continued)

Test Number	Captive Column Number	Span (in)	Gage Point	Beam Stiffness (lbs/in)				
				Experimental	Analytical		Computer Model	
					No Pretension	Ideal Pretension	No Pretension	Ideal Pretension
44	20-▽	200.0	BC	402	326	333	328	347
44	20-▽	200.0	TC	371	326	333	317	339
45	20-△	200.0	AVG	391	326	333	321	343
46	20-▽	160.0	BC	761	603	623	611	665
46	20-▽	160.0	TC	693	603	623	574	639
47	20-△	160.0	AVG	709	603	623	592	651
48	20-▽	120.0	BC	1620	1284	1356	1320	1520
48	20-▽	120.0	TC	1350	1284	1356	1160	1390
49	20-△	120.0	AVG	1540	1284	1356	1240	1450
50	21-▽	200.0	BC	1410	1320	1480	1210	1490
50	21-▽	200.0	TC	1300	1320	1480	1130	1410
51	21-△	200.0	AVG	1370	1320	1480	1160	1440
52	21-▽	160.0	BC	2390	2230	2620	2010	2680
52	21-▽	160.0	TC	2100	2230	2620	1790	2440
53	21-△	160.0	AVG	2310	2230	2620	1890	2520
54	21-▽	120.0	BC	4720	4120	5190	3620	5450
54	21-▽	120.0	TC	3660	4120	5190	2980	4570
55	21-△	120.0	AVG	4150	4120	5190	3240	4840
56	22	117.6	BC	6930	6210	7810	4740	7380
57	23	117.6	BC	7030	6350	8010	4830	7560
57	23	117.6	TC	6240	6350	8010	4160	6660
58	24-▽	120.0	BC	6360	5360	6960	4680	7190
58	24-▽	120.0	TC	5240	5360	6960	3970	6130
59	24-△	120.0	AVG	5720	5360	6960	4250	6450
60	25	54.0	BC	1270	1400		1080	

TABLE 3 (Continued)

Test Number	Captive Column Number	Span (in)	Gage Point	Beam Stiffness (lbs/in) Experimental	Analytical No Pretension	Analytical Ideal Pretension	Computer Model No Pretension	Computer Model Ideal Pretension
60	25	54.0	TC	1030	1400		879	
61	26	54.0	BC	2240	2180	2850	1620	2520
61	26	54.0	TC	1980	2180	2850	1520	2380
62	27	54.0	BC	2830	3430	4720	2300	4260
62	27	54.0	TC	2460	3430	4720	2170	4030
63	28	54.0	BC	3360	3430	4720	2300	4260
63	28	54.0	TC	2910	3430	4720	2170	4030
64	29	54.0	BC	3460	3420	4710	2300	4240
64	29	54.0	TC	2820	3420	4710	2170	4020
65	30	54.0	BC	4540	4710	6220	2950	5740
65	30	54.0	TC	3760	4720	6220	2780	5460
66	31	54.0	BC	5340	5800	7250	3490	6830
66	31	54.0	TC	4400	5800	7250	3280	6520
67	32	48.0	BC	7230	6430	8330	4320	6600
67	32	48.0	TC	6990	6430	8330	4110	6320
68	33	48.0	BC	8240	7760	10600	5110	8480
68	33	48.0	TC	7370	7760	10600	4660	7790
69	34	48.0	BC	9010	7460	10100	4940	7910
69	34	48.0	TC	7410	7460	10100	4350	7010
70	35	48.0	BC	7030	6460	8380	4360	6640
70	35	48.0	TC	6520	6460	8380	4140	6350
71	36	48.0	BC	8260	7780	10600	5150	8570
71	36	48.0	TC	7340	7780	10600	4700	7860
72	37	48.0	BC	8620	7470	10100	4990	8020
72	37	48.0	TC	7370	7470	10100	4380	7090

TABLE 3 (Continued)

Test Number	Captive Column Number	Span (in)	Gage Point	Beam Stiffness (lbs/in)				
				Experimental	Analytical		Computer Model	
					No Pretension	Ideal Pretension	No Pretension	Ideal Pretension
73	38	88.0	BC	1410	1540	1850	1200	1640
73	38	88.0	TC	1340	1540	1850	1130	1560
74	38	72.0	BC	1980	2170	2700	1650	2360
74	38	72.0	TC	1850	2170	2700	1530	2210
75	38	56.0	BC	2900	3190	4100	2380	3560
75	38	56.0	TC	2610	3190	4100	2140	3230
76	39	88.0	BC	1550	1540	1850	1200	1640
76	39	88.0	TC	1490	1540	1850	1130	1560
77	39	72.0	BC	2170	2170	2700	1650	2360
77	39	72.0	TC	2090	2170	2700	1530	2210
78	39	56.0	BC	3300	3190	4100	2380	3560
78	39	56.0	TC	3120	3190	4100	2140	3230
79	40	88.0	BC	1740	1540	1850	1200	1640
79	40	88.0	TC	1690	1540	1850	1130	1560
80	40	72.0	BC	2500	2170	2700	1650	2360
80	40	72.0	TC	2410	2170	2700	1530	2210
81	40	56.0	BC	3700	3190	4100	2380	3560
81	40	56.0	TC	3470	3190	4100	2140	3230
82	41	88.0	BC	1690	2080	2540	1560	2340
82	41	88.0	TC	1600	2080	2540	1490	2250
83	41	72.0	BC	2450	3120	3990	2230	3620
83	41	72.0	TC	2280	3120	3990	2080	3420
84	41	56.0	BC	3590	4890	6670	3320	5950
84	41	56.0	TC	3290	4890	6670	3010	5430

TABLE 3 (Continued)

Test Number	Captive Column Number	Span (in)	Gage Point	Beam Stiffness (lbs/in)				
				Experimental	Analytical		Computer Model	
					No Pretension	Ideal Pretension	No Pretension	Ideal Pretension
85	42	88.0	BC	2100	2080	2540	1560	2340
85	42	88.0	TC	2020	2080	2540	1490	2250
86	42	72.0	BC	3270	3120	3990	2230	3620
86	42	72.0	TC	3140	3120	3990	2080	3420
87	42	56.0	BC	5100	4890	6670	3320	5950
87	42	56.0	TC	4730	4890	6670	3010	5430
88	43	88.0	BC	2220	2080	2540	1560	2340
88	43	88.0	TC	2150	2080	2540	1490	2250
89	43	72.0	BC	3480	3120	3990	2230	3620
89	43	72.0	TC	3350	3120	3990	2080	3420
90	43	56.0	BC	5500	4890	6670	3320	5950
90	43	56.0	TC	5120	4890	6670	3010	5430
91	44	88.0	BC	2000	2540	2960	1890	2810
91	44	88.0	TC	1930	2540	2960	1800	2720
92	44	72.0	BC	2950	3990	4900	2780	4580
92	44	72.0	TC	2870	3990	4900	2600	4360
93	44	56.0	BC	4590	6670	8770	4280	8080
93	44	56.0	TC	4450	6670	8770	3880	7400
94	45	88.0	BC	2590	2540	2960	1890	2810
94	45	88.0	TC	2560	2540	2960	1800	2720
95	45	72.0	BC	4230	3990	4900	2780	4580
95	45	72.0	TC	4020	3990	4900	2600	4360
96	45	56.0	BC	7260	6670	8770	4280	8080
96	45	56.0	TC	7080	6670	8770	3880	7400

TABLE 3 (Continued)

Test Number	Captive Column Number	Span (in)	Gage Point	Beam Stiffness (lbs/in)				
				Experimental	Analytical		Computer Model	
					No Pretension	Ideal Pretension	No Pretension	Ideal Pretension
97	46	88.0	BC	2560	2540	2960	1890	2810
97	46	88.0	TC	2430	2540	2960	1800	2720
98	46	72.0	BC	4240	3990	4900	2780	4580
98	46	72.0	TC	4000	3990	4900	2600	4360
99	46	56.0	BC	7160	6670	8770	4280	8080
99	46	56.0	TC	6450	6670	8770	3880	7400
100	47	88.0	BC	2460	2460	2770	1990	2520
100	47	88.0	TC	2400	2460	2770	1910	2440
101	47	72.0	BC	3840	3840	4470	2970	3980
101	47	72.0	TC	3660	3840	4770	2790	3790
102	47	56.0	BC	6320	6350	7750	4630	6680
102	47	56.0	TC	5800	6350	7750	4220	6160
103	48	88.0	BC	2440	2460	2780	1950	2500
103	48	88.0	TC	2350	2460	2780	1880	2430
104	48	72.0	BC	3910	3840	4500	2890	3930
104	48	72.0	TC	3710	3840	4500	2740	3760
105	48	56.0	BC	6470	6340	7810	4500	6590
105	48	56.0	TC	5940	6340	7810	4140	6120

midspan of the captive column. The column in Table 3 headed Gage Point indicates whether the deflection of the top or bottom caps was measured. In the case of triangular cross-sections with an apex up, all three caps are in contact with the load distribution frame. If there is no deformation of the frame, all three caps will deflect an equal amount, yielding an average value.

Analytical Results

Predicted beam stiffness values were obtained for each captive column flexure test that was performed. Two stiffness values are listed in Table 3 for each test. These values represent a range from the case where there is no wrap pretension to the case of ideal wrap pretension. As noted in Chapter 2, the analytical approach for predicting beam stiffness is unable to determine the extent of the cross-sectional deformation. The results listed in Table 3 represent the deflection of the neutral axis of the cross-section.

The equivalent flexural rigidity, used in computing the beam stiffness, for each captive column is listed in Table 4, along with the radius of gyration and the core significance. The core significance is defined by the following ratio:

$$\text{core significance} = \frac{(EI)_{panels} + (EI)_{center}}{(EI)_{eq}} \times 100\% \qquad (50)$$

This term represents the contribution of the core to the overall resistance of the captive column to the applied bending moment.

Computer Model Results

The computer model was also used to predict the beam stiffness for each flexure test. Again, two stiffness values are listed in Table 3,

TABLE 4

COMPUTED CAPTIVE COLUMN PROPERTIES

Captive Column Number	Radius of Gyration (in)	Core Significance (%)	Total EI(10^6 lb-in^2)
1	0.582	0.91	0.1164
2	0.570	0.17	0.3989
3	0.614	0.18	0.5741
4	0.585	0.03	2.0327
5	0.725	1.04	0.1296
6	0.721	0.20	0.4715
7	0.762	0.21	0.6564
8	0.722	0.04	2.317
9	0.547	22.98	0.1731
10	0.627	5.55	0.6890
11	0.885	1.76	4.907
12	1.829	0.36	9.222
13	1.634	0.70	8.963
14	1.793	0.18	15.48
15	1.702	0.38	15.68
16	2.891	1.40	32.96
17	3.216	0.68	61.96
18	3.451	0.16	295.9
19	3.319	1.91	277.3
20	3.815	0.75	60.15
21	4.057	0.15	300.7
22	4.297	0.24	466.0
23	4.370	0.27	488.8
24	4.058	0.13	467.2
25	1.569	0.09	33.82
25 - 28	1.565	0.09	33.65
29, 30	1.561	0.09	33.48
31	1.557	0.09	33.32
32,33,34	1.814	0.18	81.63
35,36,37	1.833	0.18	83.35
38 - 46	1.952	0.14	53.20
47	1.916	0.37	53.33
48	1.897	0.45	53.37

one for the case of no wrap pretension and the other for the case of ideal wrap pretension. The computer model is able to predict the amount of cross-sectional deformation. The stiffness values listed in Table 3 correspond to the stiffness of the top or bottom caps as determined by physical testing.

Conclusions

In general, the computer model yields a better prediction of the experimental beam stiffness than the analytical approach. Comparisons between the experimentally determined and analytically predicted beam stiffness values will be made in the latter part of the following chapter. Possible sources of error in the experimental results, as well as inadequacies in the analytical approach, will be identified there. The computer model results will be examined in Chapter 7.

CHAPTER 6

ANALYTICAL RESULTS

The influence of individual design parameters on the beam stiffness of a captive column will be discussed in this chapter. The following parameters will be investigated: 1) cross-section shape and size, 2) cap and core panel materials and dimensions, 3) wrap material, density, diameter, angle, and wrapping tension, and 4) span length. The analytical development of Chapter 2 will be used to predict the effect of a change in each of the above parameters. The experimentally determined beam stiffness values will then be studied to see whether or not the predicted behavior can be verified by experimental evidence.

Approximate Beam Stiffness

The beam stiffness for a square cross-section captive column, oriented as in Figure 6B, can be computed by using equation (47). For convenience, equation (47) is repeated below:

$$k = \frac{48(EI)_{eq}}{L^3\left[1 + \frac{24(E_{cap})^2}{L^2 G_{cap} (EI)_{eq}} (J_1 + J_2 + J_3)\right]} \tag{51}$$

It is very difficult to isolate the effect of an individual design parameter in the above equation. For this reason, the equation will be simplified by introducing approximations for some of the quantities in the equation.

The major component of the equivalent moment of inertia for a captive column is generally the product of the area of each cap and the

square of the distance from the centroid of the cap to the neutral axis. If all of the caps are made of the same material and have equal diameter, d, the flexural rigidity for a square cross-section captive column can be approximated by the following equation:

$$(EI)_{eq} \cong \frac{\pi E_{cap} d^2 D^2}{4} \tag{52}$$

For the test specimens under consideration in this research effort, the contribution of the integrals J_1 and J_3 to the sum of the three integrals $(J_1 + J_2 + J_3)$ is less than five percent. The equivalent first moment of area used in computing J_2 is primarily due to the first moment of area of the caps. By neglecting the first moment of area of the wrap and the core panels, the following equation is developed:

$$J_2 \cong \int_{h_1}^{h_2} \left[\frac{(wG)_{cap}(h_3^2 - h_2^2)}{2(wG)_{wrap} + 2(tG)_{panel}} \right]^2 \frac{[2(wG)wrap + 2\sqrt{2}(tG)panel}{G_{cap}} dy$$

$$J_2 \cong \frac{[(wG)_{wrap} + \sqrt{2}\,(tG)_{panel}][(wG)_{cap}\,(h_3^2 - h_2^2)]^2}{2\,G_{cap}\,[(wG)_{wrap} + (tG)_{panel}]^2} (h_2 - h_1)$$

This equation can be further simplified by making the following two substitutions:

$$(wG)_{cap}(h_3^2 - h_2^2) = \frac{\pi d^2 D}{4} G_{cap}$$

$$h_2 - h_1 = \frac{D}{2} - \frac{\sqrt{\pi}\, d}{4} - \frac{1}{2} w_{center}$$

Substituting the above quantities into the equation for the integral J_2 and simplifying yields the following equation for an approximation to the integral J_2:

$$J_2 \cong \frac{\pi^2 d^4 D^2 G_{cap}}{32} B_1 H_1 \tag{53}$$

where $$B_1 = \frac{(wG)_{wrap} + \sqrt{2}\,(tG)_{panel}}{[(wG)_{wrap} + (tG)_{panel}]^2}$$

$$H_1 = 0.5D - 0.443d - 0.5w_{center}$$

Approximate equations have been developed for $(EI)_{eq}$ and J_2. By setting $J_1 = J_3 = 0$, substituting equations (52) and (53) into equation (51), and simplifying, the following approximate equation for beam stiffness is developed:

$$k \cong \frac{12\pi d^2 D^2 E_{cap}}{L^3 + 3L\pi d^2 E_{cap} B_1 H_1} \tag{54}$$

Using the above equation, the effect of the previously identified parameters can more easily be determined.

The first term in the denominator of equation (54) accounts for the deflection due to the bending moment and the second term accounts for the deflection due to the shear force. If the deflection due to the shear force is neglected when computing the beam stiffness, equation (54) will become:

$$k \cong \frac{12\pi d^2 D^2 E_{cap}}{L^3} \tag{55}$$

The effect of a change in the cap material or diameter, cap centerline distance, or span length can easily be determined by examining equation (55). For example, by doubling the cap diameter, the stiffness will be increased by a factor of four.

Experimentally determined beam stiffness values indicate that the increase in stiffness due to a decrease in the span length or an increase in the cap diameter, cap elastic modulus, or cap centerline distance is not as great as the increase predicted by equation (55). The discrepancies between the experimental beam stiffness and the stiffness predicted from equation (55) indicate the need for including the deflection due to the shear force when predicting beam stiffness. Equation (54) must be used to determine the full effect of a design parameter.

Predicted Captive Column Behavior

The component materials and physical dimensions for a square cross-section captive column are listed below. This captive column will serve as the reference with respect to which the influence of the various parameters will be examined.

Caps: 3/8 inch diameter steel

Core Panels: 3/8 inch thick balsa wood

Core Centerpiece: 3/8 inch thick Douglas Fir

Wrap: 0.0132 inch diameter Kevlar, 45° angle, 10 strands/inch, assume ideal pretension

Cap Centerline Distance: 4 inches

Span Length: 72 inches

The interrelationships of the variables are complex and the effect of a change in an individual design parameter is dependent upon the values of the other parameters. For example, it will be shown that the beam stiffness is very dependent upon the wrap density, diameter, material, and angle for the captive column described above. If the core panel material is acrylic sheet instead of balsa wood, the stiffness will not be nearly as dependent upon the wrap parameters.

The effect of a change in each design parameter will be discussed independently. This will be accomplished by solving equation (54) in terms of the particular parameter under consideration. For the captive column described above, the stiffness is highly dependent upon each parameter. That is why these particular values were chosen.

Cap Elastic Modulus

An increase in the cap elastic modulus will increase the numerator of equation (54) and the term in the denominator associated with the deflection due to shear force. The following equation is obtained by expressing equation (54) in terms of the elastic modulus:

$$k = \frac{84.8\ E_{cap}}{373{,}000 + 0.00726\ E_{cap}}$$

where k and E_{cap} have units of pounds/inch and pounds/inch^2, respectively.

The beam stiffness calculated from the above equation is plotted in Figure 17 for values of the cap elastic modulus ranging from 0 to 60,000,000 pounds/inch^2. The beam stiffness computed from equation (55) is also plotted in Figure 17. When deflection due to shear force is neglected, beam stiffness is proportional to the elastic modulus. As shown in Figure 17, the difference between the beam stiffness values predicted from equations (54) and (55) increases with an increase in the elastic modulus. This can be explained by comparing the magnitude of the deflections due to the bending moment and shear force. At low values of the elastic modulus, the deflection due to shear force is negligible when compared with the deflection due to the bending moment. When this is the case, equations (54) and (55) will predict approximately the same value for the beam stiffness. As the elastic modulus is increased, the

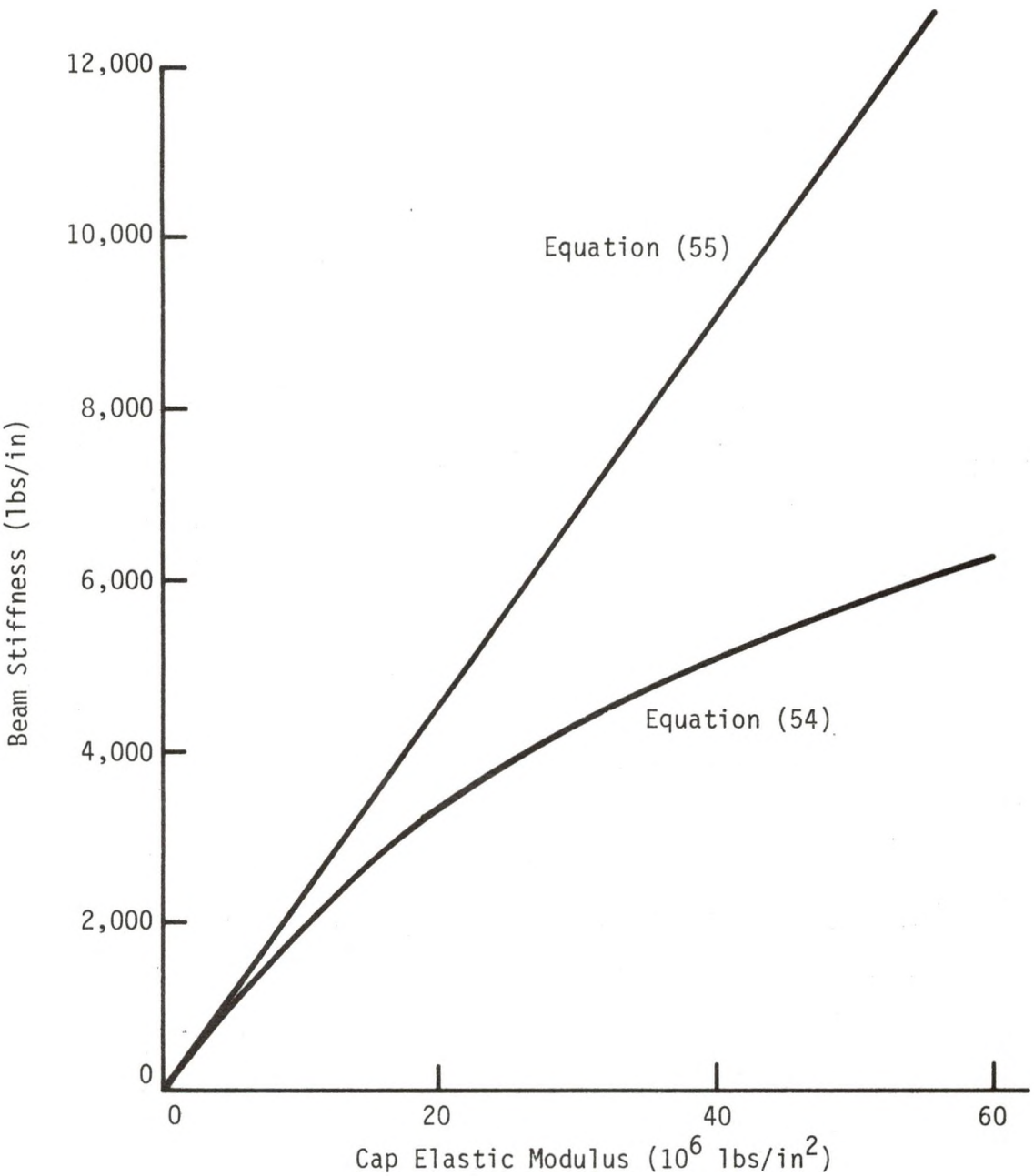

FIGURE 17 - BEAM STIFFNESS VS. CAP ELASTIC MODULUS

deflection due to shear force becomes a significant factor. When the deflection due to shear force is important, equation (55) will yield a higher prediction for the beam stiffness than equation (54).

Cap Diameter

Using steel ($E = 30{,}000{,}000\ lb/in^2$) as the cap material, the following equation is obtained for the beam stiffness as a function of the cap diameter:

$$k = \frac{18.1(10)^6 d^2}{373 + 941d^2(1.813 - 0.443d)}$$

where d has units of inches.

Beam stiffness values calculated from the above equation and from equation (55) are plotted in Figure 18 for cap diameters ranging from 0 to 1 inch. When deflection due to shear force is neglected, increasing the cap diameter by a factor of N will cause the stiffness to increase by a factor of N^2. For small cap diameters, the deflection due to shear force is negligible and equations (54) and (55) yield approximately the same value for the beam stiffness. As the cap diameter is increased, the deflection due to shear force becomes an important factor in the determination of the beam stiffness and equation (55) no longer applies.

Span Length

Using 3/8 inch diameter steel caps and varying the span length in equation (54), the following equation is obtained:

$$k = \frac{2.54(10)^9}{L^3 + 3030L}$$

where L has units of inches.

Beam stiffness values calculated from the above equation are plotted in Figure 19, along with the stiffness calculated from equation (55), for

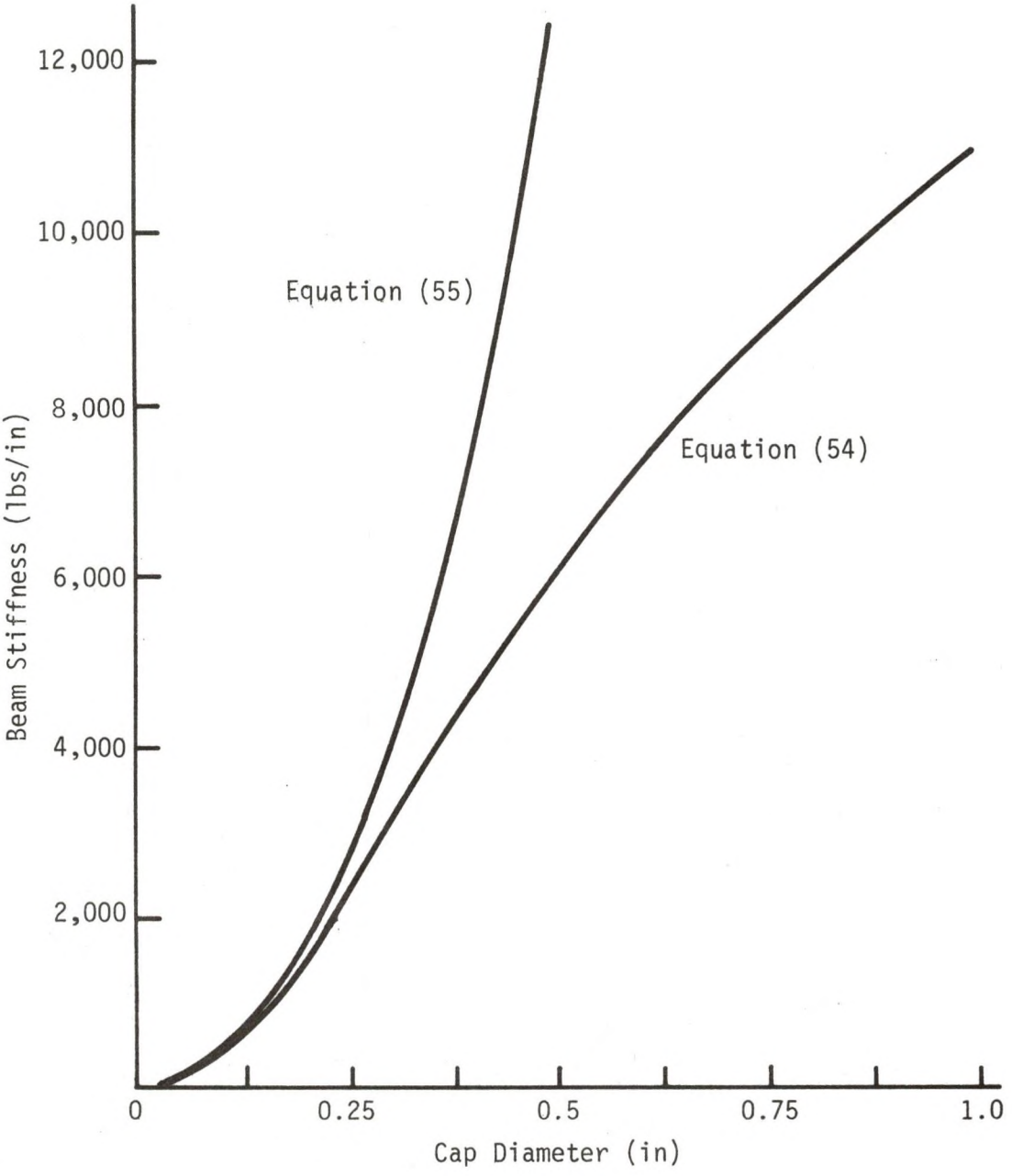

FIGURE 18 - BEAM STIFFNESS VS. CAP DIAMETER

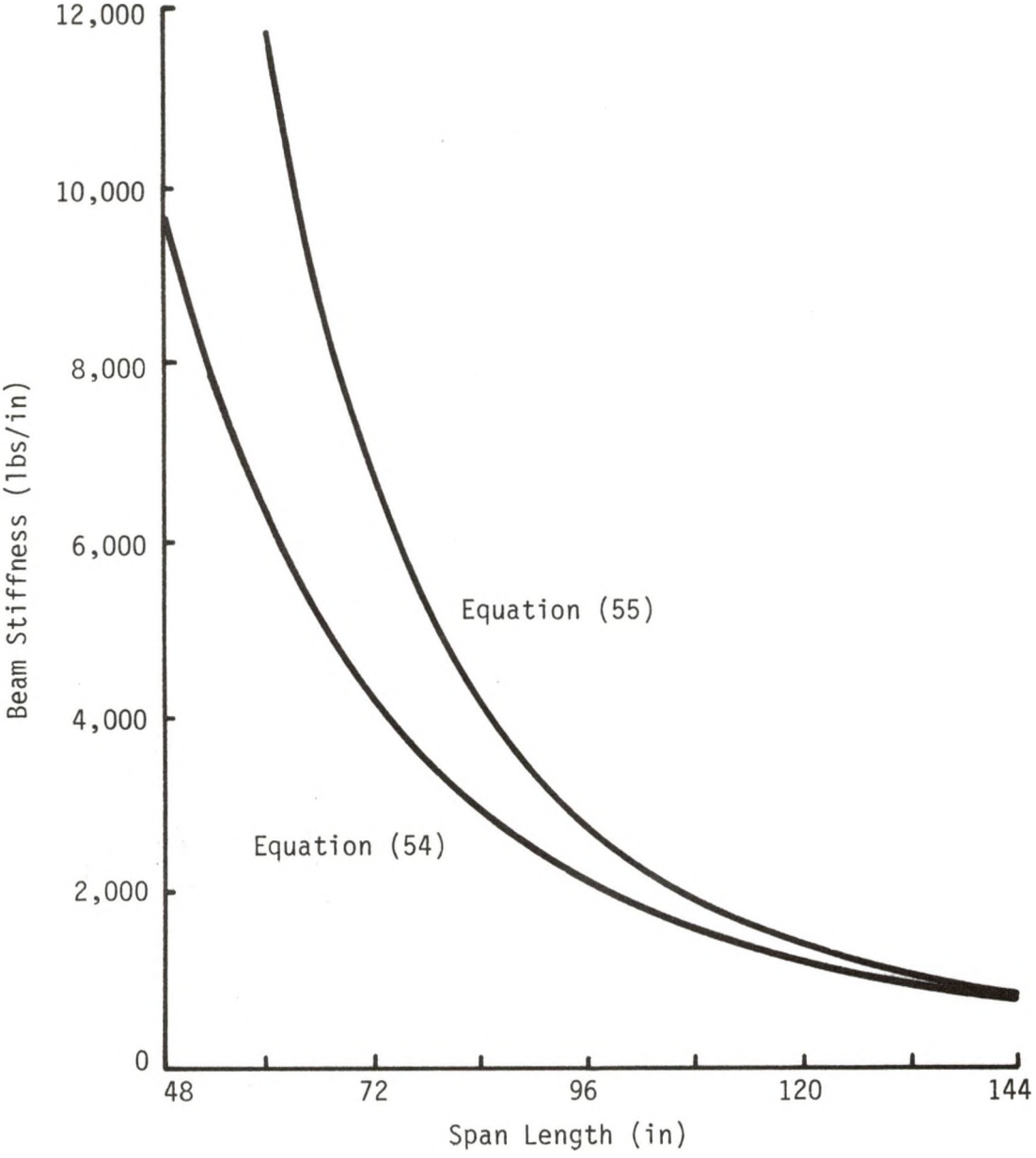

FIGURE 19 - BEAM STIFFNESS VS. SPAN LENGTH

span lengths varying from 48 to 144 inches. For long span lengths, the term in the denominator that accounts for the deflection due to the bending moment is much greater than the term that accounts for the deflection due to shear force. When this is the case, equations (54) and (55) will yield approximately the same value for the beam stiffness. As the span length is decreased, the deflection due to shear force becomes more significant relative to the deflection due to the bending moment, and therefore, the difference between the beam stiffness values predicted from equation (54) and (55) increases.

Cap Centerline Distance

With 3/8 inch diameter steel caps and a 72 inch span length, the following equation for the beam stiffness as a function of the cap centerline distance is obtained from equation (54):

$$k = \frac{159{,}000\ D^2}{373 + 132(0.5D - 0.354)}$$

where D has units of inches.

In Figure 20, the beam stiffness computed from the above equation and from equation (55) are plotted for cap centerline distances ranging from 0 to 8 inches. When the deflection due to shear force is neglected, the beam stiffness increases by a factor of N^2 when the cap centerline distance is increased by a factor of N. As the cap centerline distance is increased, the deflection due to shear force becomes more significant in the determination of the beam stiffness. As this happens, equation (55), which is accurate for relatively small centerline distances, can no longer be used to predict the beam stiffness.

The effects of changes in the four parameters found in equation (55) have been discussed. It has been found that this equation and equation

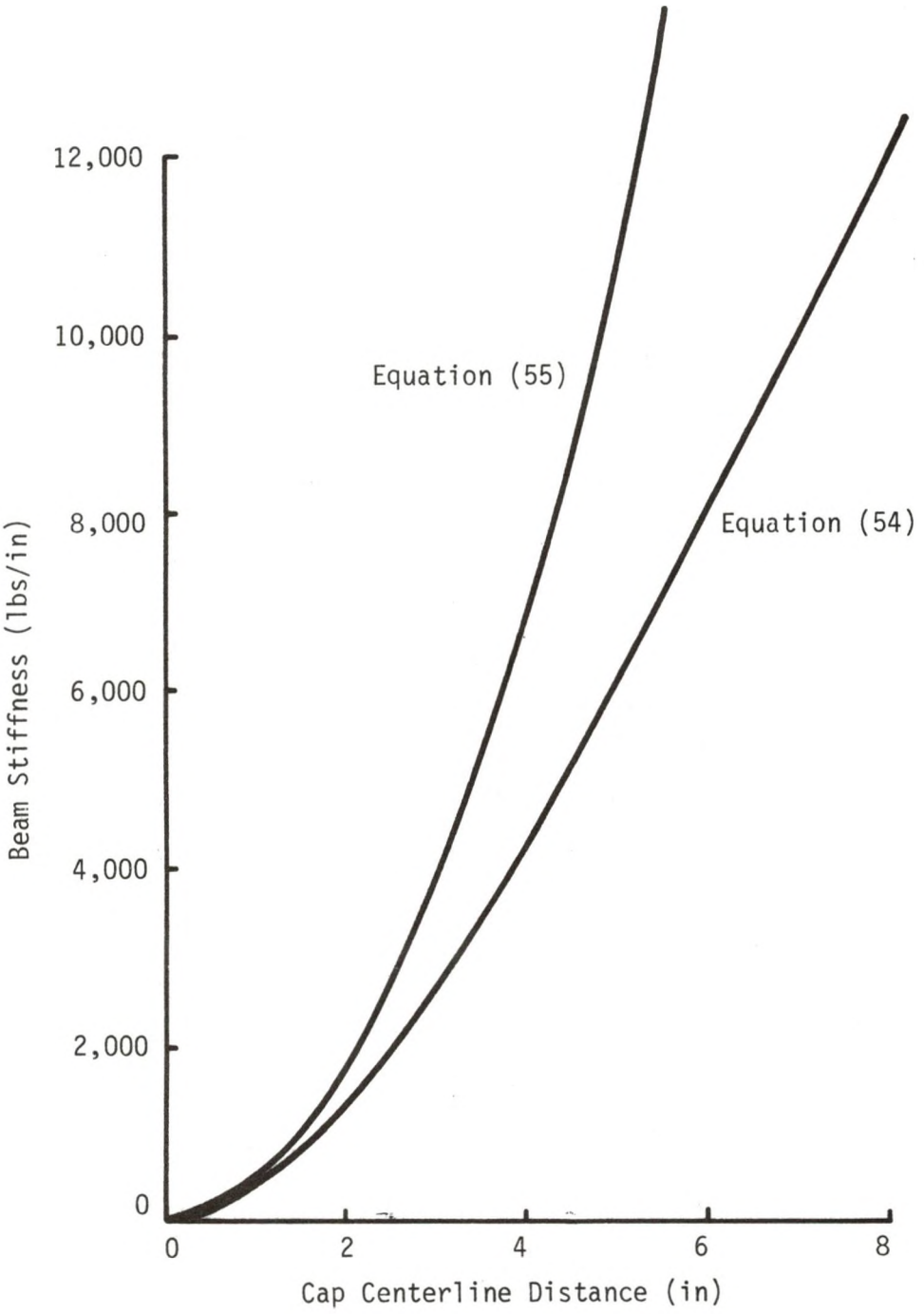

FIGURE 20 - BEAM STIFFNESS VS. CAP CENTERLINE DISTANCE

(54) yield approximately the same beam stiffness value if the following conditions are satisfied: 1) low cap elastic modulus, 2) small cap diameter, 3) long span length, and 4) small cap centerline distance. This statement leads to a conclusion that the deflection due to shear force is small when compared with the deflection due to the bending moment if the above four conditions are satisfied. As mentioned at the beginning of this section, the effect of a change in one parameter is dependent upon the values of the other parameters. For this reason it is difficult to place a numerical value on the four conditions described above.

Core Panels and Wrap

When the deflection due to shear force is not negligible, equation (54) must be used to obtain a prediction of the beam stiffness. Based on the captive column reference values presented earlier, equation (54) can be expressed as follows in terms of the core panel and wrap properties:

$$k = \frac{2.55(10)^6}{373 + 4.71(10)^6 \dfrac{[(wG)_{wrap} + \sqrt{2}\,(tG)_{panel}]}{[(wG)_{wrap} + (tG)_{panel}]^2}}$$

where w and t have units of inches and G has units of pounds/inch^2.

The equivalent wrap width multiplied by the wrap shear modulus has previously been defined to be the wrap shear stiffness. In a similar fashion, the core panel thickness multiplied by the core panel shear modulus will be defined to be the core panel shear stiffness. An increase in either of these shear stiffnesses will result in an increase in the beam stiffness.

Equation (20), which was developed in Chapter 2 and is repeated below, is used to compute the wrap shear stiffness.

$$(wG)_{wrap} = \rho\, A_s\, E_{wrap} \sin\phi \cos^2\phi$$

The above equation was developed for the case of no wrap pretension. If there is an ideal pretension applied during the wrapping operation, the effective width will be twice the value calculated above. If there is some pretension applied, but it is less than the ideal pretension, the effective width will fall within the range represented by the two values. It will be assumed in the following discussion that the wrap is ideally pretensioned, and therefore the above equation will be multiplied by two. The effect of pretension will be discussed more thoroughly later in this chapter.

By substituting the expression for the area of an individual wrap strand into the above equation and applying the pretension factor of two the following equation is obtained:

$$(wG)_{wrap} = \frac{\pi\, \rho}{2}\, d^2_{wrap}\, E_{wrap} \sin\phi \cos^2\phi \qquad (56)$$

By increasing the wrap density, diameter or elastic modulus, the magnitude of the wrap shear stiffness is increased, thus increasing the beam stiffness. For constant values of the above three parameters, the wrap angle that maximizes the wrap shear stiffness can be determined by setting the first derivative of equation (56) with respect to the wrap angle equal to zero and solving for the wrap angle:

$$(wG)_{wrap} = C \sin\phi \cos^2\phi$$

$$\frac{d}{d\phi}(wG)_{wrap} = C \cos\phi\, [\cos^2\phi - 2 \sin^2\phi] = 0$$

$$\phi = 35.3°$$

where $C = \frac{\pi\, \rho}{2}\, d^2_{wrap}\, E_{wrap} = \text{constant}$

When the wrap density is held constant, a wrap angle of 35.3 degrees will maximize the wrap shear stiffness, but this is not the only criterion to consider when choosing the wrap angle. The total amount of wrap material that is required to wrap a captive column will influence the total weight and the cost of the captive column.

The length of wrap material, l, that is required per linear inch of captive column is computed by using the following equation:

$$l = 8 \rho D \csc\phi \tag{57}$$

The wrap shear stiffness and the amount of wrap needed for a wrap density of 1 strand per inch are plotted in Figure 21 as functions of the wrap angle. As expected, the shear stiffness attains a maximum value at a wrap angle of 35.3 degrees. The amount of wrap needed decreases from a value that approaches infinity at 0 degrees to a minimum value at 90 degrees, where the wrap shear stiffness is equal to zero.

To determine the wrap angle that will yield the maximum wrap shear stiffness for a given amount of wrap, equation (57) is solved for the wrap density in terms of the wrap length:

$$\rho = \frac{l \sin\phi}{8D} \tag{58}$$

The above expression for wrap density is substituted into equation (56) yielding the following:

$$(wG)_{wrap} = \frac{\pi l}{16D} d_{wrap}^2 E_{wrap} \sin^2\phi \cos^2\phi \tag{59}$$

The amount of wrap material, the cap centerline distance, and the wrap diameter and elastic modulus will now be held constant. By differentiating the above equation with respect to the wrap angle and setting the result equal to zero the following angle is determined:

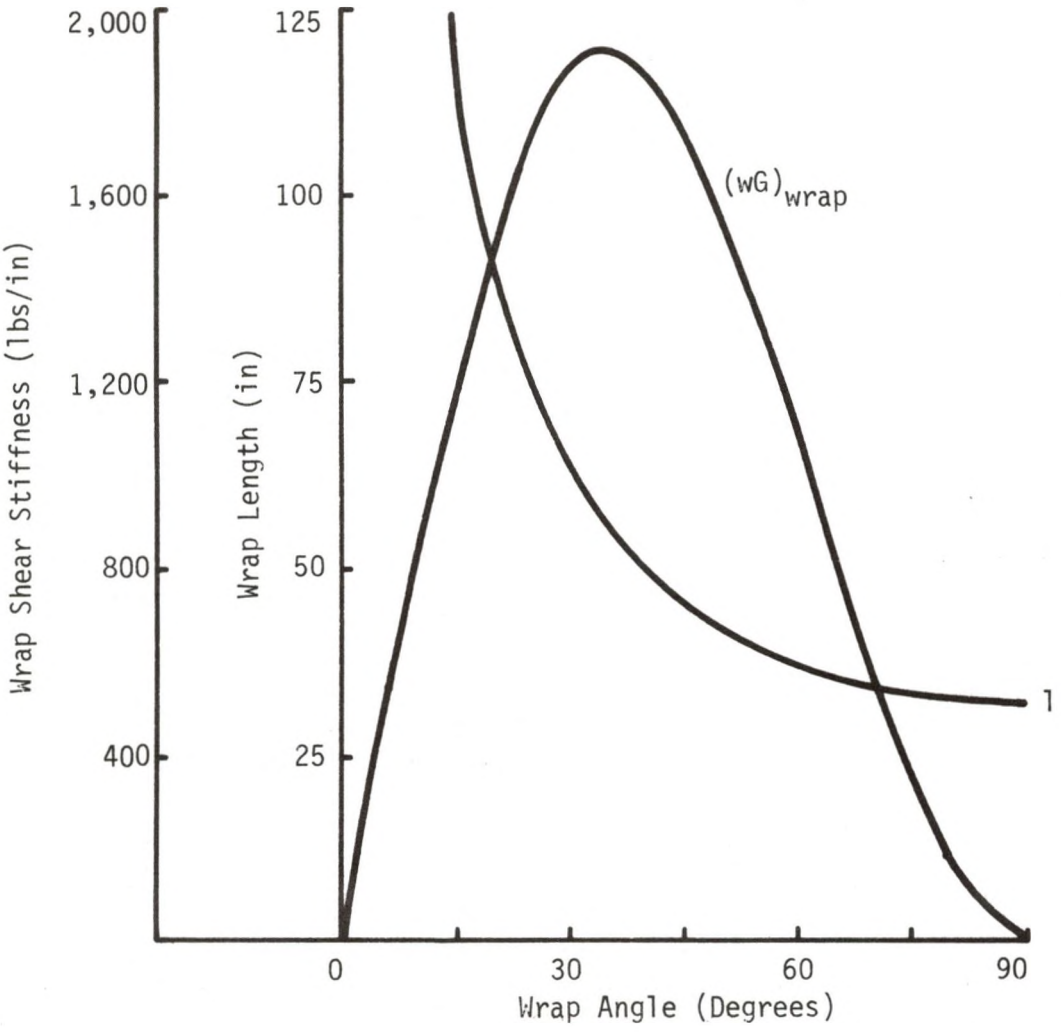

$D = 4.0$ in; $\rho = 1.0$ strand/in.; $d_{wrap} = 0.0132$ in; $E_{wrap} = 18(10)^6$ lbs/in^2

$$(wG)_{wrap} = \frac{\pi\rho}{2} d^2_{wrap} E_{wrap} \sin\phi \cos^2\phi = 4930 \sin\phi \cos^2\phi$$

$$l = 8\rho D \csc\phi = 32 \csc\phi$$

FIGURE 21 - WRAP PARAMETERS FOR CONSTANT WRAP DENSITY

$$(wG)_{wrap} = C \sin^2\phi \cos^2\phi$$

$$\frac{d}{d\phi}(wG)_{wrap} = 2C \sin\phi \cos\phi[\cos^2\phi - \sin^2\phi] = 0$$

$$\phi = 45.0°$$

where $C = \frac{\pi}{16D} \frac{1}{d^2_{wrap} E_{wrap}}$ = constant.

The wrap shear stiffness and density for a constant amount of wrap are plotted in Figure 22 as a function of the wrap angle. The amount of wrap is based on a wrap density of 1 strand/inch and a wrap angle of 45 degrees. The shear stiffness reaches a maximum value at 45.0 degrees. The shift in the wrap angle that maximizes the wrap shear stiffness from 35.3 to 45.0 degrees is due to the fact that the wrap density decreases as the wrap angle decreases.

From the above discussion, it is apparent that the optimum wrap angle for a captive column subjected to a flexural load is 45.0 degrees. This angle will maximize the wrap shear stiffness for a given amount of wrap.

The beam stiffness for a range of values of the wrap and core panel shear stiffnesses is plotted in Figure 23. These beam stiffness values are based upon the captive column described at the beginning of this section. The beam stiffness predicted from equation (55) is also plotted on Figure 23. Since equation (55) is not dependent upon the wrap or core panel shear stiffnesses, the beam stiffness is a constant value.

When the wrap and the core panel shear stiffnesses are both small, the deflection due to shear force will be greater than the deflection due to the bending moment, which will result in a low value for the beam stiffness. As the wrap and the core panel shear stiffnesses increase, the deflection due to shear force decreases, and therefore, the beam stiffness increases.

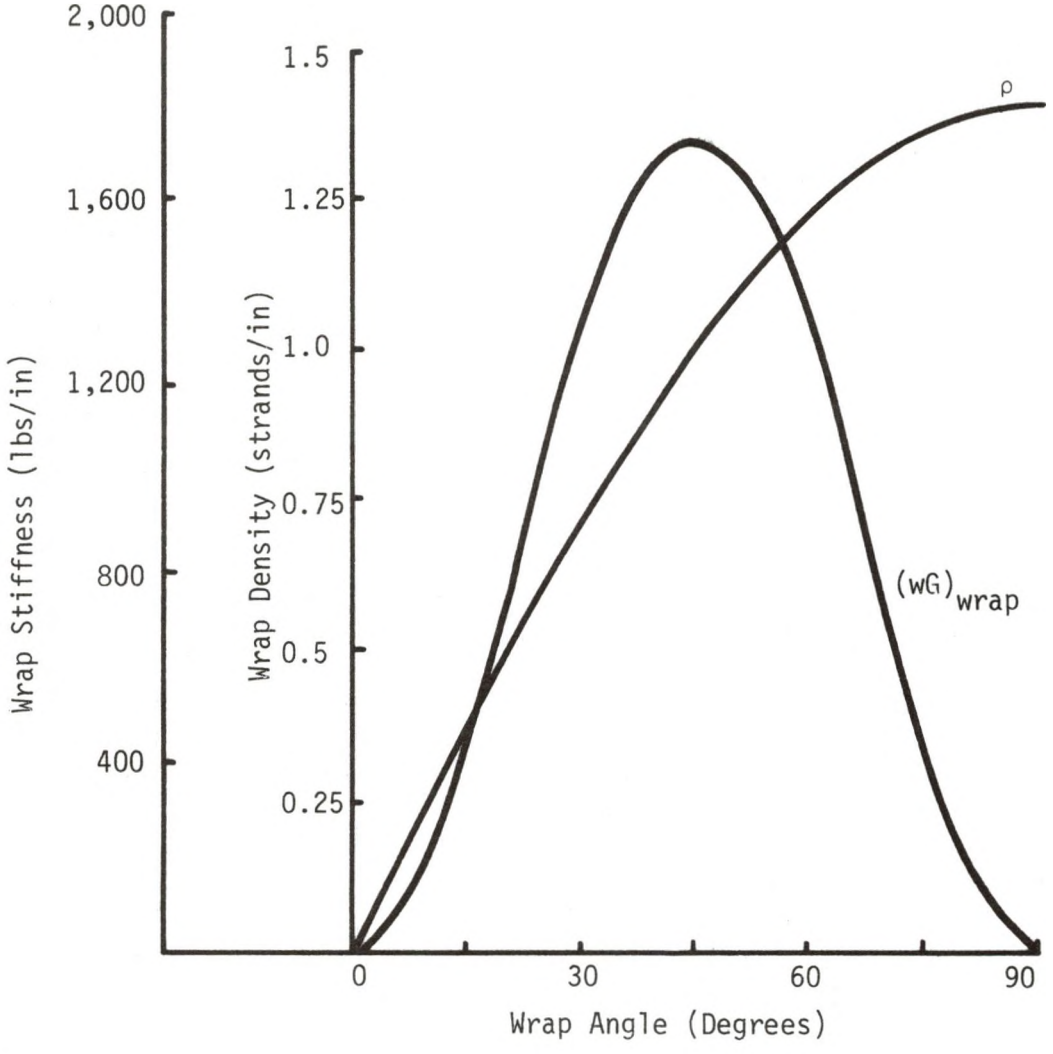

$D = 4.0$ in; $\quad d_{wrap} = 0.0132$ in; $\quad E_{wrap} = 18(10)^6$ lbs/in^2

$$l = 8\rho D \csc\phi = 32 \csc 45^\circ = 45.25 \text{ in/linear in}$$

$$(wG)_{wrap} = \frac{\pi l}{16D} d^2_{wrap} E_{wrap} \sin^2\phi \cos^2\phi = 6970 \sin^2\phi \cos^2\phi$$

$$\rho = \frac{l \sin\phi}{8D} = 1.414 \sin\phi$$

FIGURE 22 - WRAP PARAMETERS FOR CONSTANT AMOUNT OF WRAP MATERIAL

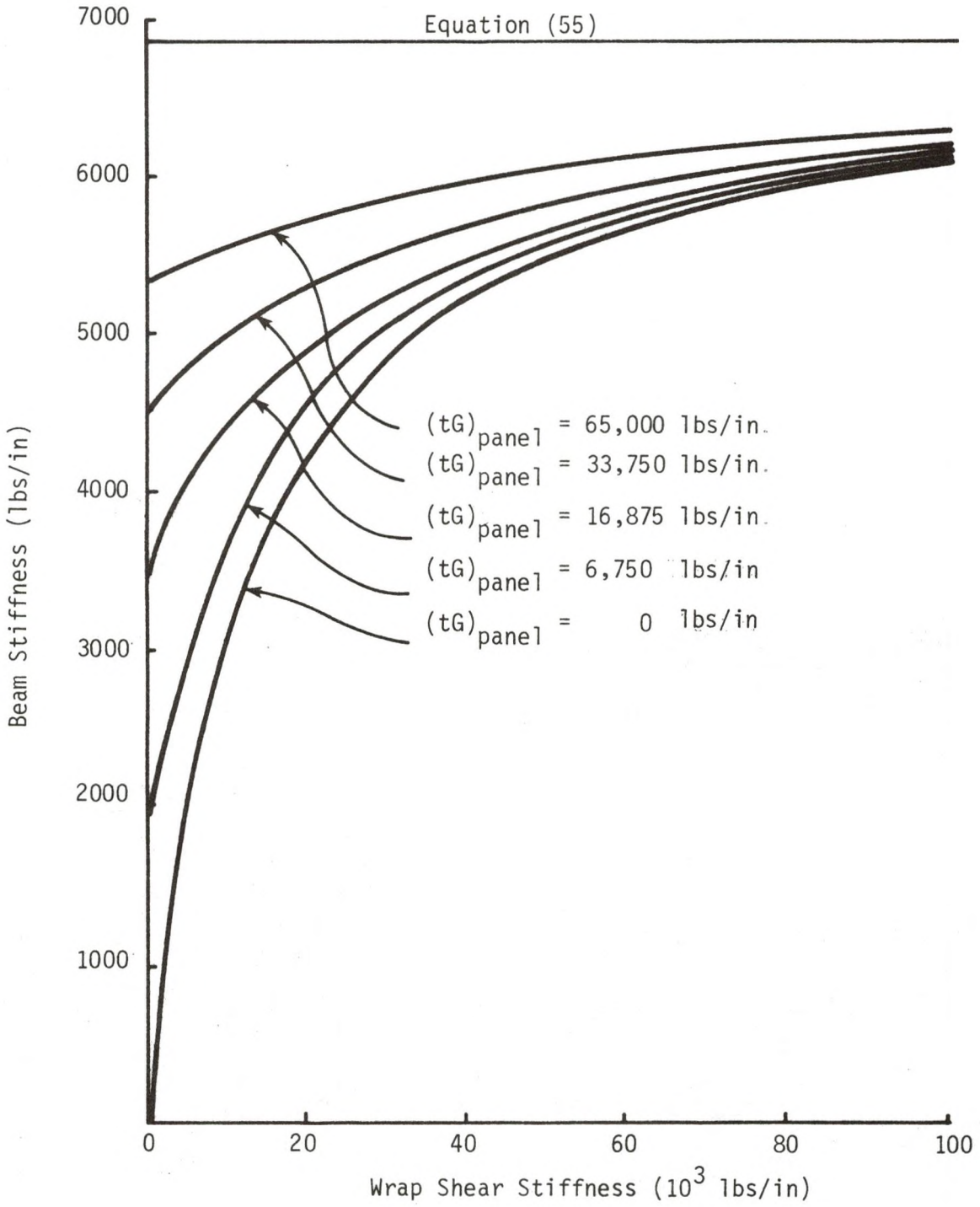

FIGURE 23 - BEAM STIFFNESS AS A FUNCTION OF CORE PANEL AND WRAP SHEAR STIFFNESSES

Figure 23 represents a good example of the interdependence of captive column design parameters. The core panel shear stiffness for 3/8 inch thick balsa wood is 6750 pounds per inch. For this core panel shear stiffness the beam stiffness is very dependent upon the wrap shear stiffness. If 3/8 inch thick acrylic sheet is used as the core panel material, the core panel shear stiffness will increase to 65,000 pounds per inch. At this value, the beam stiffness is not very dependent upon the wrap shear stiffness. The reverse situation is also true. The wrap shear stiffness for the parameters listed at the beginning of this section is 17,400 pounds per inch. For this value the beam stiffness is very dependent upon the core panel shear stiffness. As the wrap shear stiffness increases, however, the beam stiffness becomes less dependent upon the core panel shear stiffness.

Cross-Section Geometry

A square cross-section captive column, oriented as in Figure 24A has been used to describe the effect of the various design parameters. If a square cross-section captive column is rotated about its longitudinal axis, or if a different cross-section is used, the effect of a change in any given parameter may not be the same.

Equations needed to determine the beam stiffness of a square captive column, rotated to the orientation shown in Figure 24B, are developed in Appendix D. An approximate beam stiffness equation, similar in form to equation (54), is also developed and is repeated below:

$$k \cong \frac{12\pi d^2 D^2 E_{cap}}{L^3 + 3L\pi d^2 E_{cap} B_2 H_2} \qquad (60)$$

where $$B_2 = \frac{2\sqrt{2}(wG)_{wrap} + (tG)_{panel}}{[2(wG)_{wrap} + (tG)_{panel}]^2}$$

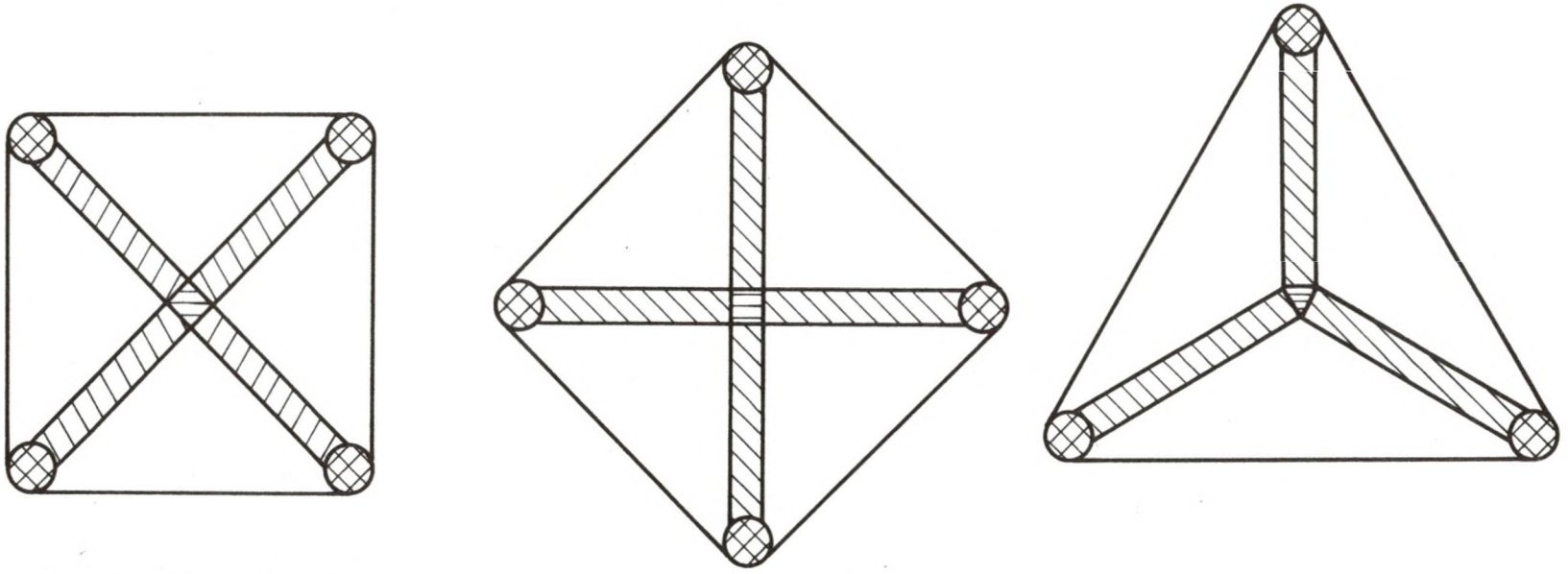

A) Square Cross-Section

B) Square Cross-Section, Rotated 45°

C) Triangular Cross-Section

FIGURE 24 - CAPTIVE COLUMN CROSS-SECTIONAL SHAPES

$$H_2 = 0.707D - 0.443d - 0.5w_{center}$$

Except for the second term in the denominator, which accounts for the deflection due to shear force, this equation is the same as equation (54). The beam stiffness computed from equation (60) will be slightly less than the stiffness computed from equation (54). Furthermore, the normal stress in two of the caps will be greater for the case when the captive column is rotated 45 degrees. This is due to the fact that the distance from these caps to the neutral axis increases as the captive column is rotated.

The above statements suggest that the best orientation for a square cross-section captive column is the one shown in Figure 24A. This conclusion is intuitively obvious due to the fact that two of the caps, as shown in Figure 24B coincide with the neutral axis when the captive column is rotated 45 degrees. These caps offer a negligible increase in the beam stiffness and in the load carrying capacity of the captive column.

A triangular cross-section captive column, as shown in Figure 24C, is also considered in Appendix D. An approximate beam stiffness equation is developed as well in the Appendix. The equation is repeated below:

$$k = \frac{6\pi d^2 D^2 E_{cap}}{L^3 + 2L\pi d^2 E_{cap}(B_3H_3 + B_4H_4)} \qquad (61)$$

where

$$B_3 = \frac{2.309(wG)_{wrap} + (tG)_{panel}}{[2(wG)_{wrap} + (tG)_{panel}]^2}$$

$$B_4 = \frac{0.577(wG)_{wrap} + (tG)_{panel}}{[(wG)_{wrap} + (tG)_{panel}]^2}$$

$$H_3 = 0.577D - 0.443d - 0.439w_{center}$$

$$H_4 = 0.289D - 0.443d - 0.219w_{center}$$

If the deflection due to shear force is neglected, equation (61) becomes:

$$k = \frac{6\pi d^2 D^2 E_{cap}}{L^3} \tag{62}$$

A comparison of equations (55) and (62) indicates that if all of the parameters are the same, a square cross-section captive column will be twice as stiff as a triangular cross-section captive column. By increasing the cap centerline distance of the triangular cross-section captive column by a factor of $\sqrt{2}$, the two captive columns will have equivalent beam stiffness.

When the deflection due to shear force is included, a comparison between equations (54) and (61) must be made. Again, the cap centerline distance of the triangular cross-section captive column will be increased by a factor of $\sqrt{2}$. When this is done, equations (54) and (61) will be equivalent, except for the second term in the denominator. In general, the beam stiffness predicted from equation (61) will be slightly less than the stiffness predicted from equation (54). An exception to this rule occurs when the cap centerline distance to cap diameter ratio is large and the wrap shear stiffness is greater than the core panel shear stiffness. When these two conditions occur simultaneously, the beam stiffness predicted from equation (61) will be slightly greater than the stiffness predicted from equation (54).

With all other design parameters the same, a triangular cross-section captive column will have approximately the same beam stiffness as a square cross-section captive column if the cap centerline distance is increased by a factor of $\sqrt{2}$. The amount of wrap, core panel, and core centerpiece material will be approximately the same for both cross-sections, and therefore, the weight and cost of the captive column

will be lower if a triangular cross-section is used because of a reduction in the number of caps. This advantage is offset by the increase in size of the cross-section and the increase in the normal stress of the cap furthest from the neutral axis. Due to the above tradeoffs, a statement cannot be made concerning the selection of a square or triangular cross-section.

Other Design Parameters

An approximate equation for the determination of beam stiffness has been developed. Using this equation, it was found that the stiffness is very dependent upon a number of design parameters. Simplifications were made in the development of the approximate equation that eliminated the effect of some design parameters. Although these parameters have only a minor effect upon the stiffness, they will be briefly discussed here for completeness.

The significance of three terms was assumed to be negligible in the development of the approximate equivalent flexural rigidity; 1) the moment of inertia of the caps about their centroidal axes, 2) the flexural rigidity of the core panels, and 3) the flexural rigidity of the core centerpiece. Including these terms would increase the equivalent flexural rigidity, which would lead to an increase in the beam stiffness.

For the captive columns considered in this research effort, the moment of inertia of the caps about their centroidal axes is less than one percent of the moment of inertia of the caps about the cross-section centroidal axis. Including the moment of inertia of the caps about their centroidal axes will therefore lead to a very slight increase in the equivalent flexural rigidity.

The combined flexural rigidity of the core panels and core

centerpiece is small when compared with the flexural rigidity of the caps. The centerpiece flexural rigidity is small because the neutral axis of the captive column passes through the centerpiece and the ratio of the centerpiece elastic modulus to the cap elastic modulus is low. The core panel flexural rigidity is small when the core panel elastic modulus to cap elastic modulus ratio is low. The core significance, which is defined by equation (50), is less than two percent for all of the captive columns that were constructed with balsa wood core panels. With these captive columns, including the core panel and core centerpiece flexural rigidities would only slightly increase the beam stiffness. When acrylic was used as the core panel material, the core significance was as high as twenty-three percent. In this case the core panel elastic modulus to cap elastic modulus is relatively high; thus the core panel flexural rigidity is more significant and including the core panels will lead to a relatively large increase in the beam stiffness.

Three simplifications were made in the development of the approximate term in equation (54) associated with the deflection due to shear force. An approximation was made for the following integral:

$$J = \int_0^{h_3} \left(\frac{Q_{eq}}{b_{eq}} \right)^2 dA$$

The first simplification concerned the integral, J_1, from the neutral axis to the vertical distance h_1. The equivalent width, b_{eq}, of the core centerpiece and the wrap is large when compared with the equivalent width of the core panels and the wrap. Furthermore, the equation is integrated over a small range of vertical distance. The combination of the above two factors leads to a small value for this integral. The

second simplification concerned the integral J_3. The equivalent width of the caps is very large in comparison with the equivalent width of the core panels and wrap. This alone leads to a small value for the integral. In the development of the approximate equations, the integrals J_1 and J_3 were assumed to be equal to zero. In the computation of the integral over the core panel area, J_2, the first moment of area of the core panels and the wrap was assumed to be equal to zero. This is due to the fact that the incremental area, dA, of the core panels and wrap is much smaller than the incremental area of the caps.

If the above three simplifications are not made, the integral will have a slightly larger value, which would lead to a small decrease in the beam stiffness. The sum of the integrals J_1 and J_3 is less than five percent of the integral J_2 for the captive columns considered in this research effort. With this small percentage, the first two assumptions are valid. The third assumption is valid when the core panel and wrap shear stiffnesses are small. As these values increase, the first moment of area of the core panels and wrap must be considered.

Experimental Verification

Beam stiffness values determined experimentally and by using the analytical method of Chapter 2 were presented in Table 3 of Chapter 5. Subsets of this data will be used to verify the applicability of the analytical method in predicting the influence of individual design parameters.

All of the captive column test specimens are described in Table 1. The only reference to materials and dimensions that will be made in this chapter will refer to the particular parameter(s) under consideration. Unless noted otherwise, all other materials and dimensions are very

nearly the same, with Table 1 being the source for the specific values.

Throughout the discussion, predicted beam stiffness will refer to the beam stiffness that is determined by using equation (47) or, in the case of triangular cross-section captive columns, equation (101). When it is mentioned, relative error will be defined by the following equation:

$$\text{relative error} = \frac{k_{pre} - k_{exp}}{k_{exp}} \times 100\%$$

where k_{pre} = predicted beam stiffness (no wrap pretension or ideal wrap pretension)

k_{exp} = experimentally determined beam stiffness.

Four square cross-section captive columns with a cap centerline distance of approximately 7.0 inches were built and tested at various span lengths. Captive column numbers 16, 17, and 18 had 3/8 inch diameter fiberglass reinforced polyester (FRP), 1/2 inch diameter FRP, and 1/2 inch diameter steel caps, respectively, with balsa wood used as the core panel material. The fourth specimen, number 19, also had 1/2 inch diameter steel caps, but acrylic was used as the core panel material.

The experimentally determined beam stiffness is plotted in Figures 25, 26, 27 and 28 for five span lengths for each specimen. The deflection of the bottom (tensile) cap was used in determining this stiffness. The predicted beam stiffnesses as a function of the span length are also plotted in each figure.

The absolute value of the relative error, based upon the predicted stiffness of either wrap pretension case, is less than twenty percent for all tests conducted with these specimens. Considering the complexities

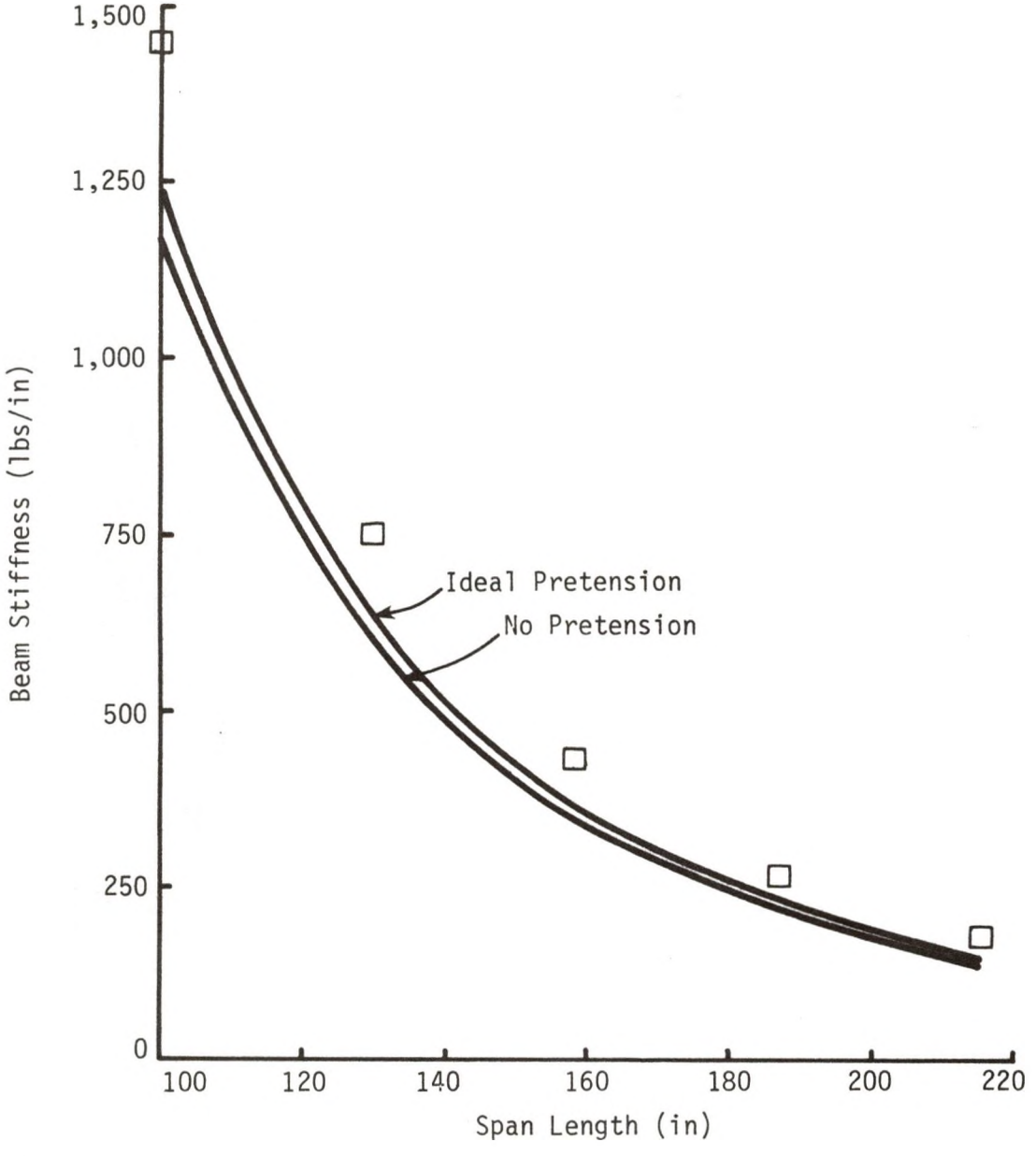

FIGURE 25 - BEAM STIFFNESS VS. SPAN LENGTH, CAPTIVE COLUMN NUMBER 16

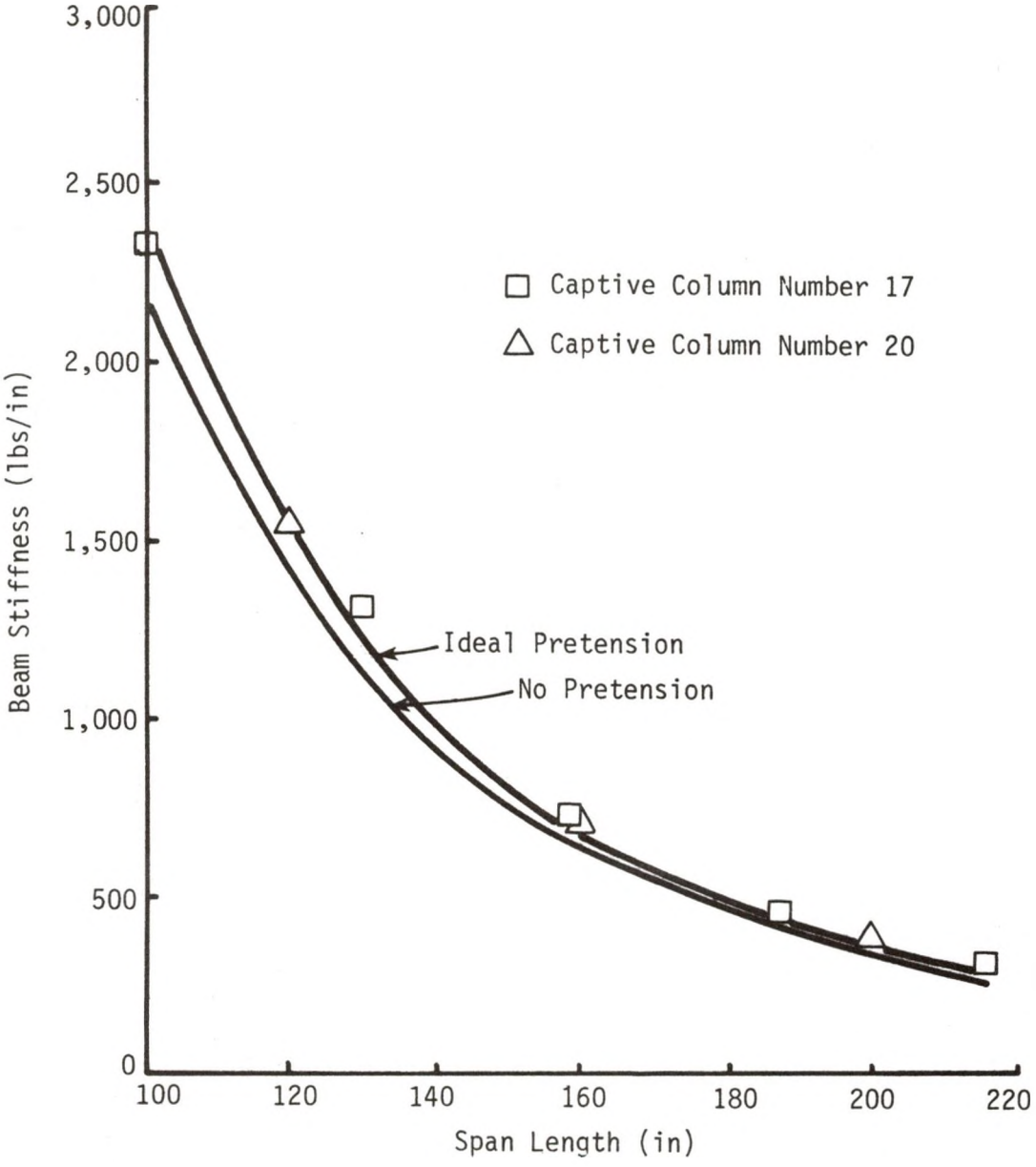

FIGURE 26 - BEAM STIFFNESS VS. SPAN LENGTH,
CAPTIVE COLUMN NUMBERS 17 AND 20

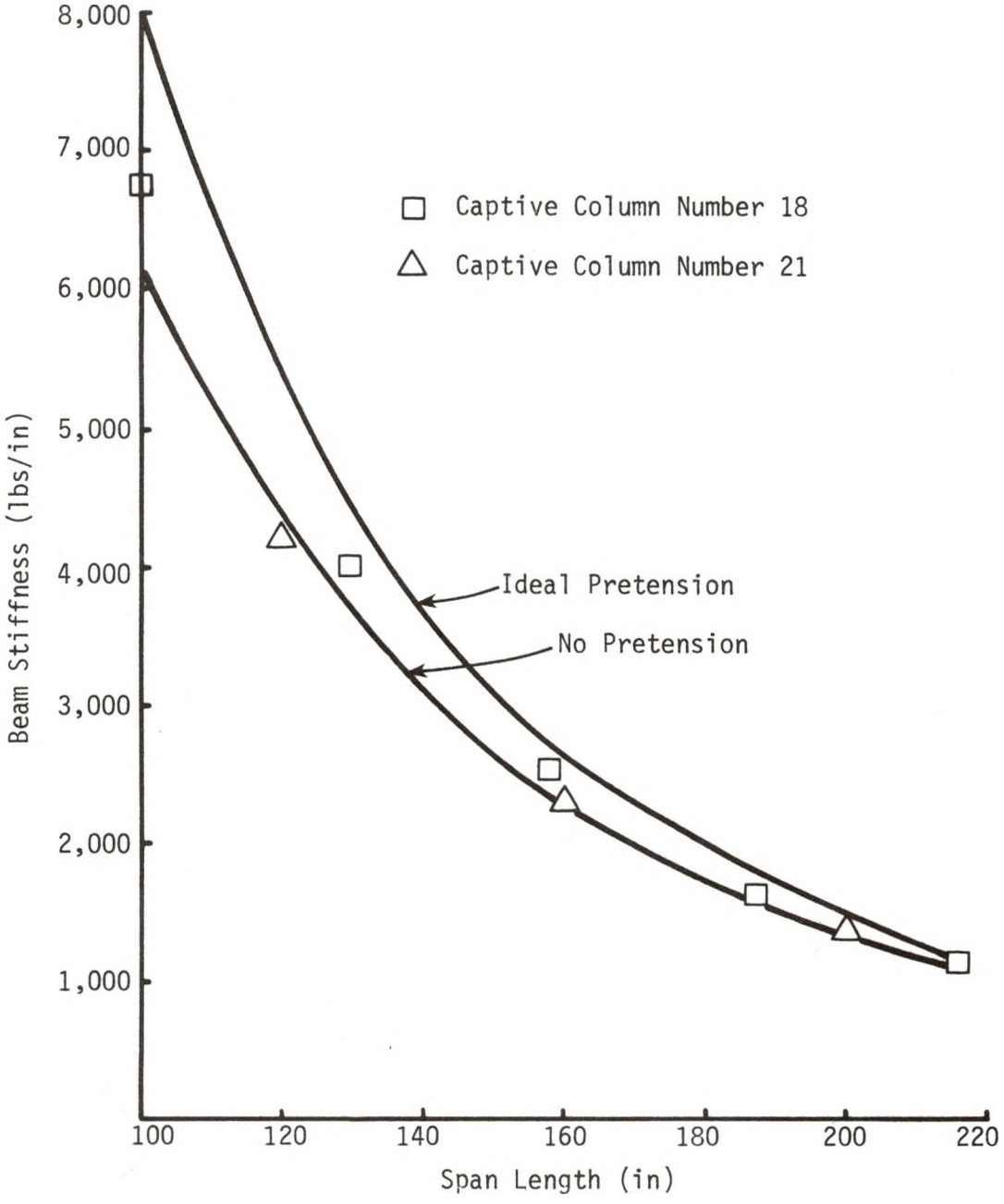

FIGURE 27 - BEAM STIFFNESS VS. SPAN LENGTH, CAPTIVE COLUMN NUMBERS 18 AND 21

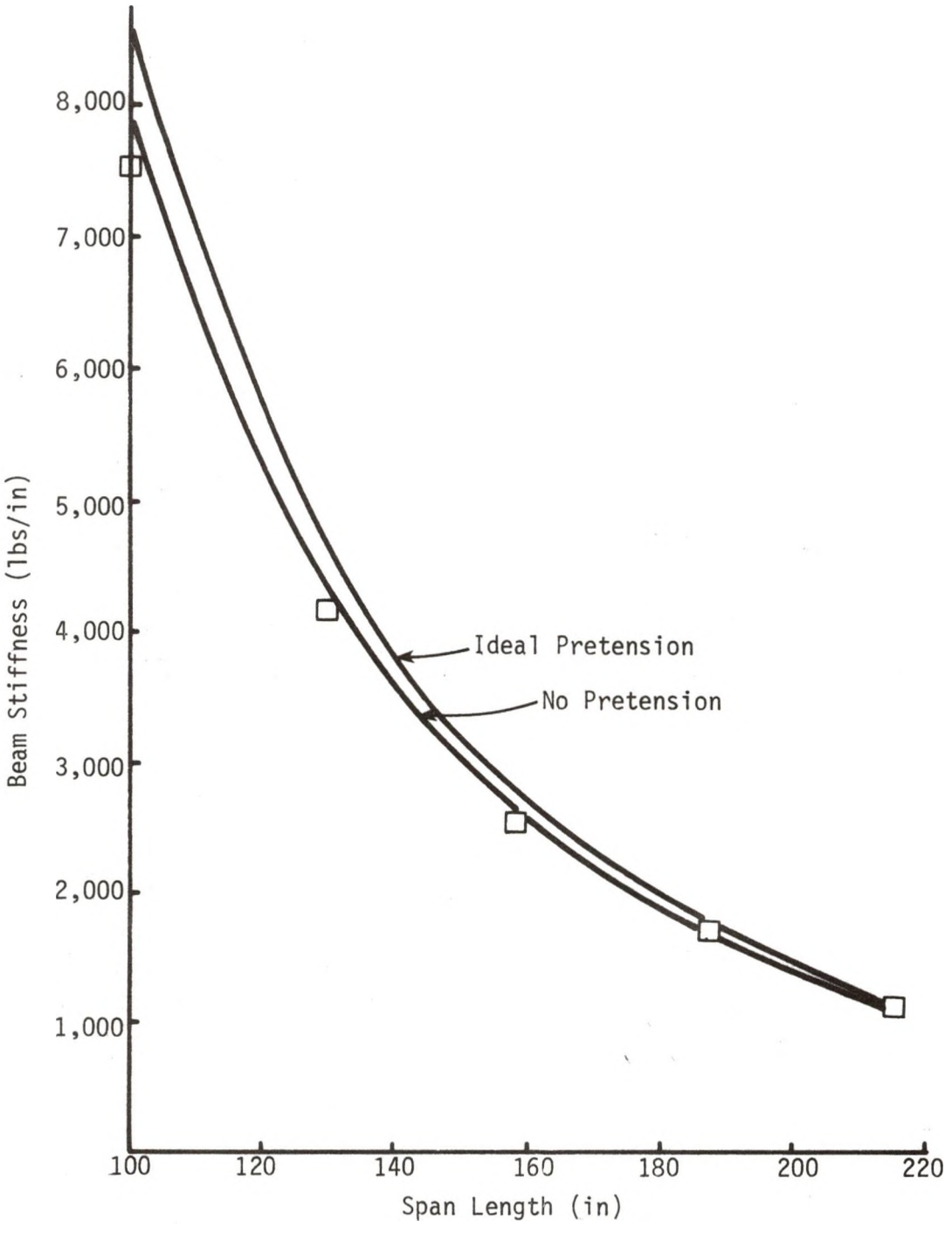

FIGURE 28 - BEAM STIFFNESS VS. SPAN LENGTH, CAPTIVE COLUMN NUMBER 19

involved in analyzing a captive column, this is a fairly low relative error, which indicates that the analytical method adequately predicts the influence of the cap diameter, the cap material, the core panel material, and the span length.

Although the magnitude of the relative error is less than twenty percent for all of the tests, the range of error is different for each specimen. It has been previously stated that the deflection due to shear force is small in comparison with the deflection due to the bending moment when the cap elastic modulus is relatively low, the cap diameter is small, and the span length is long. This statement will be used to determine possible sources of error in the predicted beam stiffnesses.

The two predicted stiffnesses, one for no wrap pretension and one for ideal wrap pretension, bracket the experimentally determined stiffness for specimen number 18. For specimen number 19, which has acrylic core panels instead of balsa wood core panels, the experimentally determined stiffness is less than both predicted stiffnesses. For both specimens, the absolute value of the relative error, for either wrap pretension case, increases as the span length decreases. This increase in the error coincides with an increase in the significance of the deflection due to shear force, which suggests that there is room for improvement in the term of equation (47) associated with the deflection due to shear force.

The only major physical difference between specimens 18 and 19 is a change in the core panel shear stiffness. The range of relative error is different for the two specimens, which implies a need for refinement of the way in which the core panels are dealt with in the development of equation (47). Another possibility for the differences in the relative

error is the use of incorrect balsa wood material properties. The properties of balsa wood are very dependent upon the weight density of the wood. This source of error will be discussed later in this chapter.

The experimentally determined beam stiffness is greater than the predicted stiffnesses when FRP is used as the cap material. Furthermore, the relative error is not nearly as dependent upon the span length for these specimens as it is for the specimens with steel caps. This is due to the fact that the deflection due to shear force is less significant because of the lower cap elastic modulus.

An error in the physical properties of the FRP rods is a possible source of error for the low predicted beam stiffness. The values for the elastic modulus and the shear modulus obtained from the manufacturer agree with values listed in other sources. If the value of the elastic modulus used in predicting the beam stiffness was increased by ten percent, the predicted stiffness would increase by approximately ten percent. This increase in the predicted stiffness may be possible due to the fact that the elastic modulus is dependent upon a number of manufacturing operations. The values obtained from the manufacturer are used due to the difficulties involved in experimentally determining the values.

Two triangular cross-section captive columns were built with a cap centerline distance of 10.0 inches, which is approximately $\sqrt{2}$ times greater than the size of the square cross-section specimens that were described above. Captive column number 20 had 1/2 inch diameter FRP caps and specimen number 21 had 1/2 inch diameter steel caps, with balsa wood core panels in both specimens.

Each captive column was tested twice, once with an apex up and once

with an apex down, at three different span lengths. The analytical method predicts that the beam stiffness does not depend upon which orientation is used; the stiffness should be the same for both cases. The experimentally determined stiffnesses, based upon the average deflection of the top and bottom caps, agree to within five percent of each other for the two test cases.

The experimentally determined stiffnesses are plotted in Figures 26 and 27 for the tests performed with an apex up. According to the exact analytical equations, the stiffness for these specimens should be approximately ten percent less than the stiffness of the square cross-section captive columns. As seen in Figures 26 and 27, the experimental results agree with the predicted results.

The close agreement between the two test orientations and the agreement with the square cross-section results indicate that the analytical method can be used to predict the stiffness of triangular cross-section captive columns.

Ten captive columns, specimen numbers 1 through 10, were used by Kipp [2] in his research effort. These captive columns were retested, and the data is presented in Table 3. This data set can also be used to make comparisons concerning the cap material and diameter, the core panel material, the span length, and the cross-sectional geometry. In general, the results obtained from tests using these specimens agree with the conclusions drawn from specimen numbers 16 to 21. This indicates the ability of the analytical method in predicting the beam stiffness of captive columns with various cap centerline distances.

Three square cross-section captive columns were constructed with the only difference in the specimens being a change in the core panel

thickness and core centerpiece width. Balsa wood with 1/4, 3/8, and 1/2 inch thicknesses and Douglas fir with 3/4, 1, and 1-1/8 inch widths were used in specimen numbers 39, 47, and 48, respectively.

Each specimen was tested using three different span lengths. The experimentally determined beam stiffness, based upon the average deflection of the top and bottom caps, is presented in Table 5 for each test. If the core panel shear modulus is the same for each specimen, the analytical method predicts that the beam stiffness will increase as the core panel thickness increases. The beam stiffnesses for specimen numbers 47 and 48 are approximately equal at any given span length, with the value nearly twice as great as the stiffness of specimen number 39.

The fact that the experimentally determined stiffness does not change when the core panel thickness is increased from 3/8 inch to 1/2 inch suggests that the shear modulus is not the same for the three specimens. The shear modulus and elastic modulus are plotted in Figure 29 as functions of the weight density [8]. The values listed in Table 2 are for balsa wood with a density of 7.0 pounds per cubic foot. The balsa wood used in specimen number 47 was purchased from a different supplier. This balsa wood had a density of 9.5 pounds per cubic foot, and therefore the material properties are higher.

The correct balsa wood material properties were used to obtain the predicted beam stiffness values listed in Table 5. The increase in the balsa wood shear modulus of specimen number 47 increased the predicted stiffness to the same values that are predicted for specimen number 48. In all of the tests, the experimentally determined stiffness is approximately equal to the predicted stiffness for the case with no wrap pretension, which indicates that the analytical method accurately predicts

TABLE 5

BEAM STIFFNESS FOR CORE THICKNESS TESTS

Captive Column Number	Span (in)	Beam Stiffness (lbs/in)		
		Experimental	Analytical Method	
			No Pretension	Ideal Pretension
39	88	1520	1540	1850
39	72	2130	2170	2700
39	56	3210	3190	4100
47	88	2430	2460	2770
47	72	3750	3840	4470
47	56	6060	6350	7750
48	88	2400	2460	2780
48	72	3810	3840	4500
48	56	6210	6340	7810

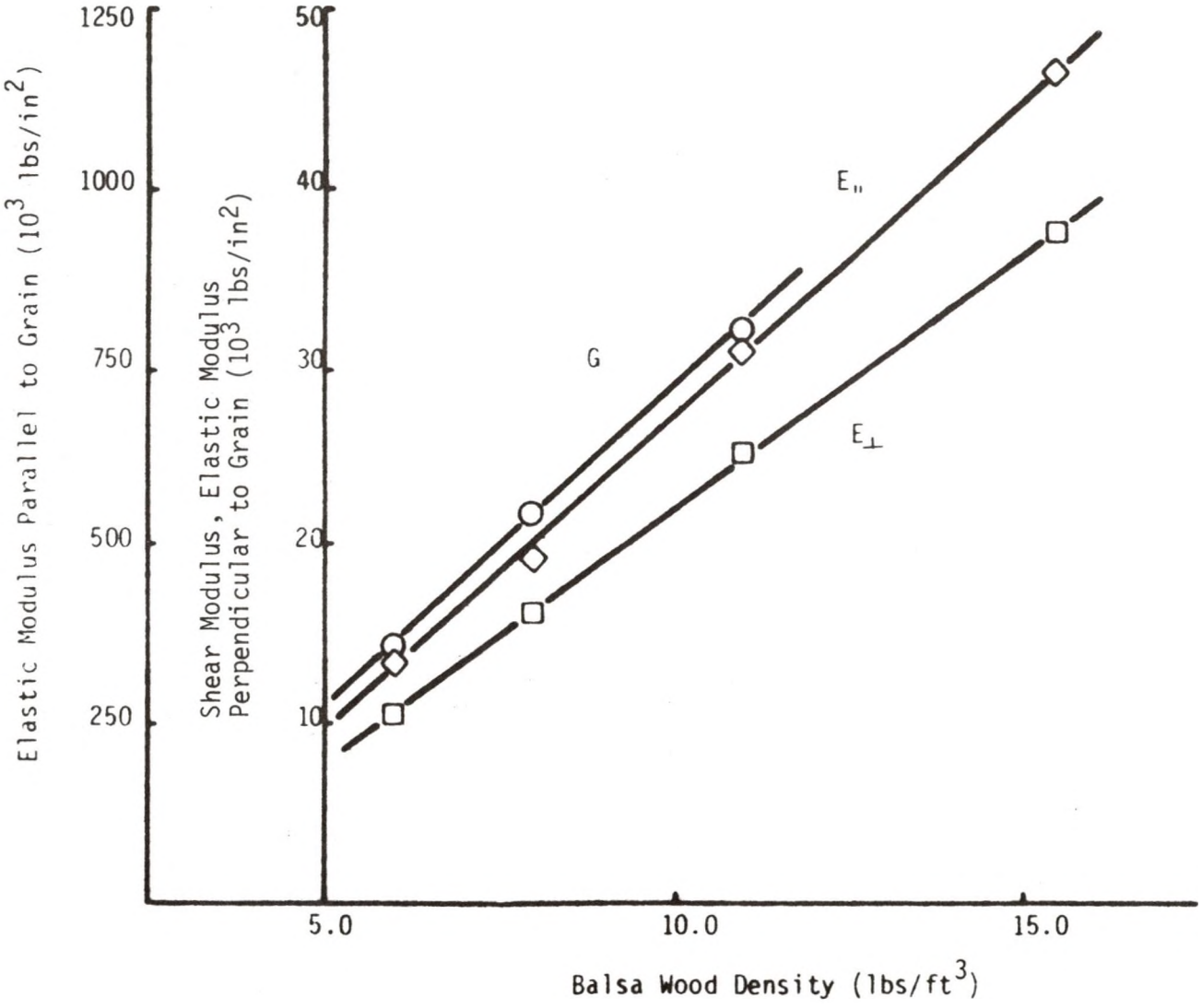

FIGURE 29 - BALSA WOOD MATERIAL PROPERTIES

the influence of a change in the core panel shear stiffness.

The weight density of the balsa wood used in the captive columns was not determined for every specimen. Excluding the above case, the density was nearly 7.0 pounds per cubic foot for all specimens in which the density was determined. Incorrect balsa wood properties are a possible source of error for specimens in which balsa wood was used as the core panel material.

Five square cross-section captive columns were built and tested to experimentally verify the influence of the wrap density. The wrap material was 0.0076 inch diameter Kevlar applied at a 45 degree angle with approximately 1.5 pounds of wrapping tension. The wrap densities were 0, 6.3, 18.9, 37.8, and 63.2 strands per inch for specimen numbers 25, 26, 28, 30, and 31, respectively.

Each captive column was tested using a 54 inch span length. The experimentally determined beam stiffness, based upon the average deflection of the top and bottom caps, is plotted in Figure 30 for each test. The predicted stiffnesses are also plotted in Figure 30 as a function of the wrap density.

The experimentally determined stiffness is less than the predicted stiffnesses for all five tests. Furthermore, if the specimen without any wrap is disregraded, the relative error increases with an increase in the wrap density. This change in the relative error may be attributable to a relaxation of some of the wrap strands during the wrapping operation. All of the strands are applied with the same amount of wrapping tension. The caps are drawn towards the core centerpiece due to this tension. As wrap is added, the amount of core deformation increases, which results in relaxation of the first strands that are applied. In effect, the

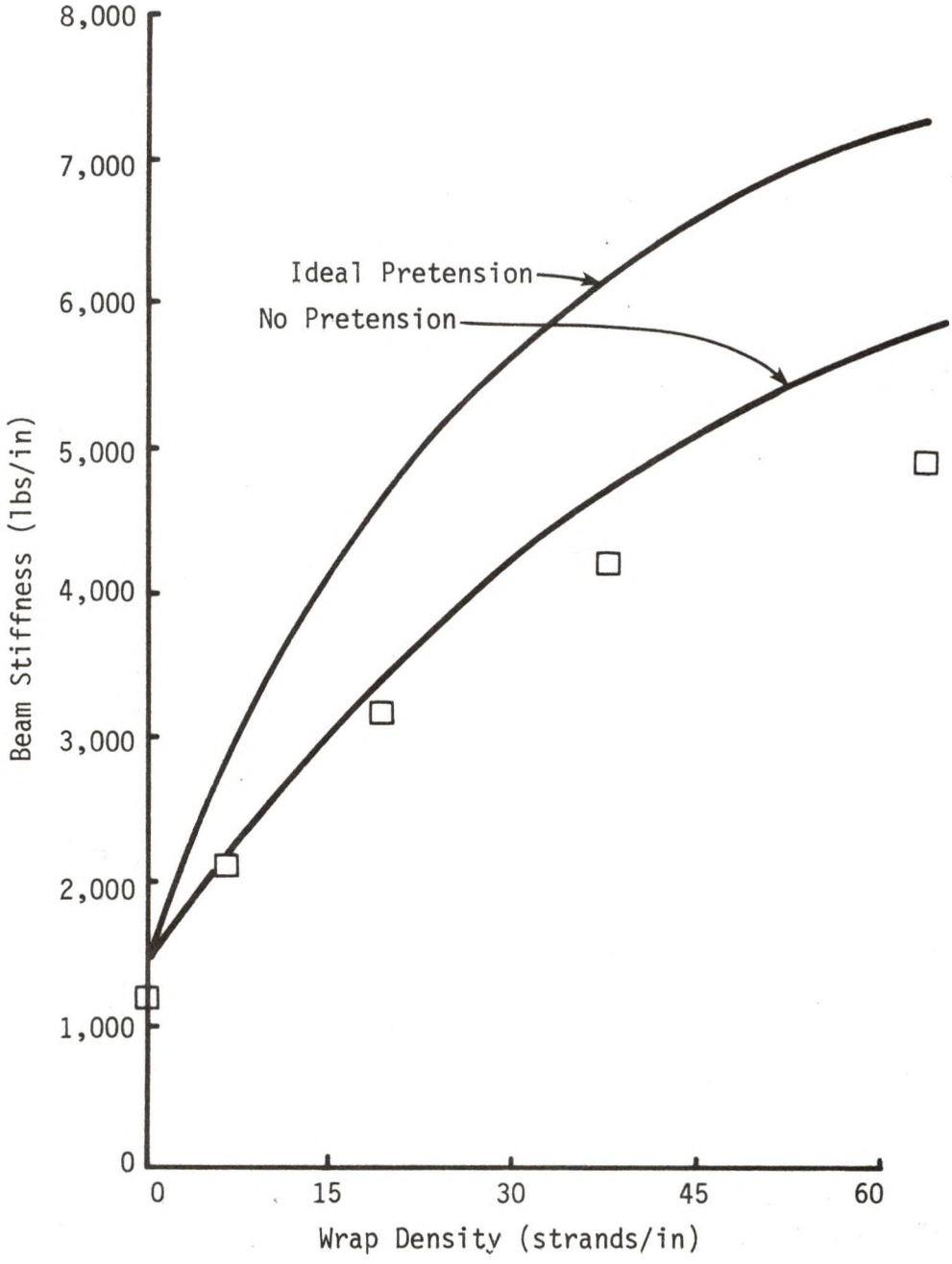

FIGURE 30 - BEAM STIFFNESS VS. WRAP DENSITY

pretension in the wrap strands that are applied last is equal to the wrapping tension and the strands that are applied first have little or no pretension, resulting in an average wrap pretension which is lower than the wrapping tension.

The relative error increases as the wrap density increases because of the decrease in the average wrap pretension. Furthermore, the amount of relaxation may be great enough to cause some of the wrap strands to become slack, and therefore the effective wrap density will be less. The predicted beam stiffnesses do not take into account this possible decrease in the wrap density.

Six square cross-section captive columns were constructed to experimentally determine the influence of the wrap angle. The cap centerline distance was 3.71 inches for specimen numbers 32, 33, and 34 and 3.75 inches for specimen numbers 35, 36, and 37. The wrap density was approximately 17 strands per inch of 0.0076 inch diameter Kevlar with a wrapping tension of 4.0 pounds. Wrap angles of 60, 45, and 30 degrees were used on specimen numbers 32 and 35, 33 and 36, and 34 and 37, respectively.

Each captive column was tested using a 48 inch span length. Since the cap centerline distance is very nearly the same for each group of specimens, the experimentally determined and the predicted beam stiffnesses are also very nearly equal. The experimentally determined beam stiffness, based upon the average deflections of the top and bottom caps for each pair of specimens at a given wrap angle is plotted in Figure 31. The predicted stiffnesses, based upon an average cap centerline distance, is also plotted in Figure 31.

The average experimentally determined stiffness of the two specimens

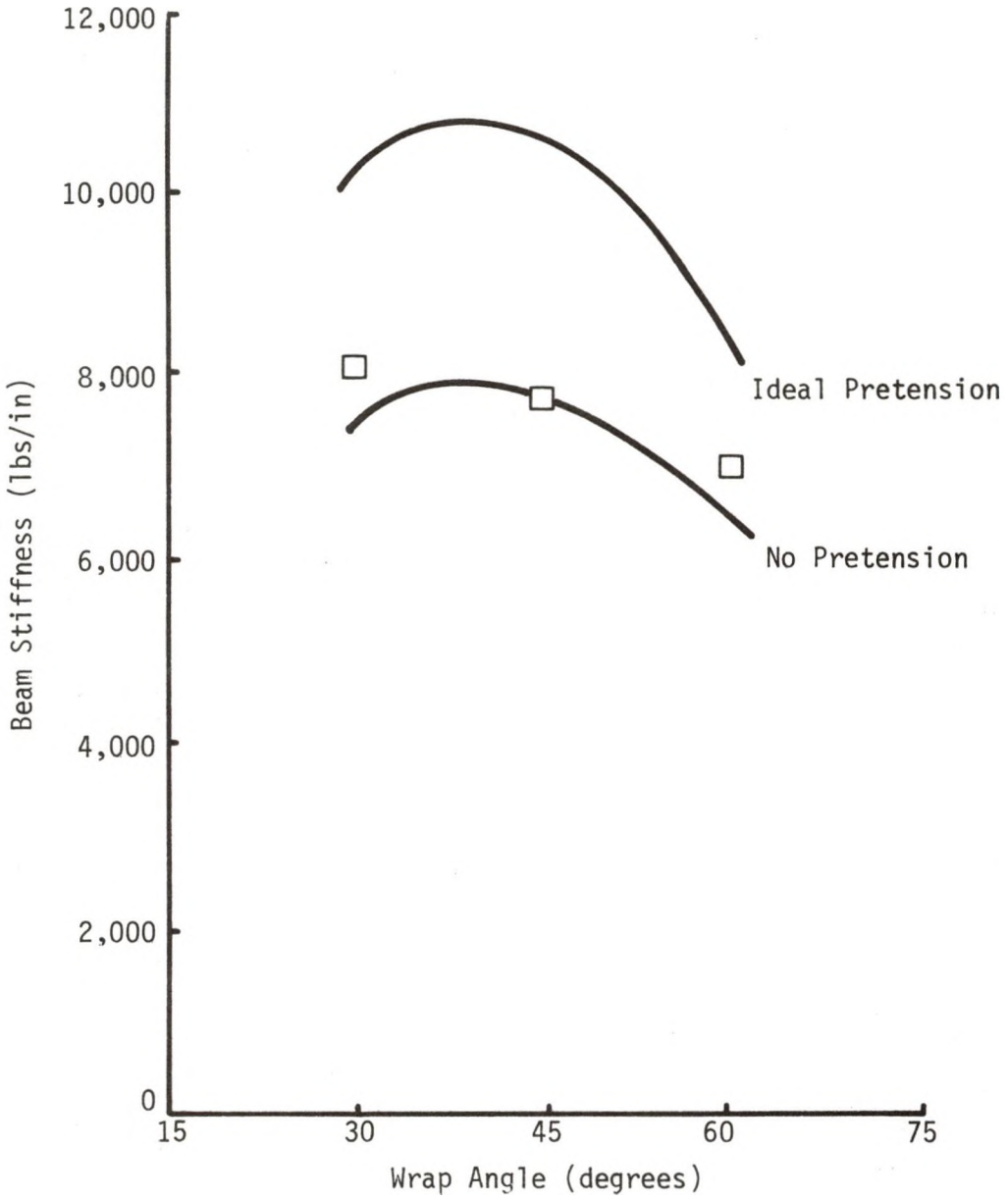

FIGURE 31 - BEAM STIFFNESS VS. WRAP ANGLE

wrapped at a 45 degree wrap angle was equal to the predicted stiffness for the case of no wrap pretension. The average experimentally determined stiffness for the other two wrap angles is in the lower range of predicted stiffnesses. The maximum beam stiffness according to the experimental data is in the vicinity of 30 degrees. This supports the previously determined analytical optimum for a constant wrap density of 35 degrees.

The relative error between the experimentally determined stiffness and either of the predicted stiffnesses is not the same for each wrap angle. This series of tests suggests that the analytical method incorrectly accounts for the influence of the wrap angle. An area that requires further study is the influence of the wrap angle in maintaining the cross-sectional geometry during the application of a load. A decrease in the cross-sectional deformation will lead to an increase in the beam stiffness. The wrap and the core resist cross-sectional deformation. It is logical to assume that the degree of deformation is dependent upon the wrap angle.

Nine captive columns were built and tested to determine the influence of the wrapping tension, and thus the wrap pretension. The wrap material was 0.0132 inch diameter Kevalar applied at a 45 degree angle. Three wrapping tensions, 1.5, 4.5, and 6.0 pounds, were used with each of three densities, 2.5, 7.5, and 15.0 strands per inch.

Each specimen was tested at span lengths of 88, 72, and 56 inches. The experimentally determined beam stiffness, based upon the average deflection of the top and bottom caps, is plotted in Figures 32, 33, and 34 for each test. The predicted stiffnesses as a function of the span length are also plotted in the figures.

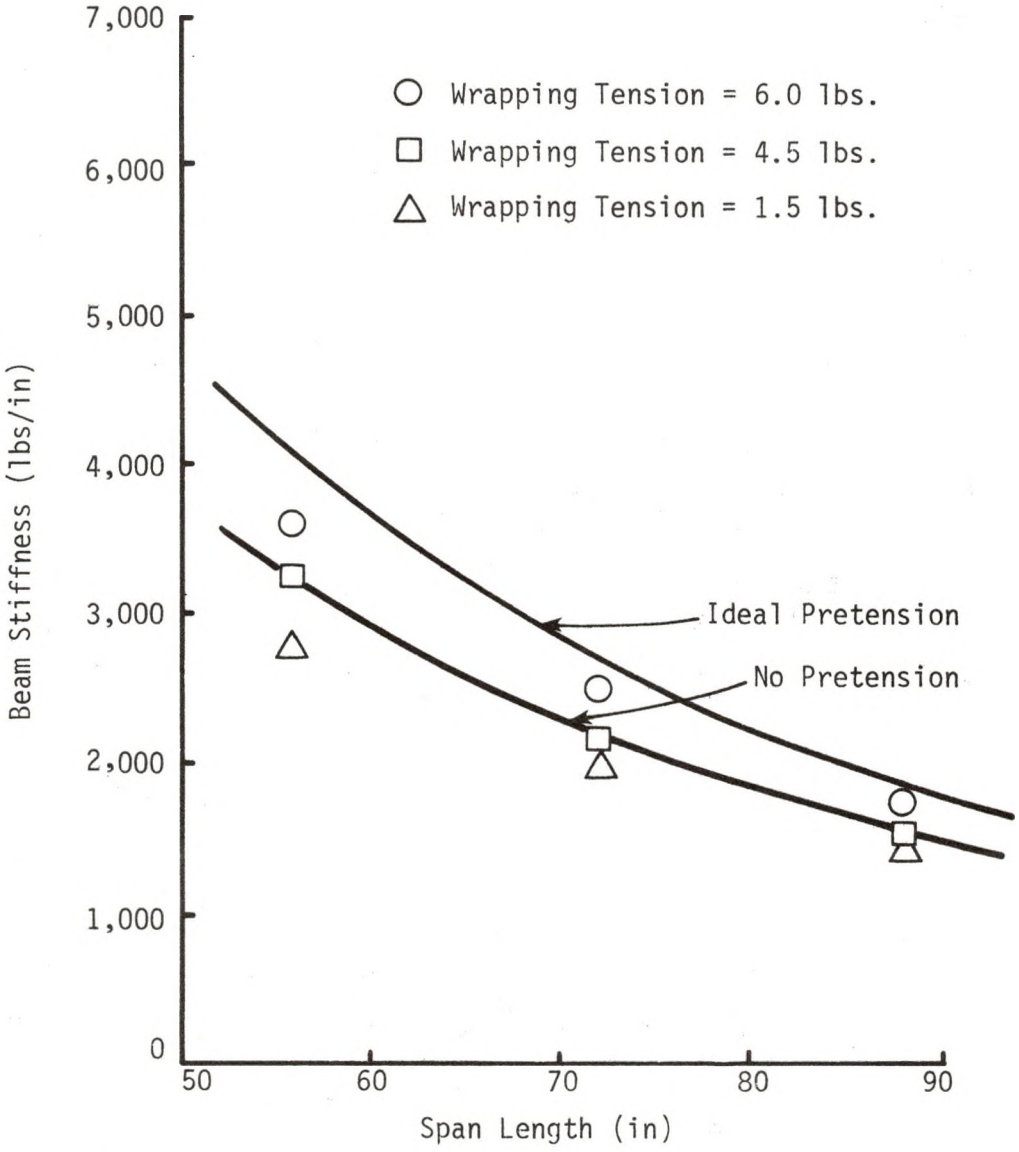

FIGURE 32 - BEAM STIFFNESS VS. SPAN LENGTH, WRAP DENSITY = 2.5 STRANDS/INCH

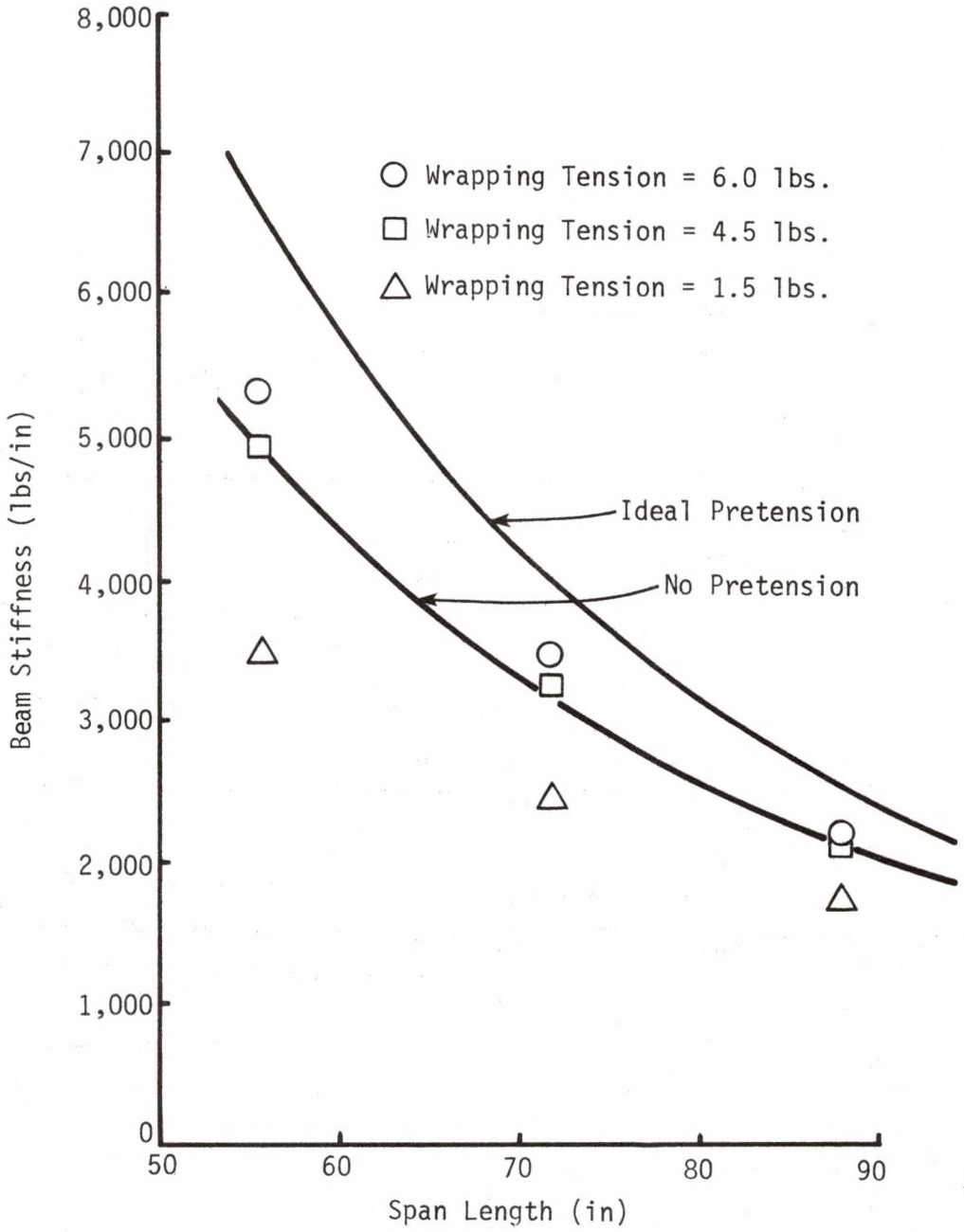

FIGURE 33 - BEAM STIFFNESS VS. SPAN LENGTH, WRAP DENSITY = 7.5 STRAND/INCH

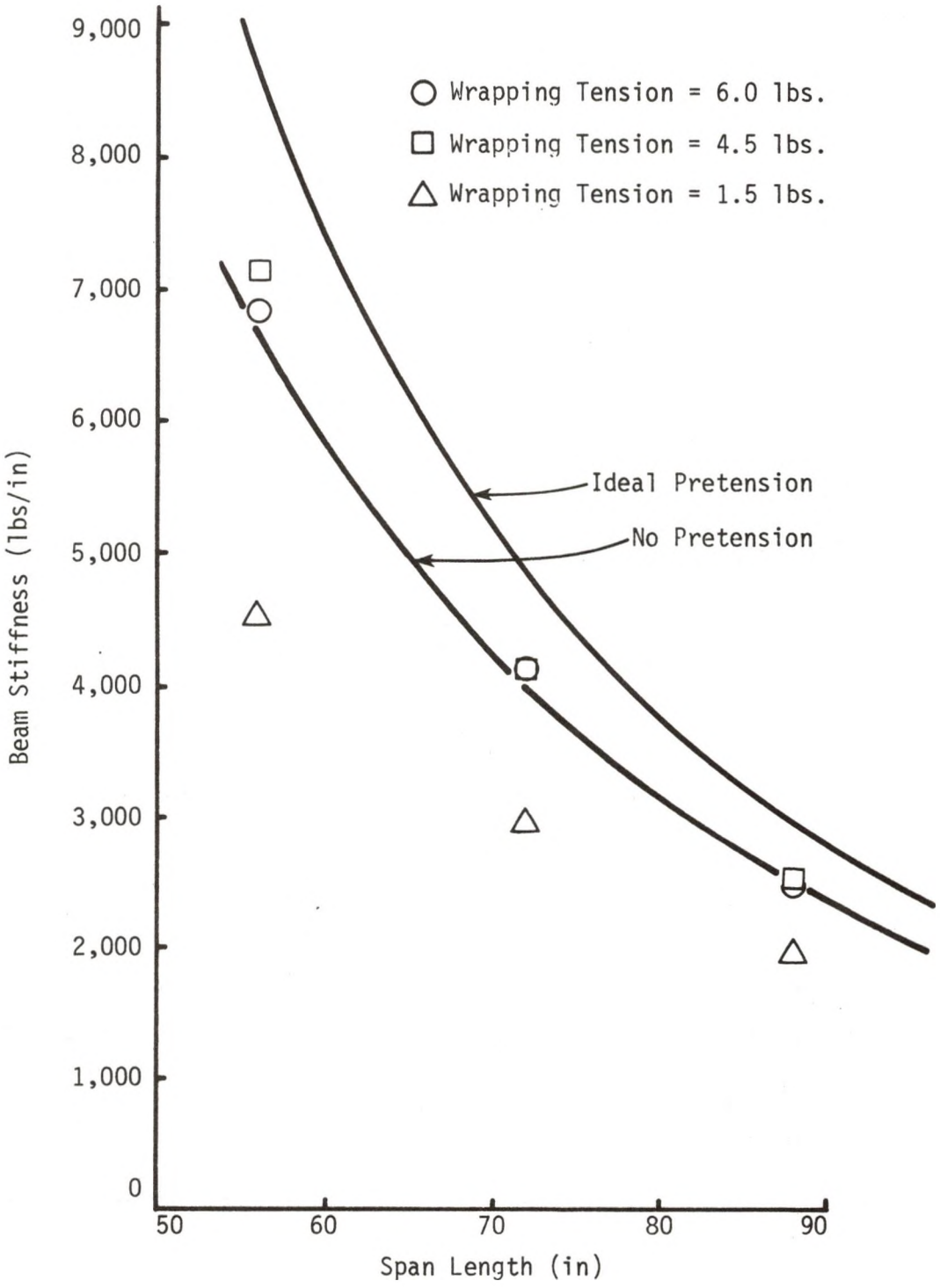

FIGURE 34 - BEAM STIFFNESS VS. SPAN LENGTH,
WRAP DENSITY = 15.0 STRANDS/INCH

The average wrap pretension is slightly less than the wrapping tension for specimens with a relatively low wrap density, with the difference between the average pretension and the wrapping tension increasing as the wrap density increases. According to the analytical method, the beam stiffness should increase with an increase in the wrap pretension. This predicted behavior is experimentally verified for the specimens wrapped with densities of 2.5 or 7.5 strands per inch. With 1.5 pounds of wrapping tension, the experimentally determined stiffness is less than the predicted stiffness for the case of no pretension. The experimentally determined stiffness when the wrapping tension is increased falls between the two predicted stiffnesses with the upper bound in all cases the predicted stiffness for ideal pretension.

For the specimens wrapped with a density of 15.0 strands per inch, the experimental results indicate that 4.5 pounds of wrapping tension produces the maximum beam stiffness. As the wrapping tension is increased, the deformation of the cross-section during the wrapping operation will increase. The net effect of the increase in the pretension of the strands that were applied last and the increase in the relaxation of the strands that were applied first is a decrease in the average wrap pretension. It is possible that this decrease in the average pretension causes a decrease in the beam stiffness, which is apparent in the experimental results.

This change in the average pretension is also apparent in the results from the specimens wrapped with a density of 7.5 strands per inch. The increase in the stiffness when the wrapping tension is increased from 4.5 to 6.0 pounds is less than the increase in the stiffness when the tension is increased from 1.5 to 4.5 pounds. This

would suggest that a further increase in the tension above 6.0 pounds would lead to only a very slight increase in the average wrap pretension. For the specimens with a density of 2.5 strands per inch, the increase in the beam stiffness is approximately the same for both increases in the wrapping tension, which suggests that the average wrap pretension will increase if the wrapping tension is increased.

It has been shown that an increase in the wrap density or wrapping tension can cause an increase in the amount of relaxation that occurs during the wrapping operation. The wrap angle will also influence the amount of relaxation that occurs. The amount of relaxation will increase as the wrap angle increases. This phenomenon was not taken into account in the discussion of the tests conducted with specimen numbers 32 through 37 and it may help explain the change in the relative error.

Determining the extent of wrap relaxation during the wrapping operation is a complex subject in itself. The relaxation can be reduced by utilizing a core panel material with a high compressive elastic modulus in the direction perpendicular to the longituidinal axis or by increasing the core panel thickness. Either one of these measures will lead to a decrease in the cross-sectional deformation. If possible, a low density of wrap material with a relatively large cross-sectional area should be used instead of a high density of wrap material with a small cross-sectional area.

Sources of Error in the Analytical Approach

Various sources of error between the experimentally determined beam stiffness and the stiffness predicted by using the analytical approach of Chapter 2 were mentioned in the preceding section. The main sources of error that were identified dealt with incorrect material properties and

the possibility of an incorrect application of some of the classical beam theory concepts. Two additional sources of error are localized discrepancies in the stress distributions and localized cross-sectional deformation. Both of these sources of error, which will be discussed in the following paragraphs, are related to the way in which the load is applied to the captive column.

As noted in Chapter 4, the experimental load is assumed to be equally distributed between two caps for a square cross-section captive column. The core and the wrap must transfer part of the load from these caps to the other two caps. The same situation occurs at each end support; the reaction is equally divided between two caps, with the core and the wrap transferring part of the reaction to the other two caps. In the case of a triangular cross-section captive column, the distribution of the load and the reaction is dependent upon the orientation of the member; the load or reaction is divided between all three caps or only two of the caps. The transfer of force from one cap to another cap causes inconsistencies in the predicted normal stresses and shear stresses in the vicinity of the concentrated load and the end supports.

The effect of these localized inconsistencies in the stress distributions is disregarded in the analytical method. It is expected that the deflection would increase if the localized inconsistencies were included in the analysis.

Deformation of the cross-section will also occur in the vicinity of the concentrated load and the end supports. The transfer of force from one cap to another is one possible explanation for this deformation. A second, and probably more significant explanation of the deformation is related to the line of action of the load or the reaction. The line of

action of the load is inclined at a 45 degree angle to the core panels. In addition to the vertical deflection of the cross-section as a whole, the two top caps will experience vertical and horizontal deflection relative to the core centerpiece. In effect, the core panels act as cantilevered beams, rigidly supported at the core centerpiece. This deflection of the caps relative to the centerpiece is resisted by the core panels and the wrap.

The above two types of cross-sectional deformation are local effects; they occur in the vicinity of the concentrated load and the end supports. The third type of cross-sectional deformation occurs at all cross-sections of the captive column. In a solid rectangular beam subjected to a pure bending moment, the longituidinal extension in the material on the convex side of the beam is accompanied by lateral contraction and the longituidinal compression on the concave side is accompanied by lateral expansion. The cross-sectional shape changes as a result of the lateral expansion and contraction. The vertical sides become inclined to each other and all straight lines parallel to the neutral axis curve so as to remain normal to the sides of the section, see Figure 35. In a captive column, it is expected that the longituidinal extension and compression of the member will result in a decrease or increase, respectively, in the cross-sectional area of the caps. An insignificant amount of deformation, as in Figure 35, will also be present, which will lead to a very slight increase in the deflection.

The analytical approach is unable to account for the cross-sectional deformation that occurs. The predicted deflection would increase if the deformation was included in the analysis.

The additional increase in the deflection attributable to the local

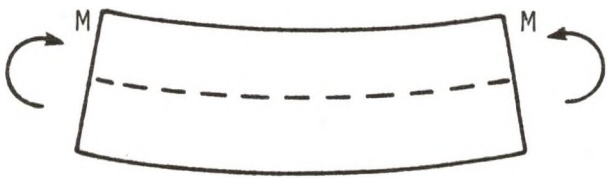

A) Section of a Rectangular Beam Subjected to a Pure Bending Moment

B) Cross-Section of the Beam

FIGURE 35 - CROSS-SECTIONAL DEFORMATION DUE TO LATERAL EXPANSION AND CONTRACTION

inconsistencies in the stress distributions and the cross-sectional deformation lead to a decrease in the beam stiffness. Since the analytical approach does not account for either increase in the deflection, the predicted stiffness values will be greater than the actual beam stiffness.

The experimental results verify the above statement. In the majority of the tests that were performed, the experimentally determined beam stiffness is below or in the lower range of stiffnesses predicted from the analytical approach. Furthermore, the predicted stiffness becomes greater, relative to the experimental stiffness, as the significance of the deflection due to shear force increases. This is an indication that the major cause of error is the local discrepancies in the shear stress distribution.

CHAPTER 7

COMPUTER MODEL RESULTS

Comparisons between the analytically predicted and the experimentally determined beam stiffnesses were made in Chapter 6. A brief discussion concerning the computer model predicted beam stiffness, relative to both the experimentally determined and the analytically predicted stiffness, will be covered in this chapter. There will also be a description of a method that may be used to model wrap pretension using the computer model, with comparisons between the stiffness obtained by using this method and the results from some of the flexure tests.

Computer Model Versus Experimentally Determined Beam Stiffness

Increases in the deflection due to localized discrepancies in the stress distribution and the deformation of the cross-section are included in the finite element analysis of a captive column in flexure. For this reason, it is expected that the computer model will yield a better prediction of the experimentally determined stiffness than the analytical approach.

As seen by an examination of Table 3 in Chapter 5, the experimentally determined stiffness is within the range of the computer predicted stiffness for 65 percent of the tests that were performed. For the tests in which the experimental stiffness is not bounded by the two extreme predicted stiffnesses, inaccurate material properties is the most likely source of error in the predicted results. This statement is based on the fact that FRP caps were used in the majority of the specimens in which the computer model predicted stiffnesses did not bound the

experimentally determined stiffness. In these cases, the experimentally determined stiffness is greater than the predicted stiffnesses. If a greater value was used for the FRP elastic modulus in the computer model, the predicted results would have been in better agreement with the experimental results, which is the same conclusion that was drawn from the analytical versus experimental results.

Computer Model Versus Analytical Beam Stiffness

The same material properties were used for all of the captive column components in the analytical approach and the computer model to obtain the predicted beam stiffness values for all of the flexure tests. By comparing the predicted stiffness values from both methods of analysis, errors in the material properties will be eliminated.

The beam stiffnesses predicted by using the analytical approach and the computer model are listed in Table 6. The deflection of the neutral axis and the average deflection of the top and bottom caps and the core centerpiece were used to obtain the stiffnesses by the two respective methods. Beam stiffnesses are listed for the cases of no wrap pretension and ideal wrap pretension for both methods.

The analytically predicted stiffness is greater than the computer model predicted stiffness for the case of no wrap pretension for all of the specimens. For the case of ideal wrap pretension, the analytically predicted stiffness is greater than the computer model predicted stiffness for the majority of the specimens. The analytically predicted stiffness becomes greater, relative to the computer model predicted stiffness, as the significance of the deflection due to shear force increases. This statement supports the claim that the major source of

TABLE 6

ANALYTICAL METHOD VS. COMPUTER MODEL

Test Number	Beam Stiffness (lbs/in)			
	Analytical		Computer Model	
	No Pretension	Ideal Pretension	No Pretension	Ideal Pretension
1	270	279	259	283
2	469	492	442	500
3	911	979	827	999
4	807	880	683	843
5	1330	1500	1070	1410
6	2370	2810	1730	2590
7	1030	1170	837	1100
8	1630	1930	1260	1790
9	2740	3450	1970	3110
10	2260	2930	1570	2540
11	3210	4400	2220	3750
12	4760	6890	3280	5840
13	238	247	245	266
14	701	787	679	827
15	858	1000	826	1060
16	1620	2180	1530	2370
17	358	359	376	382
18	1350	1370	1270	1330
19	6630	6900	4640	5460
20	1720	2000	1460	1930
21	1840	2100	1450	1910
22	2250	2730	1830	2570
23	2530	3020	1870	2610
24	147	149	144	150
25	221	226	215	226
26	352	363	339	364
27	609	636	574	636
28	1170	1250	1060	1240
29	276	283	265	283
30	416	428	394	430
31	664	692	618	696
32	1150	1220	1040	1230
33	2210	2420	1890	2440
34	1120	1220	954	1180
35	1610	1800	1330	1730
36	2410	2780	1890	2640
37	3780	4580	2800	4260
38	6300	8150	4290	7350
39	1160	1190	1080	1160
40	1720	1780	1580	1720
41	2670	2800	2380	2670
42	4430	4720	3770	4400

TABLE 6 (Continued)

Test Number	Beam Stiffness (lbs/in)			
	Analytical		Computer Model	
	No Pretension	Ideal Pretension	No Pretension	Ideal Pretension
43	7980	8730	6250	7810
44	326	333	322	343
45	326	333	321	343
46	603	623	592	651
47	603	623	592	651
48	1284	1356	1240	1450
49	1284	1356	1240	1450
50	1320	1480	1170	1450
51	1320	1480	1160	1440
52	2230	2620	1890	2550
53	2230	2620	1890	2520
54	4120	5190	3260	4960
55	4120	5190	3240	4840
56	6210	7810	4430	6970
57	6350	8010	4500	7120
58	5360	6960	4290	6610
59	5360	6960	4250	6450
60	-1400-		-978-	
61	2180	2850	1570	2450
62,63,64	3430	4720	2240	4150
65	4710	6220	2870	5600
66	5800	7250	3390	6680
67	6430	8330	4230	6470
68	7760	10600	4900	8160
69	7460	10100	4650	7480
70	6460	8380	4260	6510
71	7780	10600	4940	8230
72	7470	10100	4700	7570
73,76,79	1540	1850	1170	1600
74,77,80	2170	2700	1600	2290
75,78,81	3190	4100	2270	3410
82,85,88	2090	2540	1530	2300
83,86,89	3120	3990	2160	3530
84,87,90	4890	6670	3170	5700
91,94,97	2540	2960	1850	2770
92,95,98	3990	4900	2690	4480
93,96,99	6670	8770	4090	7750
100	2460	2770	1960	2490
101	3840	4470	2890	3890
102	6350	7750	4440	6440
103	2460	2780	1920	2470
104	3840	4500	2820	3860
105	6340	7810	4340	6370

error in the analytical approach is the local discrepancies in the shear stress distribution.

Cross-Sectional Deformation

The deflection of both the top and bottom caps was determined for approximately half of the flexure tests that were performed. The experimentally determined beam stiffnesses and the stiffnesses predicted by using the computer model, based upon the deflection of the top and bottom caps, are listed in Table 3 of Chapter 5. The relative error between the experimentally determined and the computer model predicted stiffnesses is approximately the same for the top caps and the bottom caps for any given test. This is an indication that the computer model correctly predicts the effect of the cross-sectional deformation.

The wrap and the core resist the deformation of the cross-section. Since the computer model includes this deformation in the analysis, it is expected that the wrap will have a much greater effect upon the computer model predicted stiffness than on the analytically predicted stiffness. By comparing the range of stiffness values in Table 6, with the lower bound being the case of no wrap pretension and the upper bound being the case of ideal wrap pretension, it is apparent that the wrap does affect the computer model predicted stiffness to a much greater extent. The range of computer model predicted stiffness is much greater than the range of analytically predicted stiffness, which indicates that the wrap has a much greater role in the computer model than resisting shear forces.

Wrap Pretension

During the application of a concentrated midspan load to a simple-supported captive column, approximately half of the wrap strands

on the sides of the captive column will be subjected to a compressive force. Since the wrap strands can carry only tensile forces, these strands will merely relax and do not contribute to the beam stiffness of the captive column. If the wrap strands are pretensioned, they will be able to carry the compressive force. As the load is applied, the tensile force in the strands, due to pretension introduced during the wrapping operation, will be reduced because of the compressive force attributable to the load.

Ideal wrap pretension has been defined to be the pretension in the wrap needed to keep all of the strands in tension during a given load application. The computer model can easily be used to compute the ideal pretension. With all of the wrap truss elements in place in the finite element computer model, the design load is applied and produces tensile forces in some of the wrap truss elements and compressive forces in the other wrap truss elements. The wrap truss element is modeling a group of individual wrap strands. To determine the maximum compressive force in an individual wrap strand, the maximum compressive wrap truss element force is divided by the number of individual strands that the truss element is modeling. To keep this strand in tension for the given load, an equal tensile force must be applied to the strand. This tensile force is the ideal pretension.

The ideal pretension for a given captive column is dependent upon the load that will be applied to the member. As the load is increased, the compressive forces in the wrap truss elements will increase, and therefore the ideal pretension will increase.

The problem of wrap relaxation during winding was introduced in the previous chapter. The average wrap pretension is less than the wrapping

tension because of the compressive forces that are exerted on the core during the wrapping operation. The average pretension can be determined in a relatively straightforward manner by using the thermal stress capabilities of the computer model. With all of the wrap truss elements in place in the computer model, a thermal stress is applied to the wrap truss elements. The thermal stress is equal to the product of the wrapping tension multiplied by the number of wrap strands that the truss elements are modeling. The thermal stress will compress the plane stress elements that represent the core panels, and thus the tension in each truss element will be reduced. The average wrap pretension is determined by dividing the reduced truss element tensile force by the number of strands that the truss element is modeling.

The process needed to determine the ideal wrap pretension and the average wrap pretension have been described. The maximum beam stiffness is obtained when the average wrap pretension is equal to the ideal wrap pretension. An increase in the average pretension, above the ideal pretension, will not increase the beam stiffness; it will only cause an increase in the force in each wrap strand and the compressive stress in the core panels. If the average wrap pretension is less than the ideal pretension, the beam stiffness will fall within the range of beam stiffness values bounded by the case where there is no wrap pretension and the case where there is ideal wrap pretension. The determination of this beam stiffness will be discussed in the following paragraphs.

For the following discussion, assume that the average wrap pretension is less than the ideal wrap pretension and that the load is gradually applied from no load to the design load. During the initial phase of the load cycle, all of the wrap truss elements are in tension

and the beam stiffness is equal to the stiffness produced if there is ideal wrap pretension. As the load is applied, the tension in the truss elements is reduced due to the compressive forces induced by the load. At some point in the load cycle, the tension in some of the truss elements is reduced to zero. These truss elements are then removed from the computer model, which reduces the beam stiffness. As the load is further increased, the tension in other truss elements is reduced to zero. These elements are also removed from the model causing a further decrease in the stiffness. This process is repeated until the design load is reached.

In essence, removing the wrap truss elements when their tension is reduced to zero causes a stepped decrease in the beam stiffness. An average beam stiffness can be determined by summing the products of the beam stiffness in each step multiplied by the load over which this stiffness was in effect. The quantity that is obtained is then divided by the design load to obtain the average beam stiffness.

The preceding methods for dealing with wrap pretension will be used to analyze some of the specimens that were built and tested in flexure. A total load of 600 pounds was applied to captive column numbers 44, 45, and 46. At this load, the maximum compressive wrap strand force, when all of the truss elements are in place, is 2.16 pounds for each span length; 88, 72, or 56 inches. A wrap pretension of 2.16 pounds must be introduced into the wrap strands during the wrapping operation in order to achieve the maximum beam stiffness. Using the thermal stress capabilities of the computer model, it is determined that a 1.0 pound wrapping tension results in an average wrap pretension of 0.72 pounds. Since the computer program is linear, a wrapping tension of 3.0 pounds

(2.16/0.72 = 3.0) is needed to achieve the maximum stiffness.

If the wrapping tension is less than 3.0 pounds, the average beam stiffness will be between the two stiffnesses represented by the cases of no wrap pretension and ideal wrap pretension. In Figure 36, the beam stiffness is plotted as a function of the load for the case of a wrapping tension of 1.0 pound and a span length of 88 inches. The ideal wrap pretension, no wrap pretension, and average beam stiffnesses are also plotted. The average deflection of the core centerpiece node and the top and bottom cap nodes was used in the determination of the stiffnesses.

The average beam stiffness for an 88 inch span length is plotted in Figure 37 as a function of the wrapping tension. The experimentally determined beam stiffnesses, based upon the average deflection of the top and bottom caps, for three wrapping tensions are also plotted.

The beam stiffness predicted by the computer model is greater than the experimentally determined stiffness. This is possibly due to the way in which the pretension was modeled. In the method that was used, it is assumed that the pretension is the same for all of the wrap strands. In the actual specimen, the pretension is very nearly equal to the wrapping tension in the outer strands with little or no pretension in the inner strands. Some of the inner strands may be totally slack, and therefore the wrap density should be decreased until the tensile force due to the applied load causes these strands to become taut.

The analytical method of Chapter 2 can also be modified to account for the wrap pretension. The tension in the wrap strands due to the wrapping operation produces deformation of the core. A relationship between the wrapping tension and the average wrap pretension can be developed by examining the deformation of the core produced by the

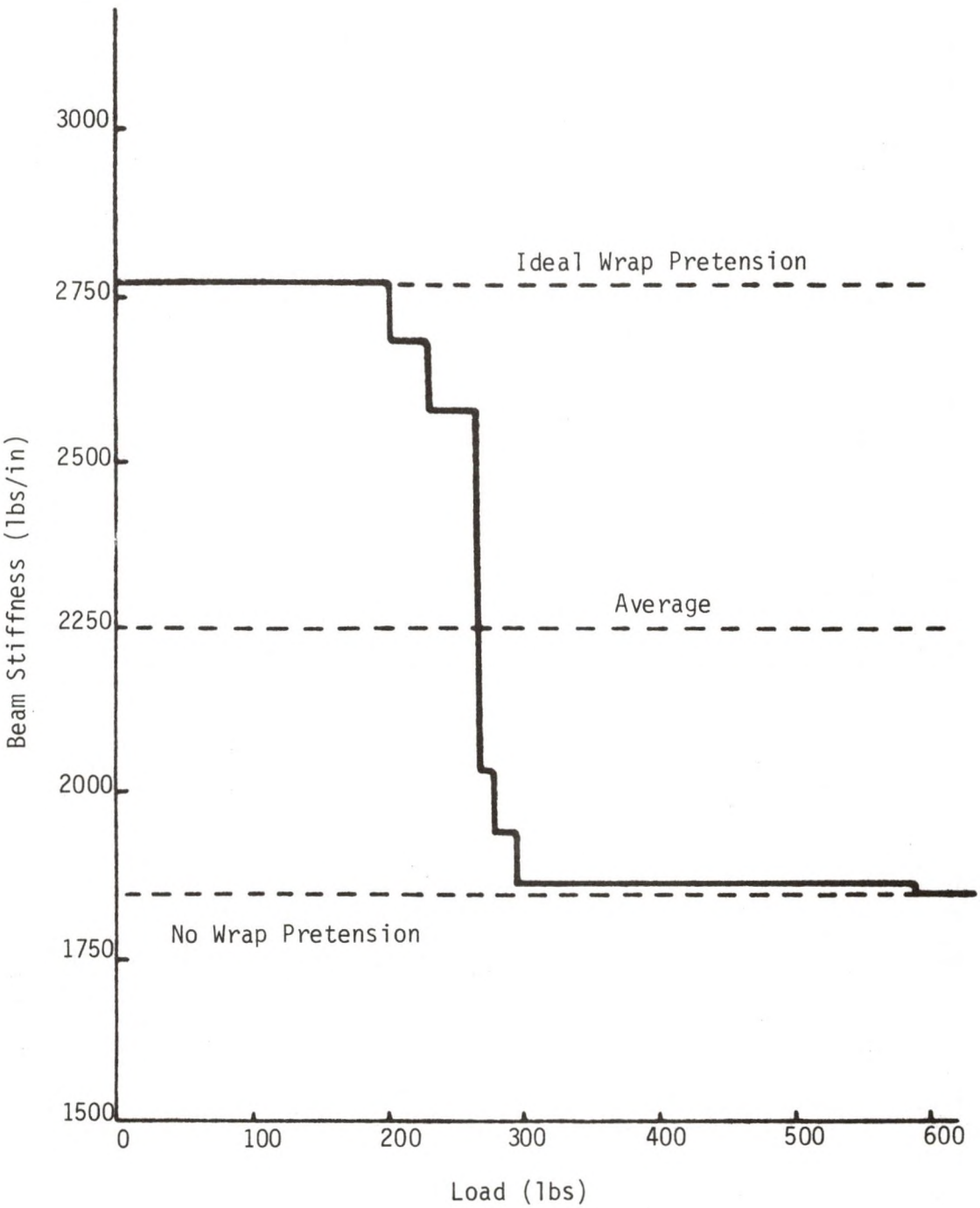

FIGURE 36 - BEAM STIFFNESS VERSUS LOAD FOR 1.0 POUND OF WRAPPING TENSION

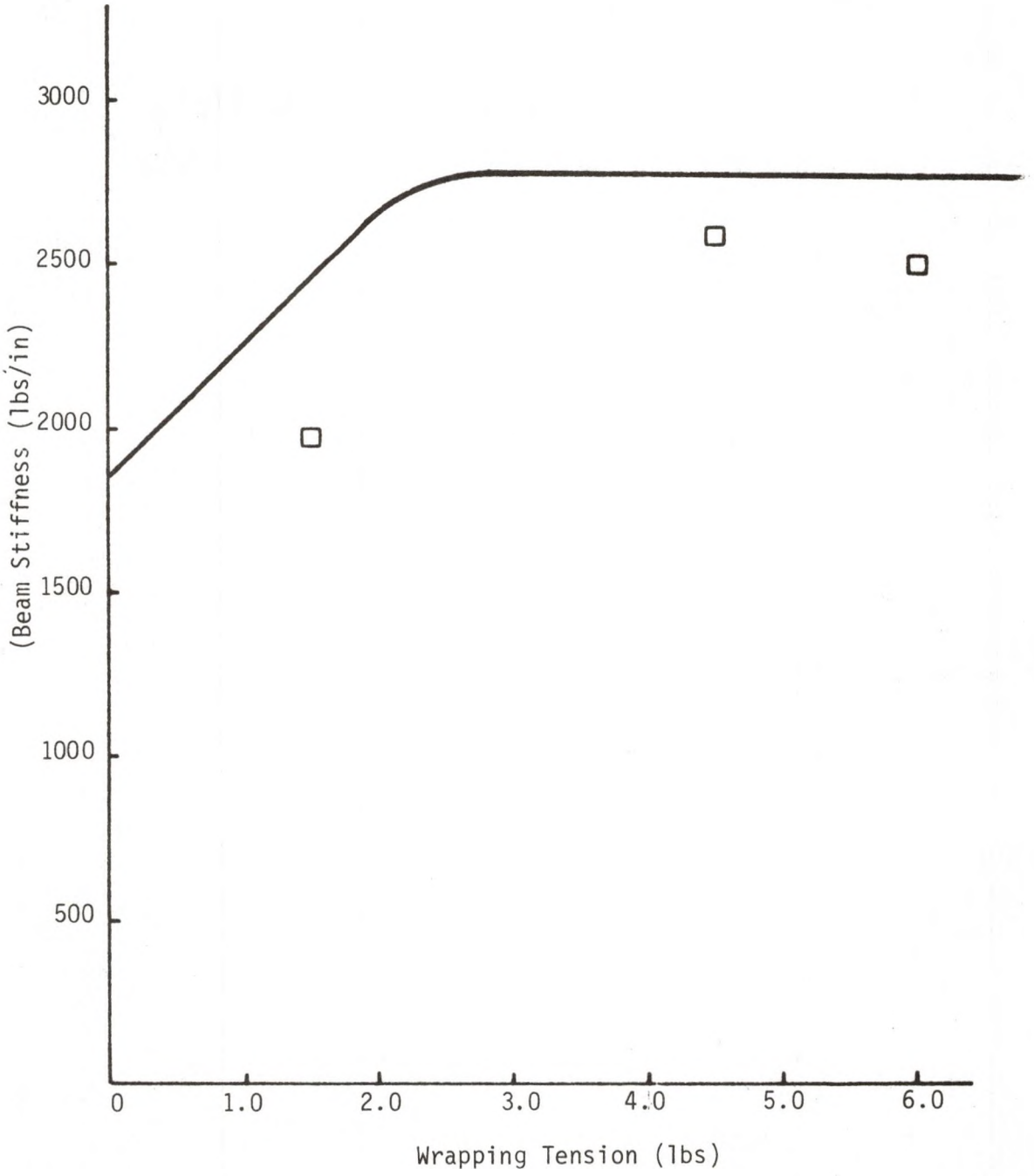

FIGURE 37 - BEAM STIFFNESS VERSUS WRAPPING TENSION

wrapping operation. The ideal wrap pretension can be determined by relating the deformation of an equivalent wrap panel, due to the percentage of the shear force that the wrap panel carries, to the tensile and compressive forces in the wrap strands that make up the panel.

In a similar fashion, the beam stiffness for a captive column in which the average wrap pretension is less than the ideal pretension can be determined. The stiffness will be equal to the ideal pretension stiffness until the load is great enough to cause relaxation of some of the wrap strands. Since the shear force is uniform along the length of the captive column for a midspan load, all of the wrap strands that relax will relax at the same load. Instead of the multiple step decrease in the beam stiffness that is predicted from the computer model, there will be a one step decrease in the stiffness from the ideal pretension stiffness to the no pretension stiffness. After the load at which the decrease in the beam stiffness occurs is determined, an average stiffness can be found.

These methods for dealing with the wrap pretension are included here for completeness only. The computer model method requires multiple execution of the program, one execution for each beam stiffness, with a resulting increase in the necessary computer time. The use of the analytical method for predicting the effect of wrap pretension requires further study and is beyond the scope of this research effort. It is recommended that the effect of wrap pretension be disregarded in the initial design of a captive column for a specific application. After a preliminary design has been chosen, the effect of wrap pretension can be included, which may result in minor changes in the preliminary design to meet all of the design requirements.

CHAPTER 8

OTHER FLEXURAL LOADING CONDITIONS

The primary emphasis of this research effort has been the analysis of a captive column loaded as a simple-supported beam with a concentrated midspan load. The computer model can easily be used to model other flexural loading conditions by assigning the necessary boundary conditions and applying the desired load. The analytical development of Chapter 2 is limited to the determination of the midspan deflection of a captive column subjected to the previously described load condition. The applicability of the analytical approach for predicting the deflection at points other than the location of the load and for other flexural loading conditions will be investigated in this chapter.

Castigliano's Theorem

Castigliano's theorem states that the displacement of an elastic body under the point of application of a force, in the direction of that force, is given by the partial derivative of the total elastic strain energy with respect to that force [5]. For a captive column subjected to a flexural load, there is elastic strain energy due to normal bending stresses and shear stresses. Castigliano's theorem is represented by the following equation:

$$\delta = \frac{\partial U_{normal}}{\partial F} + \frac{\partial U_{shear}}{\partial F} \tag{63}$$

where δ = deflection at the applied force in the direction of the force

F = applied force

U_{normal} = elastic strain energy due to normal bending stresses

U_{shear} = elastic strain energy due to shear stresses.

Equation (9), which was developed in Chapter 2 and is repeated below, can be used to determine the elastic strain energy due to the normal bending stress if the cross-section is uniform along the length of the member:

$$U_{normal} = \int_0^L \frac{M^2 \, dx}{2EI} \tag{9}$$

where M = bending moment due to the applied force, F, and any other loads

L = span length

EI = flexural rigidity

The bending moment is the only term in equation (9) that is dependent upon the applied force, and therefore the derivative of the elastic strain energy due to the normal bending stress with respect to the force is equal to the following:

$$\frac{\partial U_{normal}}{\partial F} = \frac{1}{EI} \int_0^L M \frac{\partial M}{\partial F} \, dx \tag{64}$$

Substituting equation (12) into equation (5) results in the following expression for the elastic strain energy due to shear stresses:

$$U_{shear} = \int_{Volume} \frac{1}{2G} \left(\frac{VQ}{Ib} \right)^2 dV \tag{65}$$

where G = shear modulus

V = shear force due to the applied force, F, and any other loads

Q = first moment of area

I = moment of inertia

b = width of the cross-section

dV = incremental volume.

If the cross-section is uniform along the length of the member, then the shear modulus, first moment of area, moment of inertia, and cross-section width will all be independent of the axial position. Furthermore, the shear force is not a function of the cross-sectional shape, and equation (65) can be simplified to the following expression:

$$U_{shear} = \frac{1}{2GI^2} \int_{area} \left(\frac{Q}{b}\right)^2 dA \int_0^L V^2 \, dx \tag{66}$$

The shear force is the only term in equation (66) that is dependent upon the applied force, and therefore the derivative of the elastic strain energy due to the shear stress with respect to the force is equal to the following:

$$\frac{\partial U_{shear}}{\partial F} = \frac{1}{GI^2} \int_{area} \left(\frac{Q}{b}\right)^2 dA \int_0^L V \frac{\partial V}{\partial F} \, dx \tag{67}$$

Substituting equations (64) and (67) into equation (63) yields the following:

$$\delta = \frac{1}{(EI)_{eq}} \int_0^L M \frac{\partial M}{\partial F} \, dx + \frac{1}{G_{cap}} \left[\frac{E_{cap}}{(EI)_{eq}}\right]^2 \int_{area} \left(\frac{Q_{eq}}{b_{eq}}\right)^2 dA \int_0^L V \frac{\partial V}{\partial F} \, dx \tag{68}$$

In this equation, equivalent quantities were used for the flexural rigidity, moment of inertia, first moment of area, and cross-section width. From the development of equation (42) in Chapter 2, the following expression is obtained for a square cross-section captive column:

$$\int_{area} \left(\frac{Q_{eq}}{b_{eq}}\right)^2 dA = 2[J_1 + J_2 + J_3] \tag{69}$$

The integrals J_1, J_2, and J_3 are defined by equations (43), (44), and (45) respectively. From the development of equation (94) in Appendix D, the following expression is obtained for a triangular cross-section captive column:

$$\int_{area} \left(\frac{Q_{eq}}{b_{eq}}\right)^2 dA = J_1 + J_2 + J_3 + J_4 + J_5 + J_6 \tag{70}$$

The integrals J_1 through J_6 are defined by equations (95) to (100), respectively.

After the equivalent flexural rigidity and the term represented by equation (69) or (70) have been determined, equation (68) can be used to determine the deflection at any location on the longituidinal axis of a square or triangular cross-section captive column subjected to any flexural loading condition. The deflection curve for two loading cases will be considered in the remainder of this chapter.

Cantilevered Beam, Uniform Load

Consider a captive column loaded as a cantilevered beam with a uniform load of W pounds per linear inch. It is necessary to determine the lateral deflection at a distance x_o from the support. In order to do this, an arbitrary force F will be applied at the distance x_o in the direction in which the deflection is desired, see Figure 38. The arbitrary force will be set equal to zero after the integration in equation (68) is performed and therefore the force will not add to the deflection of the captive column.

The total bending moment and shear force are represented by the following expressions:

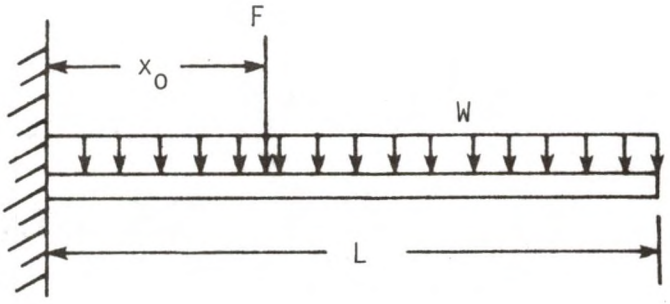

FIGURE 38 - CANTILEVERED BEAM, UNIFORM LOAD

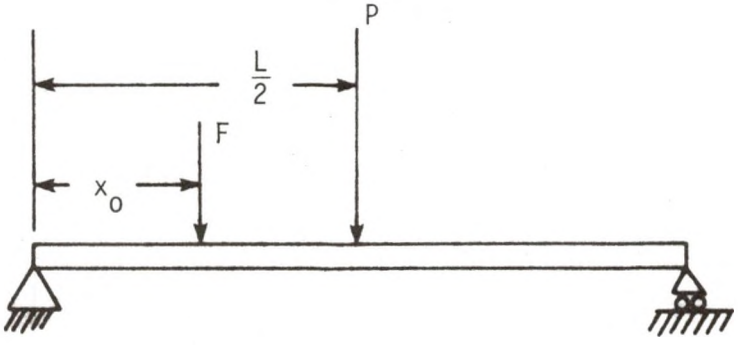

FIGURE 39 - SIMPLE-SUPPORTED BEAM, CONCENTRATED MIDSPAN LOAD

$$M = \frac{-W}{2}(L-x)^2 + F(x-x_o), \quad 0 < x < x_o$$

$$M = \frac{-W}{2}(L-x)^2, \quad x_o < x < L$$

$$V = W(L-x) + F, \quad 0 < x < x_o$$

$$V = W(L-x), \quad x_o < x < L$$

The above equations are used to obtain the following results:

$$\int_0^L M \frac{\partial M}{\partial F}\, dx = \int_0^{x_o} \left[\frac{-W}{2}(L-x)^2 + F(x-x_o)\right](x-x_o)\, dx + \int_{x_o}^{L} \frac{-W}{2}(L-x)^2 (0)\, dx$$

$$= \frac{W x_o^2}{24}(6L^2 - 4L x_o + x_o^2) + \frac{F x_o^2}{3} \tag{71}$$

$$\int_0^L V \frac{\partial V}{\partial F}\, dx = \int_0^{x_o} [W(L-x) + F](1)\, dx + \int_{x_o}^{L} [W(L-x)](0)\, dx$$

$$= W x_o \left(L - \frac{x_o}{2}\right) + F \tag{72}$$

Setting F equal to zero in equations (71) and (72), and substituting these equations into equation (68) yields the following:

$$\delta = \frac{W x_o^2}{24(EI)_{eq}}(6L^2 - 4L x_o + x_o^2)$$

$$+ \frac{W x_o \left(L - \frac{x_o}{2}\right)}{G_{cap}} \left[\frac{E_{cap}}{(EI)_{eq}}\right]^2 \int_{area} \left(\frac{Q_{eq}}{b_{eq}}\right)^2 dA \tag{73}$$

By making the appropriate substitutions, the lateral deflection at the distance x_o can be obtained from equation (73). By varying x_o from 0 to L in equation (73), the total deflection curve is obtained.

Simple-Supported, Concentrated Midspan Load

Equation (46), which was developed in Chapter 2, can be used to determine the lateral deflection of the midspan of a captive column loaded as a simple-supported beam with a concentrated midspan load. In order to determine the entire deflection curve, Castigliano's theorem must be used.

As in the previous example, an arbitrary force F will be applied at a distance x_o from the left support, see Figure 39. When x_o is less than one-half of the span length, the total bending moment and shear force are represented by the following expressions:

$$M = \frac{Px}{2} + \frac{F(L - x_o)x}{L}, \quad 0 < x < x_o$$

$$M = \frac{Px}{2} + \frac{Fx_o(L-x)}{L}, \quad x_o < x < \frac{L}{2}$$

$$M = \frac{P(L-x)}{2} + \frac{Fx_o(L-x)}{L}, \quad \frac{L}{2} < x < L$$

$$V = \frac{P}{2} + \frac{F(L - x_o)}{L}, \quad 0 < x < x_o$$

$$V = \frac{P}{2} - \frac{Fx_o}{L}, \quad x_o < x < \frac{L}{2}$$

$$V = \frac{-P}{2} - \frac{Fx_o}{L}, \quad \frac{L}{2} < x < L$$

The above equations are used to obtain the following results:

$$\int_0^L M \frac{\partial M}{\partial F}\, dx = \int_0^{x_o} \frac{Px}{2} \frac{(L-x_o)}{L}\, dx + \int_{x_o}^{L/2} \frac{Px}{2} \frac{x_o(L-x)}{L}\, dx + \int_{L/2}^{L} \frac{P(L-x)}{2} \frac{x_o(L-x)}{L}\, dx$$

$$= \frac{Px_o}{48}(3L^2 - 4x_o^2) \qquad (74)$$

$$\int_0^L V \frac{\delta V}{\delta F}\, dx = \int_0^{x_o} \frac{P}{2} \frac{(L-x_o)}{L}\, dx + \int_{x_o}^{L/2} \frac{P}{2} \frac{(-x_o)}{L}\, dx + \int_{L/2}^{L} \frac{-P}{2} \frac{(-x_o)}{L}\, dx$$

$$= \frac{Px_o}{2} \qquad (75)$$

In the development of equations (74) and (75), the arbitrary force F was set equal to zero after the derivatives with respect to the force were obtained, but before the integration was performed. This method is easier to use than the method used in the previous example and will yield the same end result. Substituting equations (74) and (75) into equation (68) results in the following:

$$\delta = \frac{Px_o}{48(EI)_{eq}}(3L^2 - 4x_o^2) + \frac{Px_o}{2G_{cap}} \left[\frac{E_{cap}}{(EI)_{eq}}\right]^2 \int_{area} \left(\frac{Q_{eq}}{b_{eq}}\right)^2 dA \qquad (76)$$

Equation (76) can be used to obtain the lateral deflection for x_o in the range from 0 to L/2, with the symmetry of the loading being used to obtain the deflection from L/2 to L. For x_o equal to L/2, with equation (69) being used to compute the cross-sectional area integral, equation (76) reduces to equation (46), which is the expected result.

These are just two of the many possible flexural loading conditions that a captive column may be exposed to. With the aid of Castigliano's theorem, the analytical development of Chapter 2 can be used to obtain the deflection curve for all loading conditions.

CHAPTER 9

CONCLUSION

A method for applying classical beam theory to the prediction of the stiffness of a captive column loaded as a simple-supported beam with a concentrated midspan load has been presented in this thesis. Results obtained from tests performed using a number of captive column specimens indicate that, in general, the method yields predicted beam stiffness values that are in agreement with experimental results. The test results were also used to verify that the analytical method adequately predicts the effects of changes in individual design parameters.

Although the discussion provided in this thesis answers a number of questions concerning the structural behavior of captive columns, many questions are still unanswered. Recommendations regarding future research efforts are presented in this chapter.

Physical Testing

There are three areas of physical testing that require further study in order to fully verify the applicability of the analytical method presented in this thesis. The first area involves the construction and testing of more captive column specimens. The captive columns that were built and tested in this research effort were limited to square and triangular cross-sections with balsa wood and acrylic sheet, FRP and steel rods, and Kevlar used as the core, cap, and wrap, respectively. As previously mentioned, these cross-sectional shapes and component materials represent a small part of the many possible design alternatives. Captive columns with other cross-sectional shapes and

different materials should be constructed. Results obtained from tests performed using these specimens will indicate the ability of the analytical method in predicting the structural behavior of captive columns with the new design parameters.

Testing of the component materials should be conducted in conjunction with the above area of study. The use of incorrect material properties for some of the materials was a possible, and very probable, source of error between the experimental results and the analytical or computer model results. It is recommended that whenever possible, the mechanical properties obtained from a manufacturer be verified by experimental testing.

The second area of study may be conducted with new or existing test specimens. In the preceding chapter, equations were developed for applying the analytical method to the prediction of the deflection curve of a captive column subjected to any flexural loading condition. Results obtained from physical testing using loading conditions other than a simple-supported beam with a concentrated midspan load should be compared with the analytically predicted results, thus yielding information concerning the applicability of the analytical method for other loading conditions.

The determination of the stresses within the individual components is the final area of study recommended. This will involve the use of strain gages and strain rosettes to determine the strain distribution, and thus the stress distribution, in each component. Results obtained from physical testing can then be compared with analytical and computer model predicted values. Some work has been done in this area. Results

obtained from these tests can be found in previous reports concerning captive column structural behavior [2,3].

Analytical Development

The analytical method presented in this thesis is a great improvement over the previous method that was used to predict captive column beam stiffness. Including the deflection due to shear force in the computation of the stiffness is the main reason for this improvement.

It has been suggested that deformation of the cross-section and inconsistencies in the stress distribution in the vicinity of the concentrated load or the end supports are possible sources of error between the experimental and analytical results. The analytical method neglects the increase in the deflection caused by these localized effects. To obtain predicted stiffnesses which are in better agreement with experimentally determined results, these localized effects should be included in the analysis.

Although the conservation of energy approach is based upon the normal stress and shear stress distributions, the determination of these distributions is not explicitly obtained in the development found in Chapter 2. By expanding the development of Chapter 2, the stress distributions may be determined for the entire captive column cross-section. Stresses obtained in this fashion may be compared with experimental results and results obtained from the computer model. Special attention will be required to account for the localized inconsistencies in the stress distribution.

The determination of the wrap pretension due to the wrapping tension and the load at which the pretensioned wrap strands become slack is related to the above determination of the stress distributions. By

determining these two factors, the beam stiffness within the range represented by the cases of no wrap pretension and ideal wrap pretension may be obtained.

Computer Model

A number of element combinations were considered by Kipp [2] before the current model was obtained. The current model was chosen because it yielded relatively accurate predictions of actual captive column structural behavior and was adaptable to a wide variety of captive column geometries, component materials, and loading conditions. In this research effort, a method has been developed to account for the effect of wrap pretension. Including the effect of wrap pretension narrows the predicted beam stiffness from a range of stiffness values, no wrap pretension stiffness to ideal wrap pretension stiffness, to a single value.

It is the author's belief that improvements in the computer model, beyond the inclusion of the effect of wrap pretension, are not possible with the finite element program (SAP IV) that is currently being used. If improved results using the computer model are desired, one of the following course of action should be taken: 1) modify SAP IV to improve the results, 2) use other commercially available finite element structural analysis programs, or 3) develop a specialized finite element program for captive columns. If either of the first two courses of action are taken, it is recommended that the program be modified to allow for easier data input and specialized data output.

Dynamic Analysis

Very little investigation has been performed concerning the response

of captive columns to dynamically applied loads. There are three main areas of interest that will be addressed in the following paragraphs.

The first area of interest is the determination of the natural frequencies of a captive column. Exciting a structure as its natural frequency leads to increases in the amplitude of vibration and may result in premature failure of the structure. The effect of rotary inertia and deformation due to shear stresses should be included in the determination of the natural frequencies of the overall captive column. Furthermore, the natural frequencies of individual components may be an important factor.

The second area of interest is the expected life of a captive column subjected to cyclic loading. A different material may be used for each component in a captive column, with various methods used to bond the components into an integral structure. The effect of cyclic loading of each component, as well as the bonds holding the components together, must be understood in order to properly design a captive column.

The last area of interest is the rate of application of a load. In the development found on Chapter 2 it was assumed that the concentrated load was gradually applied to the captive column, and therefore the external work was equal to one-half of the total load multiplied by the deflection. If the load is suddenly applied, the external work will be different. Impact factors are used to account for the sudden application of a load. The behavior of a captive column subjected to suddenly applied loads may be different that conventional structures, and therefore a new set of impact factors may have to be developed.

APPENDICES

APPENDIX A

MOMENT OF INERTIA EQUATIONS

The equations needed to determine the moments of inertia of the caps, the core panels, and the core centerpiece for square and triangular cross-section captive columns are presented in this appendix. The equations are obtained from standard moment of inertia equations. Due to the symmetry of the cross-sections, the moment of inertia is independent of the angular orientation of the members.

Square Cross-Section

$$I_{caps} = 4\left(\frac{\pi d^4}{64}\right) + 2\left(\frac{\pi d^2}{4}\right)\left(\frac{\sqrt{2}D}{2}\right)^2$$

$$I_{caps} = \frac{\pi d^4}{16} + \frac{\pi d^2 D^2}{4}$$

$$h_{panel} = \frac{\sqrt{2}\,D}{2} - \frac{d}{2} - \frac{w_{center}}{2}$$

$$I_{panels} = 2\left(\frac{h_{panel}\,t_{panel}^3}{12}\right) + 2\left(\frac{t_{panel}\,h_{panel}^3}{12}\right) + 2\,(h_{panel}\,t_{panel})\left(\frac{h_{panel} + w_{center}}{2}\right)^2$$

$$I_{panel} = \frac{h_{panel}\,t_{panel}^3}{6} + \frac{t_{panel}\,h_{panel}^3}{6} + \frac{h_{panel}\,t_{panel}}{2}\,(h_{panel} + w_{center})^2$$

$$I_{center} = \frac{w_{center}^4}{12}$$

Triangular Cross-Section

$$I_{caps} = 3\left(\frac{\pi d^4}{64}\right) + 1.5\left(\frac{\pi d^2}{4}\right)\left(\frac{\sqrt{3}\ D}{3}\right)^2$$

$$I_{caps} = \frac{3\pi d^4}{64} + \frac{\pi d^2 D^2}{8}$$

$$h_{panel} = \frac{\sqrt{3}\ D}{3} - \frac{d}{2} - \frac{\sqrt{3}\ w_{center}}{6}$$

$$I_{panels} = 1.5\left(\frac{h_{panel}\ t_{panel}^3}{12}\right) + 1.5\left(\frac{t_{panel} h_{panel}^3}{12}\right)$$

$$+ 1.5\ (h_{panel}\ t_{panel})\ \frac{h_{panel}}{2} + \frac{3\ w_{center}}{6}$$

$$I_{panel} = \frac{h_{panel} t_{panel}^3}{8} + \frac{t_{panel} h_{panel}^3}{8}$$

$$+ \frac{(h_{panel} t_{panel})(\sqrt{3} h_{panel} + w_{center})^2}{}$$

$$I_{center} = \frac{\sqrt{3}\ w_{center}^4}{96}$$

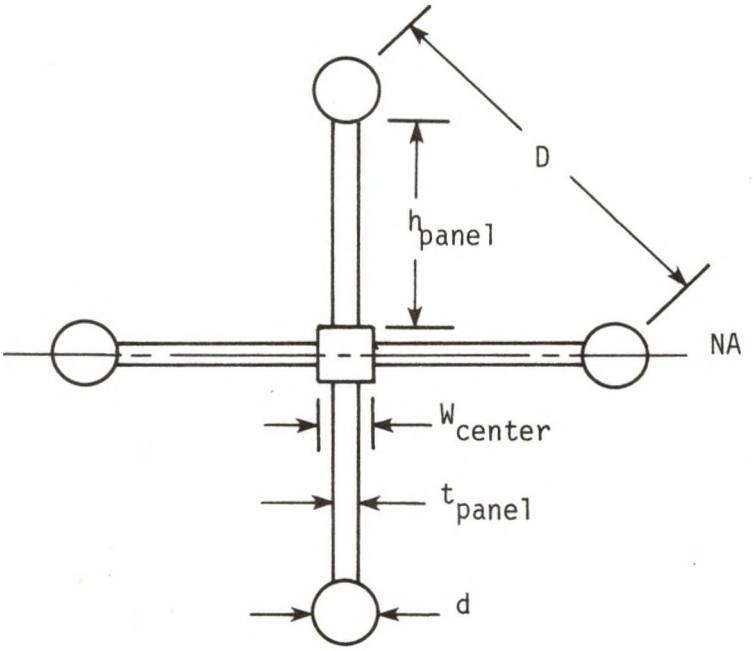

A) SQUARE CROSS-SECTION

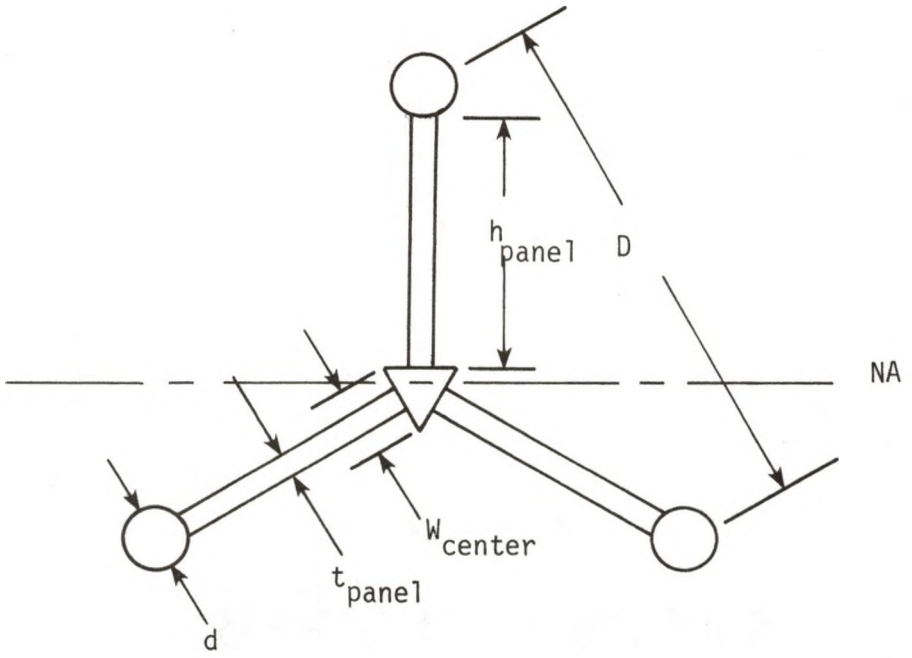

B) TRIANGULAR CROSS-SECTION

FIGURE 40 - CAPTIVE COLUMN CROSS-SECTIONS

APPENDIX B

WRAP SHEAR STIFFNESS AND EQUIVALENT WIDTH

In the development of the relationship for the stored elastic strain energy due to shear force, an equivalent wrap width must be developed for a panel of wrap strands. The development of the equivalent width is based on the angular distortion of a wrap panel due to an applied shear stress.

Four rigid links connected by frictionless pins are shown in Figure 41A, with the wrap strands, for one direction of wrap only, connected to the links. The application of a shear stress will produce the deformation shown in Figure 41B, where n is a number between zero and one. An equivalent load case is obtained by multiplying the shear stress on each side of the wrap panel by the area of each respective side. The components are vectorally added to obtain the equivalent forces, P_{eq}, shown in Figure 41C:

$$P_{eq} = (\tau D w_{wrap})^2 + \left(\frac{\tau D w_{wrap}}{\tan\phi}\right)^2$$

$$P_{eq} = \frac{\tau D w_{wrap}}{\sin\phi} \qquad (77)$$

$$\text{angle} = \tan^{-1} \frac{\tau D w_{wrap}}{\tau D w_{wrap}/\tan\phi}$$

$$\text{angle} = \phi$$

where P_{eq} = equivalent force

τ = shear stress

D = length of vertical edge (corresponds with cap centerline distance)

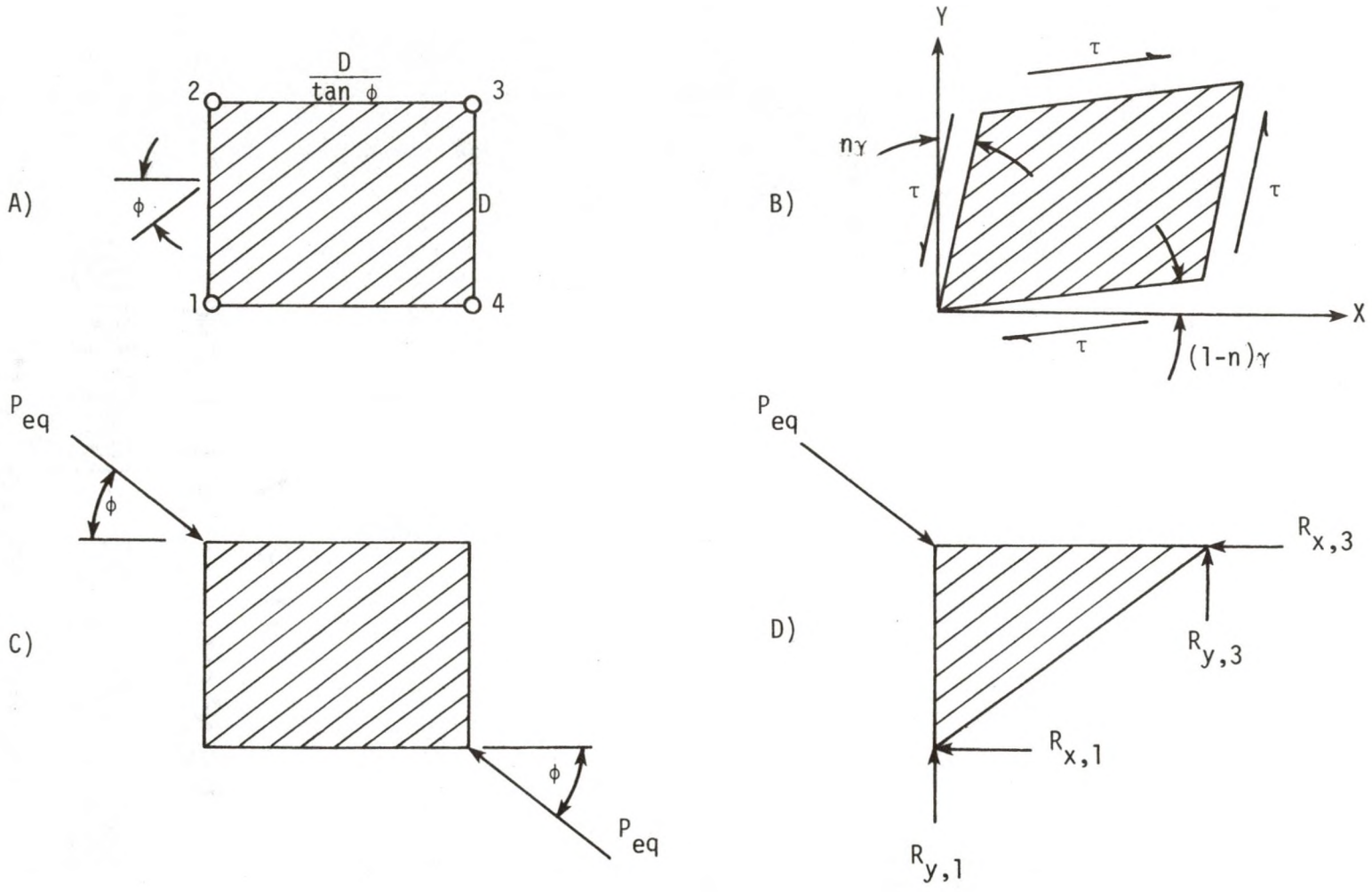

FIGURE 41 - PANEL OF WRAP STRANDS, ONE DIRECTION OF WRAP

E)

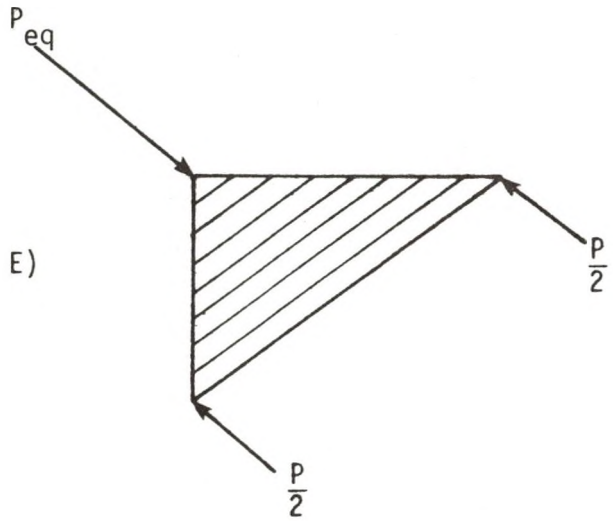

F)

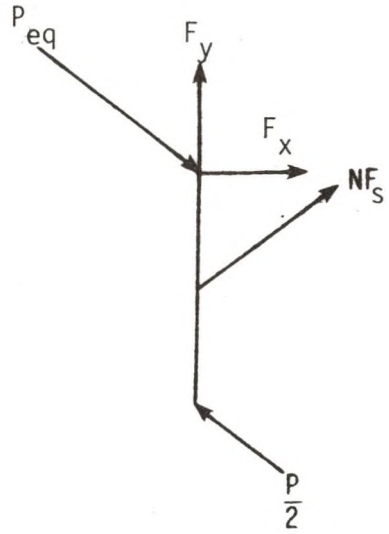

G)

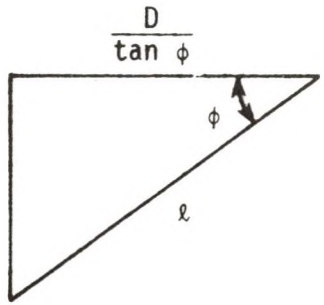

H)

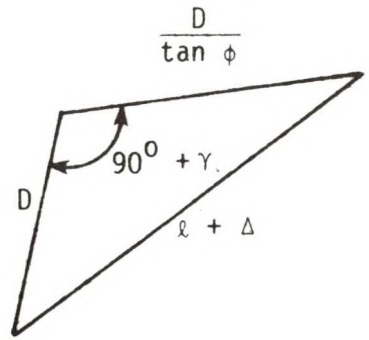

FIGURE 41 - (CONTINUED)

w_{wrap} = equivalent wrap width

ϕ = wrap angle.

For small deformations in the elastic range, the shear stress is equal to the shear modulus multiplied by the shear strain, which is the angle of deformation, γ. Substituting this definition of the shear stress into Equation (77) and simplifying yields the following expression:

$$P_{eq} = \frac{\gamma D(wG)_{wrap}}{\sin\phi} \tag{78}$$

where γ = shear strain

G = equivalent wrap shear modulus

$(wG)_{wrap}$ = wrap shear stiffness.

The wrap strands provide resistance to the deformation of the assemblage in the form of axial tensile forces. The shear strain increases as the equivalent force increases, which results in an increase in the tensile force in each wrap strand. An expression can be developed for the equivalent force in terms of the number of strands and the tensile force in each strand. The system shown in Figure 41D, which is statically equivalent to the system of Figure 41C, will be used for this development. Setting the summation of forces in the vertical and horizontal directions, and the summation of moments about any point equal to zero results in the two reactions shown in Figure 41E. A free body diagram is obtained by passing a cutting plane through pin 2 and the wrap strands, see Figure 41F. The tensile force is the same for each wrap strand, and therefore the total force due to the wrap strands is equal to the force in one strand multiplied by the number of strands. This force acts at any angle ϕ to the horizontal through the midpoint of the link.

The following expression is obtained by setting the summation of moments about pin A equal to zero:

$$\frac{D}{2} NF_s \cos\phi - D \frac{P_{eq}}{2} \cos\phi = 0$$

$$P_{eq} = NF_s \tag{79}$$

where N = number of wrap strands.

The force in each wrap strand is determined by considering the geometry of the deformed and undeformed assemblage. Two links and one wrap strand are shown in Figure 41G, with the length of the wrap strand given by the following equation:

$$\ell = \frac{D}{\sin\phi} \tag{80}$$

where ℓ = length of wrap strand.

The application of the equivalent force produces the deformation shown in Figure 41H. The following relationship is obtained from the Cosine law:

$$(\ell + \Delta)^2 = \ell^2 - 2 \frac{D^2}{\tan\phi} \cos (90° + \gamma) \tag{81}$$

where Δ = change in the wrap strand length.

By assuming that the shear strain is small, Equation (81) can be solved for Δ in the following way:

$$\ell^2 + 2\ell\Delta + \Delta^2 = \ell^2 - \frac{2D^2}{\tan\phi} \gamma$$

$$\Delta^2 + 2\ell\Delta - \frac{2\gamma D^2}{\tan\phi} = 0$$

$$\Delta = -\ell \pm \ell \sqrt{1 + \frac{2\gamma D^2}{\ell^2 \tan\phi}}$$

$$\Delta \cong -\ell + \ell \left(1 + \frac{\gamma D^2}{\ell^2 \tan\phi}\right)$$

$$\Delta \cong \frac{\gamma D}{\ell \tan\phi} = \frac{\gamma D \sin\phi}{\tan\phi}$$

$$\Delta \cong \gamma D \cos\phi \tag{82}$$

A relationship for the axial deflection of the wrap strand as a function of the force in the wrap strand and the geometric and material properties is shown below:

$$\Delta = \frac{F_s \ell}{A_s E_{wrap}} \tag{83}$$

where A_s = cross-sectional area of the wrap strand

E_{wrap} = elastic modulus of the wrap.

Equating Equations (82) and (83) and simplifying results in the following equation

$$\frac{F_s \ell}{A_s E_{wrap}} = \frac{F_s D}{A_s E_{wrap} \sin\phi} = \gamma D \cos\phi$$

$$F_s = \gamma A_s E_{wrap} \sin\phi \cos\phi \tag{84}$$

Substituting Equations (78) and (84) into Equation (79) and simplifying results in the following:

$$P_{eq} = NF_s$$

$$\frac{\gamma D(wG)_{wrap}}{\sin\phi} = N\gamma A_s E_{wrap} \sin\phi \cos\phi$$

$$(wG)_{wrap} = \frac{N}{D} A_s E_{wrap} \sin^2\phi \cos\phi \qquad (85)$$

The number of wrap strands is equal to the wrap density multiplied by the length of a horizontal link. The final equation for the wrap shear stiffness is obtained by substituting this expression into equation (85):

$$N = \frac{\rho D}{\tan\phi} = \frac{\rho D \cos\phi}{\sin\phi}$$

$$(wG)_{wrap} = \rho A_s E_{wrap} \sin\phi \cos^2\phi \qquad (86)$$

where ρ = wrap density.

By dividing this equation by the equivalent shear modulus of the wrap, an equivalent wrap panel width is obtained:

$$w_{wrap} = \frac{\rho A_s E_{wrap} \sin\phi \cos^2\phi}{G_{wrap}} \qquad (87)$$

Equations (86) and (87) represent the shear stiffness and equivalent width, respectively, of a panel of wrap strands for one direction of wrap only. Both directions of wrap are shown in Figure 42A. Under the application of the shear stress, the strands in the direction from pin 1 to pin 3 will be subjected to tensile force and the other strands will be subjected to compressive. Since the wrap strands cannot carry compressive forces, the strands that are subjected to compressive force will merely relax. If there is pretension in all of the strands, the

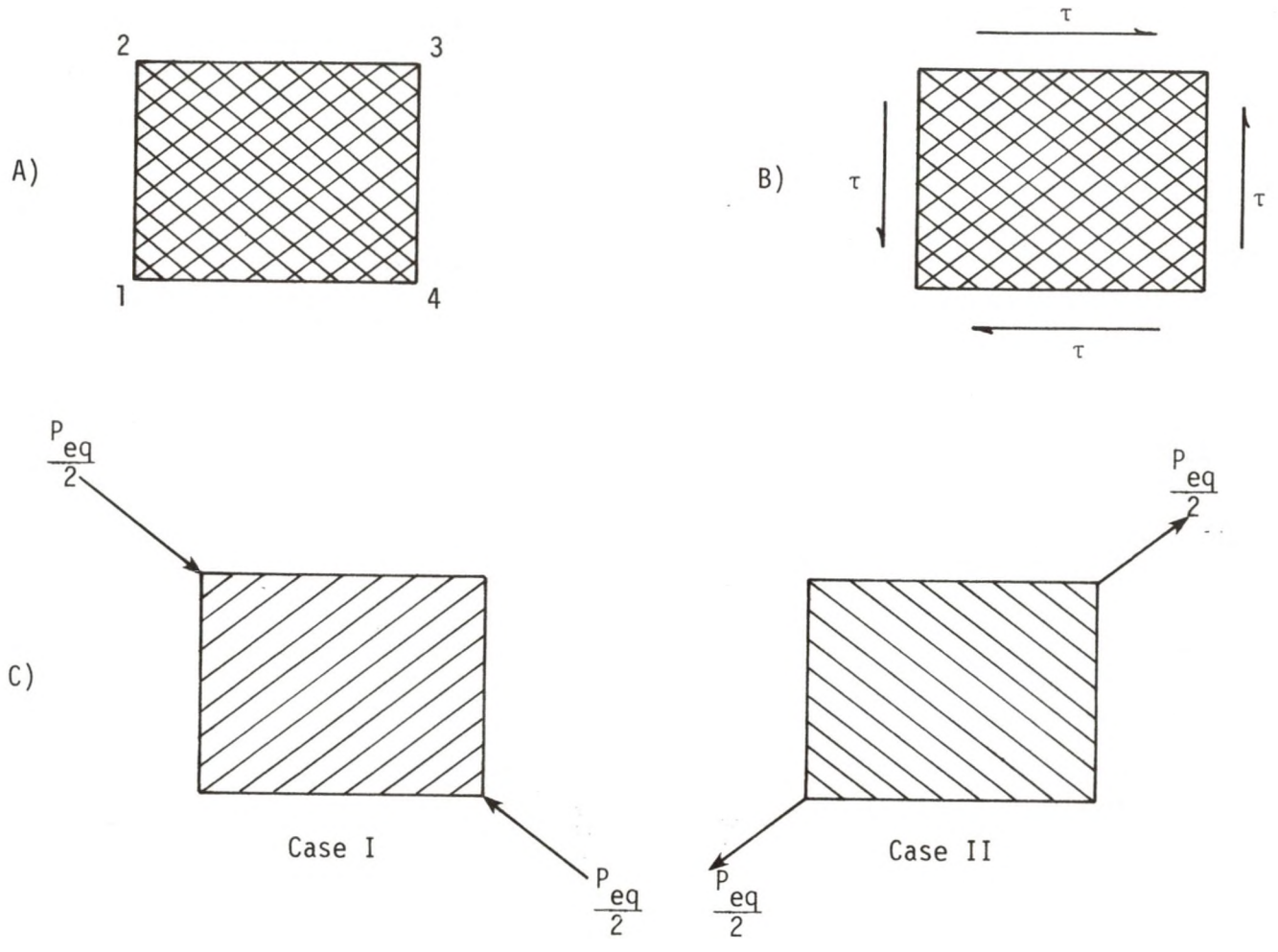

FIGURE 42 - PANEL OF WRAP STRANDS, TWO DIRECTIONS OF WRAP

compressive force will decrease the tensile force due to the pretension. In this case, all of the wrap strands will be able to resist the shear stress.

The load case shown in Figure 42B can be divided into the two cases shown in Figure 42C. The summation of the stiffnesses from these two cases will be the total shear stiffness. The analysis of the case where the strands are subjected to compressive force is similar to the previously developed analysis. It can be shown that the total shear stiffness or equivalent wrap width is equal to twice the values computed from Equations (86) and (87), respectively.

APPENDIX C

SOLUTION OF THE INTEGRALS NEEDED FOR THE ELASTIC STRAIN ENERGY DUE TO SHEAR STRESS

The solution of the three integrals needed in Equation (42) of Chapter 2 are found in this Appendix. Equations (18) and (19) are used to obtain the equivalent first moments of area and the equivalent widths of the cross-section. Equations (39), (40), and (41) are used to obtain the incremental areas.

First Integral

$$J_1 = \int_0^{h_1} \left(\frac{Q_{eq}}{b_{eq}}\right)^2 dA$$

$$Q_{eq} = \frac{(h_3^2 - h_2^2)\,(wG)_{cap} + 2(h_2^2 - h_1^2)\,(tG)_{panel} + \frac{h_1^2 - y^2}{2}\,(wG)_{center} + (h_2^2 - y^2)\,(wG)_{wrap}}{G_{cap}}$$

$$b_{eq} = \frac{2(wG)_{wrap} + (wG)_{center}}{G_{cap}}$$

$$dA = \frac{2(wG)_{wrap} + (wG)_{center}}{G_{cap}}\,dy$$

$$J_1 = c_1 \int_0^{h_1} (c_2 - c_3\,y^2)^2\,dy$$

$$J_1 = c_1 \left[c_2^2 h_1 - \frac{2}{3}\,c_2 c_3 h_1^3 + \frac{c_3^2}{5}\,h_1^5\right]$$

$$c_1 = \frac{1}{G_{cap}\left[2(wG)_{wrap} + (wG)_{center}\right]}$$

$$c_2 = (h_3^2 - h_2^2)\,(wG)_{cap} + \sqrt{2}(h_2^2 - h_1^2)\,(tG)_{panel} + \frac{h_1^2}{2}\,(wG)_{center} + h_2^2\,(wG)_{wrap}$$

$$c_3 = \frac{1}{2}\,(wG)_{cap} + (wG)_{wrap}$$

Second Integral

$$J_2 = \int_{h_1}^{h_2} \left(\frac{Q_{eq}}{b_{eq}}\right)^2 dA$$

$$Q_{eq} = \frac{(h_3^2 - h_2^2)\,(wG)_{cap} + \sqrt{2}(h_2^2 - y^2)\,(tG)_{panel} + (h_2^2 - y^2)(wG)_{wrap}}{G_{cap}}$$

$$b_{eq} = \frac{2(wG)_{wrap} + 2(tG)_{panel}}{G_{cap}}$$

$$dA = \frac{2(wG)_{wrap} + 2\sqrt{2}\,(tG)_{panel}}{G_{cap}}\,dy$$

$$J_2 = c_4 \int_{h_1}^{h_2} (c_5 - c_6 y^2)^2\,dy$$

$$J_2 = c_4 \left[c_5^2\,(h_2 - h_1) - \frac{2}{3}\,c_5 c_6\,(h_2^3 - h_1^3) + \frac{c_6^2}{5}\,(h_2^5 - h_1^5)\right]$$

$$c_4 = \frac{(wG)_{wrap} + 2\,(tG)_{panel}}{2\,G_{cap}\left[(wG)_{wrap} + (tG)_{panel}\right]^2}$$

$$c_5 = (h_3^2 - h_2^2)\,(wG)_{cap} + h_2^2\left[\sqrt{2}\,(tG)_{panel} + (wG)_{wrap}\right]$$

$$c_6 = \sqrt{2}\,(tG)_{panel} + (wG)_{wrap}$$

Third Integral

$$J_3 = \int_{h_2}^{h_3} \left(\frac{Q_{eq}}{b_{eq}}\right)^2 dA$$

$$Q_{eq} = (h_3^2 - y^2)\, w_{cap}$$

$$b_{eq} = 2\, w_{cap}$$

$$dA = 2\, w_{cap}\ dy$$

$$J_3 = c_7 \int_{h_2}^{h_3} (c_8 - c_9\, y^2)^2\ dy$$

$$J_3 = c_7 \left[(c_8^2(h_3 - h_2) - \frac{2}{3}\, c_8 c_9 (h_3^3 - h_2^3) + \frac{c_9^2}{5}\, (h_3^5 - h_2^5)\right]$$

$$c_7 = \frac{1}{2\, w_{cap}}$$

$$c_8 = h_3^2\, w_{cap}$$

$$c_9 = w_{cap}$$

APPENDIX D

BEAM STIFFNESS FOR OTHER CAPTIVE COLUMN CROSS-SECTIONS

The development of the equations needed to find the elastic strain energy due to shear force for a square cross-section captive column rotated 45° and for a triangular cross-section captive column can be found in this appendix. The development will begin with Equation (17) and will continue in a similar fashion to the development in Chapter 2. The equations needed to determine the beam stiffness for the captive columns can also be found in this appendix, along with approximate beam stiffness equations.

Square Cross-Section Rotated 45°

The square cross-section captive column shown in Figure 43A is simplified to the cross-section shown in Figure 43B. The equivalent wrap width is determined by using Equation (21). Since the equivalent wrap panels are oriented at a 45° angle to the neutral axis, the wrap panels are treated in the same way that the core panels were treated in Chapter 2.

In general, the shear modulus of the core panels is much smaller than the cap shear modulus, and therefore, the core panels that lie along the neutral axis will be neglected in this analysis. Furthermore, the two caps that lie on the neutral axis are transformed into rectangular regions with the height equal to the core centerpiece width and the width equal to the dimension necessary to have equivalent area in the round and rectangular regions. The above two approximations are made in order to simplify the analysis. Any error introduced by making these two simplifications will be insignificant.

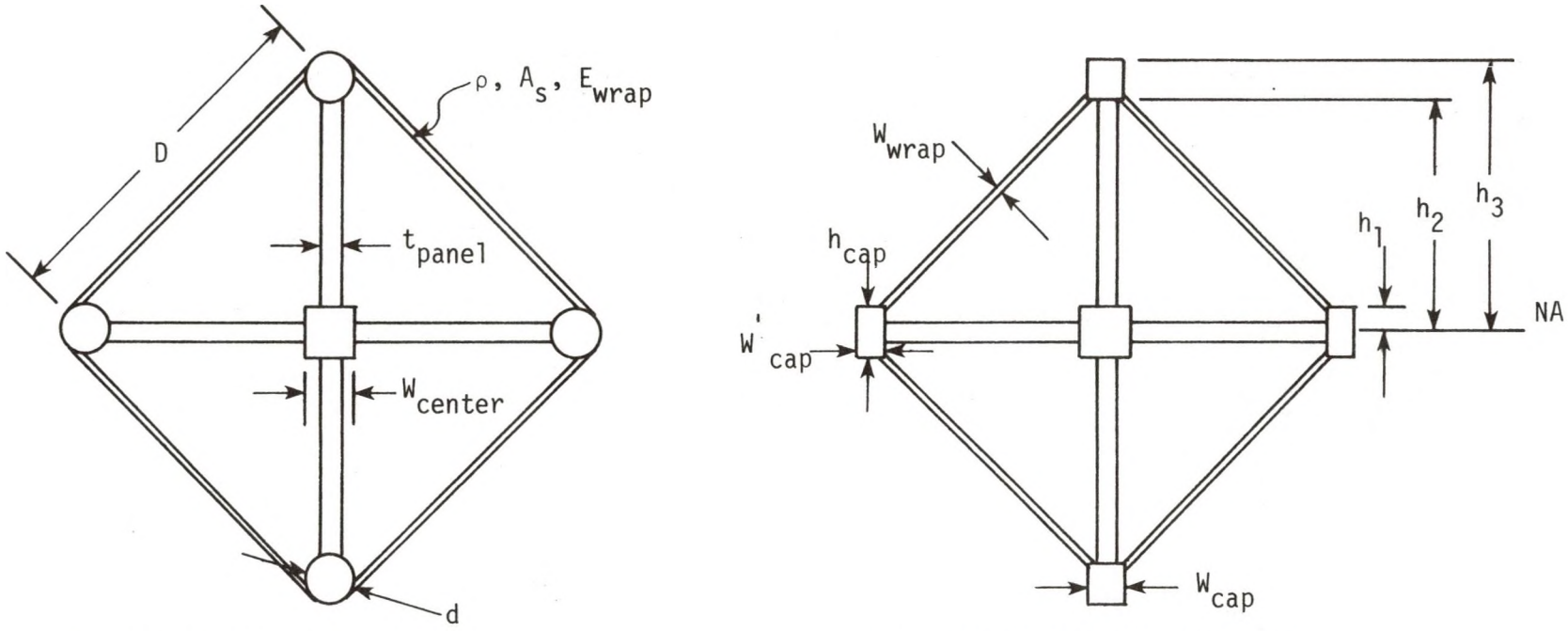

A) ACTUAL CROSS-SECTION

B) APPROXIMATE CROSS-SECTION

FIGURE 43 - SQUARE CROSS-SECTION CAPTIVE COLUMN, ROTATED 45°

$$U_{shear} = \frac{P^2 L}{8G} \left[\frac{E_{cap}}{(EI)_{eq}} \right]^2 \int_{area} \left(\frac{Q_{eq}}{b_{eq}} \right)^2 dA$$

$$w_{wrap} = \frac{\rho A_s E \sin\phi \cos^2\phi}{G_{wrap}}$$

$$w_{cap} = \frac{\sqrt{\pi} d}{2}$$

$$w'_{cap} = \frac{\pi d^2}{4 w_{center}}$$

$$h_1 = \frac{w_{center}}{2}$$

$$h_2 = (\sqrt{2} D - w_{cap}) / 2$$

$$h_3 = (\sqrt{2} D + w_{cap}) / 2$$

Caps

$$Q(0,h_1) = w'_{cap} (h_1^2 - y^2) + \frac{w_{cap}}{2} (h_3^2 - h_2^2)$$

$$Q(h_1,h_2) = \frac{w_{cap}}{2} (h_3^2 - h_2^2)$$

$$Q(h_2,h_3) = \frac{w_{cap}}{2} (h_3^2 - y^2)$$

Core Panels

$$Q(0,h_1) = \frac{t_{panel}}{2} (h_2^2 - h_1^2)$$

$$Q(h_1,h_2) = \frac{t_{panel}}{2} (h_2^2 - y^2)$$

Core Centerpiece

$$Q(h_2,h_3) = 0$$

$$Q(0,h_1) = \frac{w_{center}}{2} (h_1^2 - y^2)$$

$$Q(h_1,h_3) = 0$$

Wrap

$$Q(0,h_1) = \sqrt{2}\, w_{wrap} (h_2^2 - h_1^2)$$

$$Q(h_1,h_3 = \sqrt{2}\, w_{wrap} (h_2^2 - y^2)$$

$$Q(h_2,h_3) = 0$$

$$b_{caps} = 2\, w'_{cap} \qquad \text{for} \qquad 0<y<h_1$$

$$b_{caps} = w_{cap} \qquad \text{for} \qquad h_2<y<h_3$$

$$b_{panel} = t_{panel}$$

$$b_{wrap} = 2\, w_{wrap}$$

$$b_{center} = w_{center}$$

$$dA = \frac{[2(w'G)_{cap} + (wG)_{center}]}{G_{cap}}\, dy \qquad \text{for } 0<y<h_1$$

$$dA = \frac{[2\sqrt{2}(wG)_{wrap} + (tG)_{panel}]}{G_{cap}}\, dy \qquad \text{for } h_1<y<h_2$$

$$dA = w_{cap}\, dy \qquad \text{for } h_2<y<h_3$$

Using the horizontal plane of symmetry, and dividing the integral into three parts, the following equation is obtained:

$$U_{shear} = K[J_1 + J_2 + J_3] \tag{88}$$

where

$$K = \frac{P^2 L}{4G_{cap}} \left[\frac{E_{cap}}{(EI)_{eq}}\right]^2$$

$$J_1 = \int_0^{h_1} \left(\frac{Q_{eq}}{b_{eq}}\right)^2 dA$$

$$J_2 = \int_{h_1}^{h_2} \left(\frac{Q_{eq}}{b_{eq}}\right)^2 dA$$

$$J_3 = \int_{h_2}^{h_3} \left(\frac{Q_{eq}}{b_{eq}}\right)^2 dA$$

By substituting the appropriate values into the three integrals and performing the integrations, the following results are obtained:

$$J_1 = c_1[c_2^2 h_1 - \frac{2}{3} c_2 c_3 h_1^3 + \frac{c_3^2}{5} h_1^5] \tag{89}$$

$$J_2 = c_4[c_5^2(h_2 - h_1) - \frac{2}{3} c_5 c_6 (h_2^3 - h_1^3) + \frac{c_6^2}{5} (h_2^5 - h_1^5)] \tag{90}$$

$$J_3 = c_7[c_8^2(h_3 - h_2) - \frac{2}{3} c_8c_9(h_3^3 - h_2^3) + \frac{c_9^2}{5} (h_3^5 - h_2^5)] \qquad (91)$$

where

$$c_1 = \frac{1}{G_{cap}\,[2(w'G)_{cap} + (wG)_{center}]}$$

$$c_2 = \left[(w'G)_{cap} + \frac{(wG)_{center}}{2}\right] h_1^2 + \frac{(wG)_{cap}}{2} (h_3^2 - h_2^2)$$
$$+ \left[\sqrt{2}(wG)_{wrap} + \frac{(tG)_{panel}}{2}\right] (h_2^2 - h_1^2)$$

$$c_3 = (w'G)_{cap} + \frac{(wG)_{center}}{2}$$

$$c_4 = \frac{2\sqrt{2}(wG)_{wrap}\quad (tG)_{panel}}{G_{cap}[2(wG)_{wrap} + (tG)_{panel}]^2}$$

$$c_5 = \frac{(wG)_{cap}}{2} (h_3^2 - h_2^2) + \left[\sqrt{2}(wG)_{wrap} + \frac{(tG)_{panel}}{2}\right] h_2^2$$

$$c_6 = \frac{(wG)_{cap}}{2} + \sqrt{2}\,(wG)_{wrap}$$

$$c_7 = \frac{1}{w_{cap}}$$

$$c_8 = \frac{w_{cap}}{2}\ h_3^2$$

$$c_9 = \frac{w_{cap}}{2}$$

The solution to the integrals may be obtained in a similar fashion to the solution found in Appendix C.

The above equation for the elastic strain energy is similar to Equation (42), with the differences found in the constant values c_1 through c_9. The elastic strain energy due to the bending moment is found by using Equation (11). Equation (47) is used to find the beam stiffness for a square captive column in either orientation, provided that the appropriate constant values are used.

The method outlined in the beginning of Chapter 6 will now be used to develop an approximate beam stiffness equation. The moment of inertia is independent of the angular orientation, and therefore Equation (51) is used to find the approximate moment of inertia. The integrals J_1 and J_3 will be set equal to zero. By neglecting the first moment of area of the core panels and the wrap, the following equation is obtained for the integral J_2:

$$J_2 = \int_{h_1}^{h_2} \left(\frac{Q_{eq}}{b_{eq}}\right)^2 dA$$

$$J_2 \cong \frac{\pi^2 d^4 D^2 \text{ cap}}{32} \; B_2 \; H_2 \qquad (92)$$

where

$$B_2 = \frac{2\sqrt{2}(wG)_{wrap} + (tG)_{panel}}{[2(wG)_{wrap} + (tG)_{panel}]^2}$$

$$H_2 = \frac{D}{\sqrt{2}} - \frac{\sqrt{\pi}\, d}{4} - \frac{w_{center}}{2}$$

Approximate equations have been developed for the equivalent flexural rigidity and the integral J_2. By setting $J_1 = J_3 = 0$, substituting Equations (51) and (92) into Equation (47), and simplifying, the, following approximate equation for beam stiffness is obtained:

$$k \cong \frac{12\pi d^2 D^2 E_{cap}}{L^3 + 3Ld^2 E_{cap} B_2 H_2} \tag{93}$$

Triangular Cross-Section

The triangular cross-section captive column shown in Figure 44A is simplified to the cross-section shown in Figure 44B. The equivalent wrap panels and the core panels below the neutral axis are treated in a similar fashion to the way in which the core panels were treated in Chapter 2. The triangular centerpiece is transformed into a square region with the same cross-sectional area as the actual centerpiece. As before, this transformation is made in order to simplify the analysis. Any error introduced by making this transformation will be negligible.

$$U_{shear} = \frac{P^2 L}{8G} \left[\frac{E_{cap}}{(EI)_{eq}}\right]^2 \int_{area} \left(\frac{Q_{eq}}{b_{eq}}\right)^2 dA$$

$$w_{wrap} = \frac{\rho A_s E \sin\phi \cos^2\phi}{G_{wrap}}$$

$$w_{cap} = \frac{\sqrt{\pi}\, d}{2}$$

$$w'_{center} = \frac{3^{1/4}}{2} w_{center}$$

$$\tan 30° = \frac{1}{\sqrt{3}} = 0.577 \qquad \frac{2}{\sqrt{3}} = 1.155 \qquad \frac{4}{\sqrt{3}} = 2.309$$

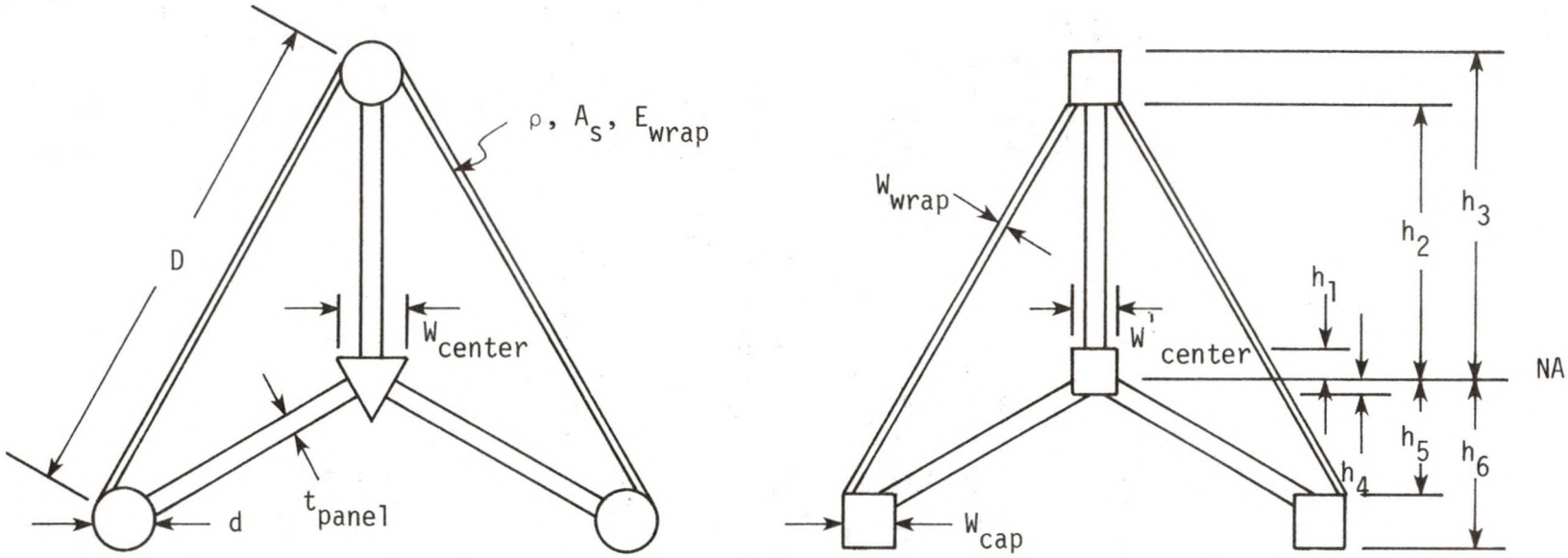

A) ACTUAL CROSS-SECTION

B) APPROXIMATE CROSS-SECTION

FIGURE 44 - TRIANGULAR CROSS-SECTION CAPTIVE COLUMN

$$h_1 = \frac{2}{3} w'_{center} = 0.439\ w_{center}$$

$$h_2 = 0.577\ D - \frac{w_{cap}}{2}$$

$$h_3 = 0.577\ D + \frac{w_{cap}}{2}$$

$$h_4 = \frac{1}{3} w'_{center} = 0.219\ w_{center}$$

$$h_5 = \frac{0.577D - w_{cap}}{2}$$

$$h_6 = \frac{0.577D - w_{cap}}{2}$$

Caps

$$Q(0,h_2) = \frac{w_{cap}}{2} (h_3^2 - h_2^2)$$

$$Q(h_2,h_3) = \frac{w_{cap}}{2} (h_3^2 - y^2)$$

$$Q(0,h_5) = w_{cap} (h_6^2 - h_5^2)$$

$$Q(h_5,h_6) = w_{cap} (h_6^2 - y^2)$$

Core Panels

$$Q(0,h_1) = \frac{t_{panel}}{2} (h_2^2 - h_1^2)$$

$$Q(h_1,h_2) = \frac{t_{panel}}{2} (h_2^2 - y^2)$$

$$Q(0,h_4) = 2\ t_{panel} (h_5^2 - h_4^2)$$

$$Q(h_4,h_5) = 2\ t_{panel} (h_5^2 - y^2)$$

$$Q(h_2,h_3) = Q(h_5,h_6) = 0$$

Core Centerpiece

$$Q(0,h_1) = \frac{w'_{center}}{2}(h_1^2 - y^2)$$

$$Q(0,h_4) = \frac{w'_{center}}{2}$$

$$Q(h_1,h_3) = Q(h_4,h_6) = 0$$

Wrap

$$Q(0,h_2) = \frac{2}{\sqrt{3}} w_{wrap}(h_2^2 - y^2)$$

$$Q(0,h_5) = \frac{2}{\sqrt{3}} w_{wrap}(h_5^2 - y^2)$$

$$Q(h_2,h_3) = Q(h_5,h_6) = 0$$

Above Neutral Axis

$$b_{cap} = w_{cap}$$

$$b_{panel} = t_{panel}$$

$$b_{center} = w'_{center}$$

$$b_{wrap} = 2\, w_{wrap}$$

Below Neutral Axis

$$b_{cap} = 2\, w_{cap}$$

$$b_{panel} = 2\, t_{panel}$$

$$b_{center} = w'_{center}$$

$$b_{wrap} = 2\, w_{wrap}$$

$$dA = \frac{[2.309(wG)_{wrap} + (w'G)_{center}}{G_{cap}}\, dy \qquad \text{for } 0<y<h_1$$

$$dA = \frac{[2.309(wG)_{wrap} + (tG)_{panel}}{G_{cap}} \, dy \qquad \text{for } h_1<y<h_2$$

$$dA = w_{cap} \, dy \qquad \text{for } h_2<y<h_3$$

$$dA = \frac{[2.309(wG)_{wrap} + (w'G)_{center}}{G_{cap}} \, dy \qquad \text{for } h_2<y<h_3$$

$$dA = \frac{[2.309(wG)_{wrap} + 4(tG)_{panel}}{G_{cap}} \, dy \qquad \text{for } h_4<y<h_5$$

$$dA = 2 \, w_{cap} \, dy \qquad \text{for } h_5<y<h_6$$

Dividing the integral into six parts, the following equation is obtained:

$$U_{shear} = \frac{K}{2} [J_1 + J_2 + J_3 + J_4 + J_5 + J_6] \tag{94}$$

where

$$K = \frac{P^2 L}{4G} \left[\frac{E_{cap}}{(EI)_{eq}}\right]^2$$

$$J_1 = \int_0^{h_1} \left(\frac{Q_{eq}}{b_{eq}}\right)^2 dA$$

$$J_2 = \int_{h_1}^{h_1} \left(\frac{Q_{eq}}{b_{eq}}\right)^2 dA$$

$$J_3 = \int_{h_2}^{h_3} \left(\frac{Q_{eq}}{b_{eq}}\right)^2 \, dA$$

$$J_4 = \int_{0}^{h_4} \left(\frac{Q_{eq}}{b_{eq}}\right)^2 \, dA$$

$$J_5 = \int_{h_4}^{h_5} \left(\frac{Q_{eq}}{b_{eq}}\right)^2 \, dA$$

$$J_6 = \int_{h_5}^{h_6} \left(\frac{Q_{eq}}{b_{eq}}\right)^2 \, dA$$

By substituting the appropriate values into the six integrals and performing the integrations, the following results are obtained:

$$J_1 = c_1 \left[c_2^2 h_1 - \frac{2}{3} c_2 c_3 h_1^3 + \frac{c_3^2}{5} h_1^5\right] \tag{95}$$

$$J_2 = c_4 \left[c_5^2 (h_2 - h_1) - \frac{2}{3} c_5 c_6 (h_2^3 - h_1^3) + \frac{c_6^2}{5} (h_2^5 - h_1^5)\right] \tag{96}$$

$$J_3 = c_7 \left[c_8^2 (h_3 - h_2) - \frac{2}{3} c_8 c_9 (h_3^2 - h_2^3) + \frac{c_9^2}{5} (h_3^5 - h_2^5)\right] \tag{97}$$

$$J_4 = c_{10} \left[c_{11}^2 h_4 - \frac{2}{3} c_{11} c_{12} h_4^3 + \frac{c_{12}^2}{5} h_4^5\right] \tag{98}$$

$$J_5 = c_{13} \left[c_{14}^2 (h_5 - h_4) - \frac{2}{3} c_{14} c_{15} (h_5^3 - h_4^3) + \frac{c_{15}^2}{5} (h_5^5 - h_4^5)\right] \tag{99}$$

$$J_6 = c_{16}\left[c_{17}^2(h_6 - h_5) - \frac{2}{3}c_{17}c_{18}(h_6^3 - h_5^3) + \frac{c_{18}^2}{5}(h_6^5 - h_5^5)\right] \quad (100)$$

where $$c_1 = \frac{2.309(wG)_{wrap} + (w'G)_{center}}{G_{cap}[2(wG)_{wrap} + (w'G)_{center}]^2}$$

$$c_2 = \frac{(wG)_{cap}}{2}(h_3^2 - h_2^2) + \frac{(tG)_{panel}}{2}(h_2^2 - h_1^2)$$

$$+ \frac{(w'G)_{center}}{2} h_1^2 + 1.155(wG)_{wrap} h_2^2$$

$$c_3 = \frac{(w'G)_{center}}{2} + 1.155(wG)_{wrap}$$

$$c_4 = \frac{2.309(wG)_{wrap} + (tG)_{panel}}{G_{cap}[2(wG)_{wrap} + (tG)_{panel}]^2}$$

$$c_5 = \frac{(wG)_{cap}}{2}(h_3^2 - h_2^2) + 1.155(wG)_{wrap} + \frac{(tG)_{panel}}{2} h_2^2$$

$$c_6 = \frac{(tG)_{panel}}{2} + 1.155\,(wG)_{wrap}$$

$$c_7 = \frac{1}{w_{cap}}$$

$$c_8 = \frac{w_{cap}}{2} h_3^2$$

$$c_9 = \frac{w_{cap}}{2}$$

$$c_{10} = c_1$$

$$c_{11} = (wG)_{cap}\,(h_6^2 - h_5^2) + 2\,(tG)_{panel}\,(h_5^2 - h_4^2) + \frac{(w'G)_{center}}{2}\,h_4^2 + 1.155(wG)_{wrap}\,h_5^2$$

$$c_{12} = c_3$$

$$c_{13} = \frac{0.577(wG)_{wrap} + (tG)_{panel}}{G_{cap}[(wG)_{wrap} + (tG)_{panel}]^2}$$

$$c_{14} = (wG)_{cap}(h_6^2 - h_5^2) + 2[0.577(wG)_{wrap} + (tG)_{panel}]\,h_5^2$$

$$c_{15} = 2\,[0.577(wG)_{wrap} + (tG)_{panel}]$$

$$c_{16} = \frac{1}{2w_{cap}}$$

$$c_{17} = w_{cap}\,h_6^2$$

$$c_{18} = w_{cap}$$

The solution to the integrals may be obtained in a similar fashion to the solution found in Appendix C.

The above equation for the elastic strain energy is similar to Equation (42), with the differences found in the constant values c_1 to c_9, the addition of three integrals (J_4, J_5, and J_6), and the multiplication factor of one-half. The elastic strain energy due to the bending moment is found by using Equation (11). An equation for the beam stiffness may be found by substituting Equation (11) and Equation (94) into Equation (3) and making the appropriate simplifications:

$$\frac{P\delta}{2} = U_{normal} + U_{shear}$$

$$k = \frac{P}{\delta}$$

$$k = \frac{48(EI)_{eq}}{L^3\left[1 + \frac{12\ E_{cap}^{\ 2}}{L^2\ G_{cap}(EI)_{eq}}\ (J_1 + J_2 + J_3 + J_4 + J_5 + J_6)\right]} \tag{101}$$

An approximate beam stiffness equation will now be developed. If all three caps have the same diameter and are made of the same material, the approximate flexural rigidity is given by the following equation:

$$(EI)_{eq} \cong \frac{\pi\ E_{cap} d^2 D^2}{8} \tag{102}$$

The integrals J_1, J_3, J_4, and J_6 will be set equal to zero. By neglecting the first moments of area of the core panels and the wrap, the following equations are obtained for the integrals J_2 and J_5:

$$J_2 = \int_{h_1}^{h_2} \left(\frac{Q_{eq}}{b_{eq}}\right)^2 dA$$

$$J_2 \cong \frac{\pi^2 d^4 D^2 G_{cap}}{48}\ B_3 H_3 \tag{103}$$

$$J_5 = \int_{h_4}^{h_5} \left(\frac{Q_{eq}}{b_{eq}}\right)^2 dA$$

$$J_5 = \frac{\pi^2 d^4 D^2 G_{cap}}{48}\ B_4 H_4 \tag{104}$$

where

$$B_3 = \frac{2.309(wG)_{wrap} + (tG)_{panel}}{[2(wG)_{wrap} + (tG)_{panel}]^2}$$

$$B_4 = \frac{0.577(wG)_{wrap} + (tG)_{panel}}{[(wG)_{wrap} + (tG)_{panel}]^2}$$

$$H_3 = 0.577\ D - \frac{\sqrt{\pi}\ d}{4} - 0.439\ w_{center}$$

$$H_4 = 0.289\ D - \frac{\sqrt{\pi} d}{4} - 0.219\ w_{center}$$

Approximate equations have been developed for the equivalent flexural rigidity and the integrals J_2 and J_5. By setting $J_1 = J_3 = J_4 = J_6 = 0$, substituting Equations (102), (103), and (104) into Equation (90), and simplifying, the following approximate beam stiffness equation is obtained:

$$k \cong \frac{6\pi d^2 D^4 E_{cap}}{L^3 + 2Ld^2 E_{cap}(B_3 H_3 + B_4 H_4)} \qquad (105)$$

APPENDIX E

COMPUTER PROGRAMS

THE FOLLOWING VARIABLES ARE REQUIRED AS INPUT DATA.

```
    TPAN: CORE PANEL THICKNESS (IN)
    EPAN: CORE PANEL ELASTIC MODULUS (LBS/IN)
    GPAN: CORE PANEL SHEAR MODULUS (LBS/IN)
    WCEN: CORE CENTERPIECE WIDTH (IN)
    ECEN: CORE CENTERPIECE ELASTIC MODULUS (LBS/IN)
    GCEN: CORE CENTERPIECE SHEAR MODULUS (LBS/IN)
    DCAP: CAP DIAMETER (IN)
    ECAP: CAP ELASTIC MODULUS (LBS/IN)
    GCAP: CAP SHEAR MODULUS (LBS/IN)
   DWRAP: WRAP STRAND DIAMETER (IN)
   EWRAP: WRAP STRAND ELASTIC MODULUS (LBS/IN)
     RHO: WRAP DENSITY (STRANDS/INCH)
     PHI: WRAP ANGLE (DEGREES)
       D: CAP CENTERLINE DISTANCE (IN)
   NSPAN: NUMBER OF TEST SPANS
       L: LENGTH OF TEST SPAN (IN)
```

THE FOLLOWING VARIABLES ARE DETERMINED WITHIN THE PROGRAMS.

```
    ACAP: CAP CROSS-SECTIONAL AREA
    ICAP: CAP MOMENT OF INERTIA ABOUT THE NEUTRAL AXIS
    APAN: CORE PANEL CROSS-SECTIONAL AREA
    IPAN: CORE PANEL MOMENT OF INERTIA ABOUT THE NEUTRAL AXIS
    ACEN: CORE CENTERPIECE CROSS-SECTIONAL AREA
    ICEN: CORE CENTERPIECE MOMENT OF INERTIA ABOUT THE NEUTRAL AXIS
    ASTR: CROSS-SECTIONAL AREA OF ONE WRAP STRAND
   WGCAP: CAP SHEAR STIFFNESS
   TGPAN: CORE PANEL SHEAR STIFFNESS
   WGCEN: CORE CENTERPIECE SHEAR STIFFNESS (SQUARE CROSS-SECTION)
  WPGCEN: CORE CENTERPIECE SHEAR STIFFNESS (TRIANGULAR CROSS-SECTION)
C1 TO C18: CONSTANTS USED IN THE DETERMINATION OF THE ELASTIC STRAIN
           ENERGY DUE TO SHEAR STRESSES, C10 TO C18 USED FOR
           TRIANGULAR CROSS-SECTIONS ONLY
```

THE FOLLOWING VARIABLES ARE OUTPUT DATA FROM THE PROGRAMS.

```
   EIPAN: CORE PANEL FLEXURAL RIGIDITTY (LBS*IN**2)
   EICEN: CORE CENTERPIECE FLEXURAL RIGIDITY (LBS*IN**2)
   EICAP: CAP FLEXURAL RIGIDITY (LBS*IN**2)
    EIEQ: EQUIVALENT FLEXURAL RIGIDITY (LBS*IN**2)
   EIAPP: APPROXIMATE FLEXURAL RIGIDITY (LBS*IN**2)
  CORSIG: CORE SIGNIFICANCE (PERCENT)
       R: RADIUS OF GYRATION (IN)
J1 TO J6: INTEGRALS USED IN THE DETERMINATION OF THE ELASTIC STRAIN
          ENERGY DUE TO SHEAR STRESSES, J4 TO J6 USED FOR TRIANGULAR
          CROSS-SECTIONS ONLY (IN**6)
    JAPP: APPROXIMATE SOLUTION FOR THE INTEGRALS (IN**6)
       K: BEAM STIFFNESS (LBS/IN)
```

```
      " THIS PROGRAM DETERMINES THE STIFFNESS OF A SQUARE
      " CROSS-SECTION CAPTIVE COLUMN LOADED AS A SIMPLE-SUPPORTED
      " BEAM WITH A CONCENTRATED MIDSPAN LOAD.
      "    THE FOLLOWING UNITS ARE USED:
      "    ELASTIC AND SHEAR MODULI- 1,000,000 PSI
      "    ALL LENGTH DIMENSIONS' INCHES
      "    WRAP DENSITY- STRANDS/INCH, WRAP ANGLE- DEGREES
      "    FLEXURAL RIGIDITIES- LB*IN**2
      "    CORE SIGNIFICANCE- PERCENT
      "    STIFFNESS- LB/IN


      DIMENSION J1(2), J2(2), J3(2), JAPP(2), L(10), SHEAR(5), K(5)
      REAL IOCAP, ICAP, IOPAN, IPAN, ICEN, J1, J2, J3, JAPP, K, KK, L
      PI=3.1416


      " INPUT ALL NECESSARY DATA

      WRITE(6,1)
    1 FORMAT(/,'  ENTER CORE PANEL ELASTIC MODULUS, SHEAR MODULUS AND THI
CKNESS')
      READ(5,*) EPAN, GPAN, TPAN
      EPAN=EPAN*1000000
      GPAN=GPAN*1000000
      WRITE(6,2)
    2 FORMAT('  ENTER CORE CENTERPIECE ELASTIC MODULUS, SHEAR MODULUS AND
 WIDTH')
      READ(5,*) ECEN, GCEN, WCEN
      ECEN=ECEN*1000000
      GCEN=GCEN*1000000
      WRITE(6,3)
    3 FORMAT('  ENTER CAP ELASTIC MODULUS, SHEAR MODULUS AND DIAMETER')
      READ(5,*) ECAP, GCAP, DCAP
      ECAP=ECAP*1000000
      GCAP=GCAP*1000000
      WRITE(6,4)
    4 FORMAT('  ENTER WRAP ELASTIC MODULUS, DIAMETER, DENSITY AND ANGLE')
      READ(5,*) EWRAP, DWRAP, RHO, PHI
      EWRAP=EWRAP*1000000
      PHI=PHI*0.01745
      WRITE(6,5)
    5 FORMAT('  ENTER DISTANCE BETWEEN ADJACENT CAP CENTERS')
      READ(5,*) D
      WRITE(6,6)
    6 FORMAT('  ENTER NUMBER OF TEST SPANS')
      READ(5,*) NSPAN
      WRITE(6,7)
    7 FORMAT('  ENTER TEST SPANS, ONE VALUE PER LINE')
      DO 10 I=1,NSPAN
      READ(5,*) L(I)
   10 CONTINUE
```

```
      " DETERMINE CROSS-SECTIONAL AREAS, MOMENTS OF
      " INERTIA, FLEXURAL RIGIDITIES, CORE SIGNIFICANCE,
      " AND RADIUS OF GYRATION

      IOCAP=PI*DCAP**4/64
      ACAP=PI*DCAP**2/4
      ICAP=4*IOCAP+2*ACAP*(D*0.7071)**2
      HGHT=1.4142*(D/2)-(DCAP+WCEN)/2
      IOPAN=(TPAN*HGHT**3)/6+(HGHT*TPAN**3)/6
      APAN=TPAN*HGHT
      IPAN=IOPAN+2*APAN*((WCEN+HGHT)/2)**2
      ICEN=(WCEN**4)/12
      EIPAN=IPAN*EPAN
      EICEN=ICEN*ECEN
      EICAP=ICAP*ECAP
      EIEQ=EIPAN+EICEN+EICAP
      EIAPP=4*ECAP*ACAP*(D/2)**2
      CORSIG=100*(EIPAN+EICEN)/EIEQ
      ACEN=WCEN**2
      AEEQ=4*ACAP*ECAP+4*APAN*EPAN+ACEN*ECEN
      R=SQRT(EIEQ/AEEQ)


      " OUTPUT THE FLEXURAL RIGIDITIES

      WRITE(6,20)
      WRITE(6,21) EIPAN
      WRITE(6,22) EICEN
      WRITE(6,23) EICAP
      WRITE(6,24) EIEQ
      WRITE(6,25) EIAPP
      WRITE(6,26) CORSIG
      WRITE(6,27) R
   20 FORMAT(/,8X,'EI OF THE COMPONENTS')
   21 FORMAT('          CORE=',F15.0)
   22 FORMAT('  CENTERPIECE=',F15.0)
   23 FORMAT('          CAPS=',F15.0)
   24 FORMAT('   EQUIVALENT=',F15.0)
   25 FORMAT('  APPROXIMATE=',F15.0)
   26 FORMAT(/,'   CORE SIGNIFICANCE=',F8.4)
   27 FORMAT('  RADIUS OF GYRATION=',F8.4)
```

```
      " DETERMINE SHEAR STIFFNESSES AND
      " INTERMEDIATE TERMS FOR THE INTEGRALS

      ASTR=PI*DWRAP**2/4
      WGWRAP=RHO*ASTR*EWRAP*SIN(PHI)*COS(PHI)**2
      WCAP=SQRT(PI)*DCAP/2
      WGCAP=WCAP*GCAP
      WGCEN=WCEN*GCEN
      TGPAN=TPAN*GPAN
      H1=WCEN/2
      H2=(D-WCAP)/2
      H3=(D+WCAP)/2
      H3H2=H3-H2
      H3H22=H3**2-H2**2
      H3H23=H3**3-H2**3
      H3H25=H3**5-H2**5
      H2H1=H2-H1
      H2H12=H2**2-H1**2
      H2H13=H2**3-H1**3
      H2H15=H2**5-H1**5


      " DETERMINE AND OUTPUT THE INTEGRALS

      DO 30 I=1,2
      C1=1/(GCAP*(2*WGWRAP+WGCEN))
      C2=H3H22*WGCAP+1.4142*H2H12*TGPAN+0.5*H1**2*WGCEN+H2**2*WGWRAP
      C3=0.5*WGCAP+WGWRAP
      C4=(WGWRAP+1.4142*TGPAN)/(2*GCAP*(WGWRAP+TGPAN)**2)
      C5=H3H22*WGCAP+H2**2*(1.4142*TGPAN+WGWRAP)
      C6=1.4142*TGPAN+WGWRAP
      C7=1/(2*WCAP)
      C8=H3**2*WCAP
      C9=WCAP
      J1(I)=C1*(C2**2*H1-0.667*C2*C3*H1**3+0.2*C3**2*H1**5)
      J2(I)=C4*(C5**2*H2H1-0.667*C5*C6*H2H13+0.2*C6**2*H2H15)
      J3(I)=C7*(C8**2*H3H2-0.667*C8*C9*H3H23+0.2*C9**2*H3H25)
      JAPP(I)=C4*(WGCAP*H3H22)**2*H2H1
      WGWRAP=2*WGWRAP
   30 CONTINUE
      WRITE(6,40)
      WRITE(6,41) J1(1), J2(1), J3(1), JAPP(1)
      WRITE(6,42) J1(2), J2(2), J3(2), JAPP(2)
   40 FORMAT(/,30X,'J1',10X,'J2',10X,'J3',8X,'J-APP')
   41 FORMAT('    NO WRAP PRETENSION ',4F12.4)
   42 FORMAT(' IDEAL WRAP PRETENSION ',4F12.4)
```

```
      " DETERMINE AND OUTPUT THE BEAM STIFFNESS VALUES

      WRITE(6,50)
      WRITE(6,51)
      WRITE(6,52)
   50 FORMAT(/,16X,'B E A M     S T I F F N E S S     V A L U E S')
   51 FORMAT('   TEST       BENDING           EXACT                  APPROX
IMATE')
   52 FORMAT('   SPAN        ONLY        NO WPT     IDEAL WPT    NO WPT
 IDEAL WPT')
      DO 60 I=1,NSPAN
      KK=24*ECAP**2/(L(I)**2*GCAP*EIEQ)
      SHEAR(1)=0
      SHEAR(2)=KK*(J1(1)+J2(1)+J3(1))
      SHEAR(3)=KK*(J1(2)+J2(2)+J3(2))
      KK=KK*EIEQ/EIAPP
      SHEAR(4)=KK*JAPP(1)
      SHEAR(5)=KK*JAPP(2)
      DO 65 J=1,5
      K(J)=48*EIEQ/(L(I)**3*(1+SHEAR(J)))
      IF(J.EQ.4.OR.J.EQ.5) K(J)=K(J)*EIAPP/EIEQ
   65 CONTINUE
      WRITE(6,70) L(I), (K(J),J=1,5)
   70 FORMAT(1X,F6.1,5F12.0)
   60 CONTINUE
      END
```

```
      " THIS PROGRAM DETERMINES THE STIFFNESS OF A TRIANGULAR
      " CROSS-SECTION CAPTIVE COLUMN LOADED AS A SIMPLE-SUPPORTED
      " BEAM WITH A CONCENTRATED MIDSPAN LOAD
      "    THE FOLLOWING UNITS ARE USED:
      "    ELASTIC AND SHEAR MODULI- 1,000,000 PSI
      "    ALL LENGTH DIMENSIONS- INCHES
      "    WRAP DENSITY- STRANDS/INCH, WRAP ANGLE- DEGREES
      "    FLEXURAL RIGIDITIES- LB*IN**2
      "    CORE SIGNIFICANCE- PERCENT
      "    STIFFNESS- LB/IN


      DIMENSION J1(2), J2(2), J3(2), J4(2), J5(2), J6(2)
      DIMENSION L(10), JAPP(2), SHEAR(5), K(5)
      REAL IOCAP, ICAP, IOPAN, IPAN, ICEN, J1, J2, J3, J4, J5, J6, JAPP,
K, KK, L
      PI=3.1416


      " INPUT NECESSARY DATA

      WRITE(6,1)
    1 FORMAT(/,'  ENTER CORE PANEL ELASTIC MODULUS, SHEAR MODULUS AND THI
CKNESS')
      READ(5,*) EPAN, GPAN, TPAN
      EPAN=EPAN*1000000
      GPAN=GPAN*1000000
      WRITE(6,2)
    2 FORMAT('  ENTER CORE CENTERPIECE ELASTIC MODULUS, SHEAR MODULUS AND
 WIDTH')
      READ(5,*) ECEN, GCEN, WCEN
      ECEN=ECEN*1000000
      GCEN=GCEN*1000000
      WRITE(6,3)
    3 FORMAT('  ENTER CAP ELASTIC MODULUS, SHEAR MODULUS AND DIAMETER')
      READ(5,*) ECAP, GCAP, DCAP
      ECAP=ECAP*1000000
      GCAP=GCAP*1000000
      WRITE(6,4)
    4 FORMAT('  ENTER WRAP ELASTIC MODULUS, DIAMETER, DENSITY AND ANGLE')
      READ(5,*) EWRAP, DWRAP, RHO, PHI
      EWRAP=EWRAP*1000000
      PHI=PHI*0.01745
      WRITE(6,5)
    5 FORMAT('  ENTER DISTANCE BETWEEN ADJACENT CAP CENTERS')
      READ(5,*) D
      WRITE(6,6)
    6 FORMAT('  ENTER NUMBER OF TEST SPANS')
      READ(5,*) NSPAN
      WRITE(6,7)
    7 FORMAT('  ENTER TEST SPANS, ONE VALUE PER LINE')
      DO 10 I=1,NSPAN
      READ(5,*) L(I)
   10 CONTINUE
```

```
      " DETERMINE CROSS-SECTIONAL AREAS, MOMENTS OF
      " INERTIA, FLEXURAL RIGIDITIES, CORE SIGNIFICANCE,
      " AND RADIUS OF GYRATION

      IOCAP=PI*DCAP**4/64
      ACAP=PI*DCAP**2/4
      ICAP=3*IOCAP+1.5*ACAP*(D/1.7321)**2
      HCEN=WCEN/1.7321/2
      HGHT=D/1.7321-HCEN-DCAP/2
      IOPAN=(TPAN*HGHT**3)/12+(HGHT*TPAN**3)/12
      APAN=TPAN*HGHT
      IPAN=1.5*IOPAN+1.5*APAN*(HCEN+HGHT/2)**2
      ICEN=1.7321*WCEN**4/96
      EIPAN=IPAN*EPAN
      EICEN=ICEN*ECEN
      EICAP=ICAP*ECAP
      EIEQ=EIPAN+EICEN+EICAP
      EIAPP=1.5*ECAP*ACAP*(D/1.7321)**2
      CORSIG=100*(EIPAN+EICEN)/EIEQ
      ACEN=1.7321*WCEN**2/4
      AEEQ=3*ACAP*ECAP+3*APAN*EPAN+ACEN*ECEN
      R=SQRT(EIEQ/AEEQ)


      " OUTPUT THE FLEXURAL RIGIDITIES

      WRITE(6,20)
      WRITE(6,21) EIPAN
      WRITE(6,22) EICEN
      WRITE(6,23) EICAP
      WRITE(6,24) EIEQ
      WRITE(6,25) EIAPP
      WRITE(6,26) CORSIG
      WRITE(6,27) R
   20 FORMAT(/,8X,'EI OF THE COMPONENTS')
   21 FORMAT('          CORE=',F15.0)
   22 FORMAT('  CENTERPIECE=',F15.0)
   23 FORMAT('          CAPS=',F15.0)
   24 FORMAT('   EQUIVALENT=',F15.0)
   25 FORMAT('  APPROXIMATE=',F15.0)
   26 FORMAT(/,'   CORE SIGNIFICANCE=',F8.4)
   27 FORMAT('  RADIUS OF GYRATION=',F8.4)
```

```
" DETERMINE SHEAR STIFFNESSES AND
" INTERMEDIATE TERMS FOR THE INTEGRALS

ASTR=PI*DWRAP**2/4
WGWRAP=RHO*ASTR*EWRAP*SIN(PHI)*COS(PHI)**2
WCAP=SQRT(PI)*DCAP/2
WGCAP=WCAP*GCAP
WPCEN=3**0.25*WCEN/2
WPGCEN=WPCEN*GCEN
TGPAN=TPAN*GPAN
H1=WPCEN*0.667
H2=D/1.7321-WCAP/2
H3=D/1.7321+WCAP/2
H4=H1/2
H5=D/1.7321/2-WCAP/2
H6=D/1.7321/2+WCAP/2
H3H2=H3-H2
H3H22=H3**2-H2**2
H3H23=H3**3-H2**3
H3H25=H3**5-H2**5
H2H1=H2-H1
H2H12=H2**2-H1**2
H2H13=H2**3-H1**3
H2H15=H2**5-H1**5
H6H5=H6-H5
H6H52=H6**2-H5**2
H6H53=H6**3-H5**3
H6H55=H6**5-H5**5
H5H4=H5-H4
H5H42=H5**2-H4**2
H5H43=H5**3-H4**3
H5H45=H5**5-H4**5


" DETERMINE AND OUTPUT THE INTEGRALS

DO 30 I=1,2
C1=(4/1.7321*WGWRAP+WPGCEN)/(GCAP*(2*WGWRAP+WPGCEN)**2)
C2=(H3H22*WGCAP+H2H12*TGPAN+H1**2*WPGCEN)/2+1.1547*H2**2*WGWRAP
C3=WPGCEN/2+1.1547*WGWRAP
C4=(4/1.7321*WGWRAP+TGPAN)/(GCAP*(TGPAN+2*WGWRAP)**2)
C5=H3H22*WGCAP/2+H2**2*(TGPAN/2+1.1547*WGWRAP)
C6=TGPAN/2+1.1547*WGWRAP
C7=1/WCAP
C8=H3**2*WCAP/2
C9=WCAP/2
C10=C1
C11=H6H52*WGCAP+2*H5H42*TGPAN+H4**2*WPGCEN/2+1.1547*H5**2*WGWRAP
C12=C3
```

```
      C13=(WGWRAP/1.7321+TGPAN)/(GCAP*(TGPAN+WGWRAP)**2)
      C14=H6H52*WGCAP+2*H5**2*(TGPAN+WGWRAP/1.7321)
      C15=2*(TGPAN+WGWRAP/1.7321)
      C16=1/(2*WCAP)
      C17=H6**2*WCAP
      C18=WCAP
      J1(I)=C1*(C2**2*H1-0.667*C2*C3*H1**3+0.2*C3**2*H1**5)
      J2(I)=C4*(C5**2*H2H1-0.667*C5*C6*H2H13+0.2*C6**2*H2H15)
      J3(I)=C7*(C8**2*H3H2-0.667*C8*C9*H3H23+0.2*C9**2*H3H25)
      J4(I)=C10*(C11**2*H4-0.667*C11*C12*H4**3+0.2*C12**2*H4**5)
      J5(I)=C13*(C14**2*H5H4-0.667*C14*C15*H5H43+0.2*C15**2*H5H45)
      J6(I)=C16*(C17**2*H6H5-0.667*C17*C18*H6H53+0.2*C18**2*H6H55)
      JAPP(I)=C4*(WGCAP*H3H22/2)**2*H2H1+C13*(WGCAP*H6H52)**2*H5H4
      WGWRAP=2*WGWRAP
   30 CONTINUE
      WRITE(6,40)
      WRITE(6,41) J1(1), J2(1), J3(1), J4(1), J5(1), J6(1), JAPP(1)
      WRITE(6,42) J1(2), J2(2), J3(2), J4(2), J5(2), J6(2), JAPP(2)
   40 FORMAT(/,30X,'J1',10X,'J2',10X,'J3',10X,'J4',10X,'J5',10X,'J6',8X,'
J-APP')
   41 FORMAT('    NO WRAP PRETENSION ',7F12.4)
   42 FORMAT(' IDEAL WRAP PRETENSION ',7F12.4)


      " DETERMINE AND OUTPUT THE BEAM STIFFNESS VALUES

      WRITE(6,50)
      WRITE(6,51)
      WRITE(6,52)
   50 FORMAT(/,16X,'B E A M     S T I F F N E S S     V A L U E S')
   51 FORMAT('   TEST      BENDING           EXACT                  APPROX
IMATE')
   52 FORMAT('   SPAN       ONLY       NO WPT     IDEAL WPT    NO WPT
 IDEAL WPT')
      DO 60 I=1,NSPAN
      KK=12*ECAP**2/(L(I)**2*GCAP*EIEQ)
      SHEAR(1)=0
      SHEAR(2)=KK*(J1(1)+J2(1)+J3(1)+J4(1)+J5(1)+J6(1))
      SHEAR(3)=KK*(J1(2)+J2(2)+J3(2)+J4(2)+J5(2)+J6(2))
      KK=KK*EIEQ/EIAPP
      SHEAR(4)=KK*JAPP(1)
      SHEAR(5)=KK*JAPP(2)
      DO 65 J=1,5
      K(J)=48*EIEQ/(L(I)**3*(1+SHEAR(J)))
      IF(J.EQ.4.OR.J.EQ.5) K(J)=K(J)*EIAPP/EIEQ
   65 CONTINUE
      WRITE(6,70) L(I), (K(J),J=1,5)
   70 FORMAT(1X,F6.1,5F12.0)
   60 CONTINUE
      END
```

REFERENCES

1. Larsen, C.E., "Material Selection and Design for a Captive Column Bridge Girder," Master of Engineering Design Report, University of North Dakota, Engineering Experiment Station Publication, August 1982.

2. Kipp, C.P., "A Finite Element Computer Model of the Captive Column," Master of Engineering Design Report, University of North Dakota, Engineering Experiment Station, Bulletin No. 81-12-EES-04, December 1981.

3. Apanian, R.A., and Sadler, J.P., "Application of the Captive Column Structure to Highway Related Structures," University of North Dakota, Engineering Experiment Station, Bulletin No. 82-04-EES-02, September 1982.

4. Popov, E.P., Mechanics of Materials, 2nd ed., Prentice Hill, Englewood Cliffs, 1976, pp. 120-33, 176, 528-31.

5. Timoshenko, S., Strength of Materials, Vol. 1, 3rd ed., D. Van Nostrand, Princeton, 1955, pp. 170-71, 328.

6. Bosch, L.R., "Captive Column Structure," United States Patent Office Number 3,501,880, 1970.

7. Bath, K., Wilson, E.L., and Peterson, F.E., "A Structural Analysis Program for Static and Dynamic Response of Linear Systems," EERC Report 73-11, 1973.

8. Mechanical Properties of Belcobalsa, Baltek Corporation, Northvale, N.J.